



Optimalisering av DMR prosesser for flytendegjøring av naturgass


Raluca Iloanda Manescu

Natural Gas Technology

Innlevert: februar 2016

Hovedveileder: Truls Gundersen, EPT

Norges teknisk-naturvitenskapelige universitet
Institutt for energi- og prosessteknikk



Optimization of Dual Mixed Refrigerant (DMR) Processes for Natural Gas Liquefaction

Raluca Iolanda Manescu

Natural Gas Technology Master Program


Submission date: February, 2016

Supervisor: Truls Gundersen

Norwegian University of Science and Technology

Faculty of Engineering and Technology

Department of Energy and Process Engineering



Optimization of Dual Mixed Refrigerant (DMR) Processes for Natural Gas Liquefaction

Abstract

Four DMR processes alternatives were modeled and optimized in Aspen HYSYS in order to evaluate their efficiency. The alternatives studied are processes developed by Shell, Air Products and Chemicals, Inc (APCI), Axens-IFP and Tealarc. The objective of the project was to test the Hyprotech SQP optimizer in Aspen HYSYS and report on the its performance, while comparing the energy requirements and the configuration complexity for the proposed processes. The mixed refrigerants composition, as well as their inlet pressures were the main variables in the optimization problem formulation. The degree of meeting the constraints of the process paid a crucial role when analyzing the performance of the optimizer. Exergy analysis was conducted in order to find the exergy loss and the exergy efficiency of the proposed solutions. The optimization results showed that the Shell alternative had the lowest specific power consumption of 214.8 kWh/ton , while the Tealarc alternative had the highest exergy efficiency of 56.8%. However, from the complexity point of view, Shell alternative was a better solution for the offshore floating vessels due to its lower equipment size. Further work should be conducted to improve the optimizer performance, by developing a new nonlinear programming method that would solve the optimization problem.

Preface

The “Optimization of the Dual Mixed Refrigerant (DMR) Process for Natural Gas Liquefaction” project was written at the Norwegian University of Science and Technology (NTNU), as a master thesis in the Department of Energy and Process Engineering, for the International Master’s Degree Program in Natural Gas Technology.

The project is divided into three major parts: project context and description, optimization and evaluation of the results. Project context and description contains the background and motivation, the scope and objective of the project, as well as a general description of the four DMR process alternatives that were analyzed. The optimization part contains an overview of nonlinear optimization, as well as a short description of the NLP and SQP solution algorithms. Further, the Aspen HYSYS optimizer is tested for the four proposed DMR processes. The evaluation part consists of the exergy analysis and the discussions over the results obtained from the optimization of the DMR alternatives.

Trondheim, February 28, 2016

Iolanda Manescu

Acknowledgements

I would like to thank my supervisor Truls Gundersen for his feedback, his patience and guidance during the realization of this project.

Further acknowledgement should also be given to my co-supervisor Donghoi Kim, for his technical guidance throughout the process and for his help regarding the commercial simulator Aspen HYSYS.

Table of Contents

Preface

List of Figures

List of Tables

Abbreviations

1. Introduction	15
1.1 Motivation and Background	15
1.2 The Scope and the Objective of the Project	15
1.3 Structure of the Project	16
2. Research Methods	17
2.1 Literature Study	17
2.2 Process Simulation	17
2.3 Thermodynamic Analysis	17
3. Dual Mixed Refrigerant Processes	18
3.1 Overview of the DMR Process Alternatives	18
3.2 Previous Optimization Work on LNG Processes	22
4. Numerical Optimization	27
4.1 Introduction to Numerical Optimization	27
4.2 Nonlinear Programming	29
4.3 Sequential Quadratic Programming	31
5. Aspen HYSYS Hyprotech SQP Optimizer	33
5.1 Hyprotech SQP Optimizer Configuration	33
5.2 Hyprotech SQP Optimizer Setup	35
6. Optimization of DMR Process Alternatives	38
6.1 Design Basis	38
6.2 Optimization Problem Formulation	41
6.3 APCI DMR Process Optimization	46
6.4 Shell DMR Process Optimization	57
6.5 Tealarc DMR Process Optimization	68
6.6 Liquefin DMR Process Optimization	81
6.7 Hyprotech SQP Optimizer Results	92
7. Thermodynamic Analysis	96
7.1 Physical Exergy	97
7.2 Chemical Exergy	98

7.3 Results.....	99
8. Discussions.....	105
8.1 Hyprotech SQP Performance.....	105
8.2 Power Consumption.....	108
8.3 Heat Transfer in Cryogenic Heat Exchangers.....	116
8.4 Compactness.....	119
8.5 Safety.....	123
9. Conclusions.....	126
10. Further Work.....	131
References.....	132
Appendix A: APCI DMR Process Flow Sheet.....	135
Appendix B Shell DMR Process Flow Sheet.....	136
Appendix C Tealarc Process Flow Sheet.....	137
Appendix D Liquefin Process Flow Sheet.....	138
Appendix E Composite Curves Diagram for Initial APCI Alternative.....	139
Appendix F Composite Curves Diagram for Optimized APCI Alternative.....	140
Appendix G Composite Curves Diagram for Initial Shell Alternative.....	141
Appendix H Composite Curves Diagram for Optimized Shell Alternative.....	142
Appendix I Composite Curves Diagram for Initial Tealarc Alternative Pre-Cooling.....	143
Appendix J Composite Curves Diagram for Optimized Tealarc Alternative Pre-Cooling.....	144
Appendix K Composite Curves Diagram for Initial Tealarc Alternative Liquefaction.....	145
Appendix L Composite Curves Diagram for Optimized Tealarc Alternative Liquefaction.....	146
Appendix M Composite Curves Diagram for Initial Liquefin Alternative.....	147
Appendix N Composite Curves Diagram for Optimized Liquefin Alternative.....	148
Appendix O Material Stream Values from HYSYS for Initial Shell DMR Process.....	149
Appendix P Material Stream Values from HYSYS for Initial APCI DMR Process.....	151
Appendix Q Material Stream Values from HYSYS for Initial Liquefin DMR Process.....	153
Appendix R Material Stream Values from HYSYS for Initial Tealarc Process.....	155
Appendix S Material Stream Values from HYSYS for Optimized Shell Process.....	157
Appendix T Material Stream Values from HYSYS for Optimized APCI Process.....	159
Appendix U Material Stream Values from HYSYS for Optimized Liquefin Process.....	161
Appendix V Material Stream Values from HYSYS for Optimized Tealarc Process.....	163

List of Figures

Figure 3.1-1 Shell DMR Process (Grootjans et al., 2002)	19
Figure 3.1-2 APCI DMR Process (Roberts et al., 2000).....	19
Figure 3.1-3 Liquefin DMR Process (Paradowski et al., 2000).....	20
Figure 3.1-4 Tealarc DMR Process.....	20
Figure 3.1-5 The proposed Cycle-1	25
Figure 3.1-6 The proposed Cycle-2	25
Figure 3.1-7 The proposed Cycle-3	26
Figure 4.0-1 Optimization Problems Classification (Biegler, 2010)	30
Figure 4.0-2 Solution for Newton Method.....	32
Figure 5.0-1 Variables Setup for the Derivative Utility Tab in HYSYS	33
Figure 5.0-2 Constraints Setup for the Derivative Utility Tab in HYSYS	34
Figure 5.0-3 Objective Function Setup for the Derivative Utility in Aspen HYSYS	35
Figure 5.0-4 Aspen HYSYS Optimizer Setup	35
Figure 6.0-1 Compressors Configuration.....	44
Figure 6.0-2 Optimizer Setup Parameters.....	45
Figure 6.0-3 Initial Composite Curves Diagrams for APCI Model	48
Figure 6.0-4 Composite Curves Diagrams Alternative Solution for APCI Model	49
Figure 6.0-5 MR1 Composition Vs. Specific Power Consumption for APCI Model.....	51
Figure 6.0-6 MR2 Composition Vs. Specific Power Consumption for APCI Model.....	51
Figure 6.0-7 Constraints in the Optimizer for the APCI Model Optimized Solution	52
Figure 6.0-8 Maximum Iterations Variation for APCI Model	53
Figure 6.0-9 Objective Scale Factor Variation for APCI Model	54
Figure 6.0-10 Accuracy Tolerance Variation for APCI Model	54
Figure 6.0-11 Step Restriction Variation for APCI Model	55
Figure 6.0-12 Pre-cooling Stage for Shell DMR Process	58
Figure 6.0-13 Initial Composite Curves Diagrams for Shell Model	60
Figure 6.0-14 Composite Curves for the Optimized Solution for Shell Model	61
Figure 6.0-15 Molar Flow Variation for MR1 for Shell Model.....	62
Figure 6.0-16 Molar Flow Variation for MR2 for Shell Model.....	62
Figure 6.0-17 Constraints in the Optimizer for Shell Model	63
Figure 6.0-18 Maximum Iterations Variation for Shell Model.....	64
Figure 6.0-19 Objective Scale Factor Variation for Shell Model	65
Figure 6.0-20 Accuracy Tolerance Variation for Shell Model	65
Figure 6.0-21 Step Restriction Variation for Shell Model	66
Figure 6.0-22 Relative Constraint Error for Shell Model	67
Figure 6.0-23 Pressure Vs. Objective Function for Tealarc Model	70
Figure 6.0-24 Constraints Values for Solution 1 for Tealarc Model	71
Figure 6.0-25 Composite Curves Diagrams for Solution 1 of the Tealarc Model	72
Figure 6.0-26 Composite Curves Diagrams for Solution 2 of the Tealarc Model	73
Figure 6.0-27 Molar Flow Rate Variation for MR1 for Tealarc Model.....	74
Figure 6.0-28 Molar Flow Rate Variation for MR2 for Tealarc Model.....	74
Figure 7.0-1 Exergy Loss Comparison	99
Figure 7.0-2 Total Exergy Loss Initial Vs. Optimized Solution	100
Figure 7.0-3 Compressors, Pumps and Coolers Exergy Efficiencies	101

Figure 7.0-4 Cold Box Exergy Efficiencies	101
Figure 7.0-5 Overall Exergy Efficiencies	102
Figure 7.0-6 Exergy Losses for APCI Model	103
Figure 7.0-7 Exergy Losses for Shell Model	103
Figure 7.0-8 Exergy Losses for Liquefin Model.....	104
Figure 7.0-9 Exergy Losses for Tealarc Model	104
Figure 8.0-1 Objective Function Values, kWh/ton of LNG.....	105
Figure 8.0-2 Average CPU Time Comparison.....	107
Figure 8.0-3 Total Power Consumption, MW	108
Figure 8.0-4 MR1 Stream Phase Envelope APCI.....	109
Figure 8.0-5 MR2 Stream Phase Envelope APCI.....	110
Figure 8.0-6 MR1 Stream Phase Envelope Shell.....	110
Figure 8.0-7 MR2 Stream Phase Envelope Shell.....	111
Figure 8.8 MR1 Phase Envelope Tealarc.....	111
Figure 8.9 MR2 Phase Envelope Tealarc.....	112

List of Tables

Table 3.1-1 DMR Process Pre-Cooling Stage Comparison	21
Table 3.1-2 DMR Process Liquefaction Stage Comparison	21
Table 3.1-3 Recent Studies on LNG Process Design Optimization (Austbø, B., 2015).....	22
Table 3.1-4 DRM Process Alternatives, (Manescu, 2015)	24
Table 3.1-5 Comparison of Specific Power for Several Cycles, Lee et al. (2012)	24
Table 6.0-1 Natural Gas Inlet Conditions	39
Table 6.0-2 LNG Conditions	39
Table 6.0-3 Cryogenic Heat Exchangers Conditions	40
Table 6.0-4 Compressor and Pump Efficiencies.....	41
Table 6.0-5 Variables Used in Optimization	43
Table 6.0-6 Optimizer Setup Parameters Ranges	46
Table 6.0-7 APCI DMR Constraints Values.....	46
Table 6.0-8 Number of Variables for APCI DMR Process	47
Table 6.0-9 APCI Variables Starting Points	47
Table 6.0-10 Comparison of the Initial Variables Values and a Random Solution	50
Table 6.0-11 Optimized Variables Vs. Initial Values for APCI Model	52
Table 6.0-12 Variables Values Comparison for APCI Model	56
Table 6.0-13 Constraints Values Comparison for APCI Model	57
Table 6.0-14 Shell DMR Constraints Values.....	57
Table 6.0-15 Number of Variables for Shell DMR Process	58
Table 6.0-16 Variables Starting Points for Shell DMR Process	59
Table 6.0-17 Initial Vs. Optimized Variables Values for Shell Model.....	63
Table 6.0-18 Tealarc DMR Constraints and Objective Function Values	68
Table 6.0-19 Number of Variables for Tealarc DMR Model	69
Table 6.0-20 Variables Starting Points for Tealarc DMR Model	69
Table 6.0-21 Initial Vs. Optimized Solutions MR 1 Values	75
Table 6.0-22 Initial Vs. Optimized Solutions MR 2 Values	76
Table 6.0-23 Constraints Values Comparison for the Tealarc Model.....	80
Table 6.0-24 Liquefin DMR Constraints Values	81
Table 7.0-1 Exergy Loss Formulas [Venkatarathnam, 2008]	96
Table 8.0-1 Constraints Values Comparison Table	106
Table 8.0-2 Cryogenic Heat Exchangers Design Initial Solution.....	120
Table 8.0-3 Cryogenic Heat Exchangers Design Optimized Solution.....	120
Table 8.0-4 Compressor Suction Volume for the Initial Solution	121
Table 9.0-1 Summary of Parameters for the Initial DMR Alternatives	126
Table 9.0-2 Summary of Parameters for the Optimized DMR Alternatives.....	127
Table 9.0-3 Assessment of the Main Parameters	127
Table 9.0-4 Grading Assessment of the Initial DMR Alternatives	128
Table 9.0-5 Grading Assessment of the Optimized DMR Alternatives	129
Table 9.0-6 Correction Factor for the Optimized Alternatives	130
Table 9.7 Final Assessment of the Initial and Optimized Solutions	130

Abbreviations

DMR	Dual Mixed Refrigerant
EoS	Equation of State
FLNG	Floating Liquefied Natural Gas
HK	Heavy Key
LK	Low Key
LNG	Liquefied Natural Gas
LTMD	Logarithmic Mean Temperature Difference
MR	Mixed Refrigerant
MTPA	Million Ton per Annum
NLP	Nonlinear Programing
SMR	Single Mixed Refrigerant
SQP	Sequential Quadratic Programming

PART ONE: PROJECT CONTEXT AND DESCRIPTION

1. Introduction

The first part of the master thesis introduces the reader to the motivation and the background of the project. The scope and the objectives are presented together with the structure of the project. A short overview of the DMR processes follows focusing on the main differences, advantages and disadvantages for the four alternatives analyzed.

1.1 Motivation and Background

As the world turns to the search for more low emission fuels, natural gas comes more and more into the attention of the researches in the energy sector. The liquefaction process of the natural gas is an important stage in the design and operation of floating LNG devices (FLNG). The dual mixed refrigerant process is considered to be a good candidate for the liquefaction process for offshore platforms. The optimization of such process is therefore crucial to the development of safer and higher energy efficiency processes for FLNG installations (Morin et al., 2011).

The specialization project "The Dual Mixed Refrigerant Process for Natural Gas Liquefaction" (Manescu, 2015), analyses four different DMR processes, by modeling them in Aspen HYSYS and comparing their power consumption and reliability when operating on a FLNG platform. A need to further optimizing these processes was the obvious next step.

1.2 The Scope and the Objective of the Project

The scope of the master thesis is to find an optimized solution for the DMR process that can be successfully used on a floating LNG platform. Thus, the objective of the project is to test the built-in optimizer in the commercial simulator Aspen HYSYS for the four DMR processes alternatives selected. In order to achieve this objective, several tasks have been considered throughout the project:

1. Test the SQP algorithm in the HYSYS optimizer, with a focus on reducing the power consumption of the processes.

2. Analyze the optimization results and compare them with the values obtained in the specialization project and from the literature.

3. Perform an exergy analysis.

1.3 Structure of the Project

The mater thesis is divided into three major parts: the context and description of the project, the optimization and the evaluation parts. The first part introduces the motivation and the background of the project, and sets the scope and the objective that will be followed throughout the project. It also includes the research methods used such as literature study, Aspen HYSYS simulation and thermodynamic analysis. A general description of the DMR processes and the previous work that has been done is introduced here too.

The second part, the optimization, consists of three chapters. The first chapter gives an overview on the numerical optimization with a focus on non-linear optimization problems and SQP solution algorithm. The second chapter goes into the objective of the project, giving relevant information on the SQP Optimizer in HYSYS. The third chapter presents the optimization that has been done for the four DMR alternatives modeled in Aspen HYSYS.

The third part of the project, the evaluation, starts with a thermodynamic analysis of all the processes optimized, goes on with an evaluation and discussion of the results, and ends with a pertinent conclusion and further work recommendation.

2. Research Methods

In order to achieve the scope and the objective of the project, several methods were used, such as literature review, process simulation, and thermodynamic analysis.

2.1 Literature Study

Different relevant publications on numerical optimization were consulted, as well as dedicated books on nonlinear programming. Publications and scientific papers were consulted to get an overview of the previous work regarding the optimization of the LNG processes, in particular, the progress so far in the dual mixed refrigerant process. The Aspen HYSYS user guide was a good reference for understanding how the Hyprotech SQP method is used in the commercial simulator optimizer.

2.2 Process Simulation

Two commercial simulators were used during this project: Aspen HYSYS v8.6 and PROII v9.3. The Aspen HYSYS simulator was used to model the DMR process alternatives selected. Within the simulator, the Hyprotech SQP method was used to test the performance of the built-in optimizer. PROII was used to plot the phase envelopes of the mixed refrigerants streams. This was done in order to achieve a better understanding of how the composition has changed based on the performance of the optimizer.

2.3 Thermodynamic Analysis

An exergy analysis was done for the optimized DMR processes to see where improvements can be made in order to increase the overall efficiency of the process. Values for physical exergy of the streams were taken from the models simulated in HYSYS that were used for the calculation of the exergy loss and the exergy efficiency of all equipment involved in the liquefaction process. Chemical exergy was also included when calculating the exergy loss for the mixers and the phase separators present in the process. The chemical exergy was calculated based on equations taken from the specialized literature.

3. Dual Mixed Refrigerant Processes

This chapter presents an overview of the four DMR process alternatives proposed, with a focus on the differences, advantages and disadvantages of each alternative. A brief presentation of the previous work done on the optimization of the LNG processes follows.

3.1 Overview of the DMR Process Alternatives

In order to achieve the low temperature needed for the liquefaction of the natural gas, the dual mixed refrigerant process uses two different mixtures of refrigerants. Usually, a first mixed refrigerant is compressed and expanded at different pressure levels in the pre-cooling stage of the liquefaction process, while a second mixed refrigerant goes through compression and expansion in the liquefaction stage. The mixed refrigerants have different inlet pressures; usually the one with the lower pressure is called the low level mixed refrigerant and the one with the higher pressure is called the high level mixed refrigerant (Venkatarathnam, 2008).

The four DMR alternatives that were subject to optimization are the following:

1. Shell DMR Process
2. Air Products and Chemicals, Inc. (APCI)
3. Axens-IFP – “Liquefin” DMR with plate-in heat exchangers
4. Tealarc LNG Process

The Shell DMR process uses a low pressure mixed refrigerant in the pre-cooling stage and a high pressure mixed refrigerant in the liquefaction stage. The low level refrigerant goes through two pressure level changes before leaving the pre-cooling stage to the compression stage. The high pressure refrigerant, leaves the pre-cooling stage at a lower temperature, and enters a phase separator where liquid and vapor are separated, at the beginning of the second stage, the liquefaction part. Here, the mixed refrigerant goes through one pressure level change, and then leaves the liquefaction stage in order to be compressed and sent back to the pre-cooling stage of the process. Figure 3.1 presents the flow sheet of the process.

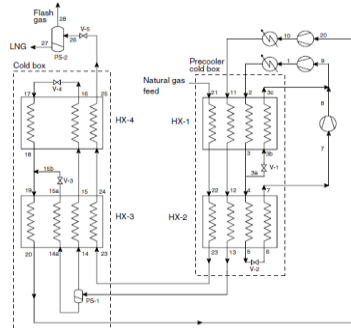


Figure 3.0-1 Shell DMR Process (Grootjans et al., 2002)

The APCI process uses one pressure level change for the low pressure refrigerant in the pre-cooling stage, and one pressure level in the liquefaction part. In the liquefaction stage, the high pressure mixed refrigerant enters a phase separator where the stream is split into vapor and liquid streams. The liquid stream is sub-cooled in the first part of the cryogenic heat exchanger, expanded and then mixed with the vapor stream before entering the same exchanger at a lower temperature. The vapor stream is cooled and sub-cooled in the same heat exchanger in the liquefaction stage, expanded after it passes the cold end of the exchanger, when its temperature is decreased and then enters back the same exchanger and is mixed with the liquid stream before it leaves the hot end of the same heat exchanger. Figure 3.2 presents the flow sheet of the process.

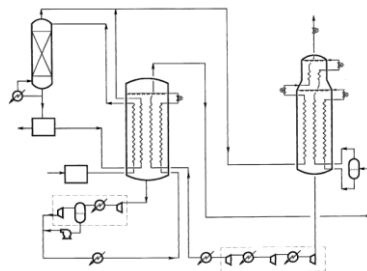


Figure 3.0-2 APCI DMR Process (Roberts et al., 2000)

The Liquefin pre-cooling stage consists of three heat exchangers, all with different pressure levels for the low pressure mixed refrigerant. The liquefaction stage consists of one pressure level change. The difference from the first two alternatives presented, is that there is no phase

separators in the second stage, the high level mixed refrigerant entering the liquefier straight from the pre-cooling stage. Figure 3.3 shows a scheme of the process taken from the patent.

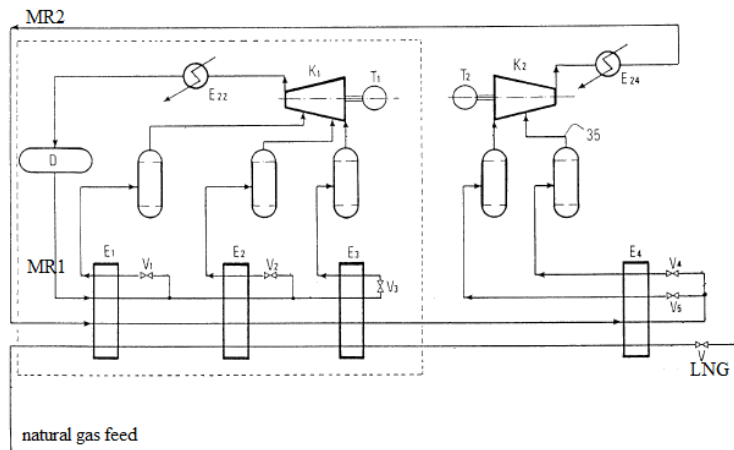


Figure 3.0-3 Liquefin DMR Process (Paradowski et al., 2000)

The Tealarc process is likewise divided in two parts. The natural gas stream is absent in the pre-cooling stage, and the first mixed refrigerant is absent from the liquefaction stage. In the first stage, the first mixed refrigerant is circulated and goes through three pressure level changes in order to get the second mixed refrigerant to a low temperature. In the second part, the liquefaction stage, the second mixed refrigerant enters first a phase separator. In this stage, the mixed refrigerant goes through one pressure level change. Figure 3.4 presents the flow scheme of the process.

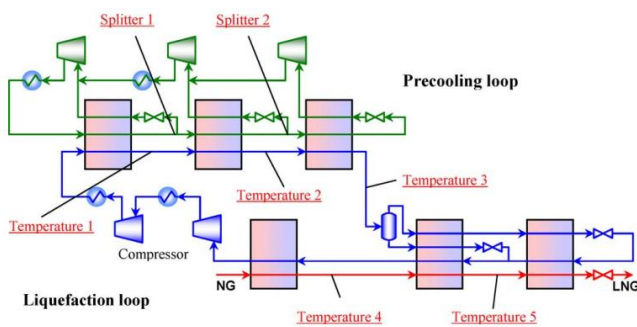


Figure 3.0-4 Tealarc DMR Process

In order to have a better overview of the four alternatives and their main differences, a short comparison of the pressure levels and number of phase separators is presented in Table 3.1 for the pre-cooling stage and Table 3.2 for the liquefaction stage. Values were taken from patents and research papers.

Table 3.0-1 DMR Process Pre-Cooling Stage Comparison

Alternative	Pressure Levels	Phase Separators
Shell	2	0
APCI	1	0
Liquefin	3	0
Tealarc	3	0

Table 3.0-2 DMR Process Liquefaction Stage Comparison

Alternative	Pressure Levels	Phase Separators
Shell	1	1
APCI	1	1
Liquefin	1	0
Tealarc	1	1

Based on the two tables presented above, a lower number of pressure levels in the pre-cooling stage will require the presence of a phase separator in order to have a competitive process efficiency. Based on this, the Tealarc alternative should have the best efficiency since it has three pressure levels in the pre-cooling stage and a phase separator in the liquefaction stage. However, the way different pressure levels and phase separators have an impact on the efficiency of the processes is presented and discussed in the Evaluation part of the project.

3.2 Previous Optimization Work on LNG Processes

An overview on the previous optimization work done for the liquefaction of the natural gas process is presented in this chapter. From literature studies, optimization has been done for different types of liquefaction processes such as DMR, C3MR, and expander based processes. In his doctoral thesis, Austbø (2015), presents a selection of recent studies done on LNG process design optimization that is shown in Table 3.3. The equations of state used in modeling these processes are SRK and PR, with the latter one being predominant.

Table 3.0-3 Recent Studies on LNG Process Design Optimization (Austbø, B., 2015)

Study	Process	Optimization Method	Modeling/Simulation
Alabdulkarem et al. (2011)	C3MR	GA	Aspen HYSYS®
Aspelund et al. (2010)	SMR	TS + NMSS	Aspen HYSYS®
Castillo and Dorao (2012)	SMR	GA	Aspen HYSYS®
Del Nogal et al. (2008)	SMR and DMR	GA	WORK
Hatcher et al. (2012)	C3MR	BOX	Aspen HYSYS®
He and Ju (2014a)	EXP	GA	Aspen HYSYS®
He and Ju (2014b)	SMR	GA	Aspen HYSYS®
Hwang et al. (2013a)	DMR	GA + SQP	Aspen HYSYS®
Hwang et al. (2013b)	DMR	GA + SQP	Aspen HYSYS®
Jensen and Skogestad (2008)	SMR	-	gPROMS®
Kamath et al. (2012)	SMR	CONOPT	GAMS
Khan and Lee (2013)	SMR	PSO	UniSim®
Khan et al. (2012)	SMR	SQP	UniSim®
Lee et al. (2012)	SMR	Mesh search	Aspen HYSYS®
Lee et al. (2014)	C3MR	SQP	Aspen HYSYS®
Morin et al. (2011)	SMR and DMR	SQP and ES	Aspen HYSYS®
Shah et al. (2009)	EXP	GA	Aspen HYSYS®
Shirazi and Mowla (2010)	SMR	GA	MATLAB®/Aspen HYSYS®
Skaugen et al. (2010)	SMR	SQP	Aspen HYSYS® / PRO/II
Taleshbahrami and Saffari (2010)	C3MR	GA	MATLAB®/Aspen HYSYS®
Wahl et al. (2013)	SMR	SQP	Aspen HYSYS®

Wang et al. (2013a)	C3MR	BOX	Aspen HYSYS®
Wang et al. (2012)	C3MR	Branch-and-cut	GAMS/Aspen Plus®
Wang et al. (2011)	C3MR	SQP	Aspen Plus®
Xu et al. (2013)	SMR	GA	Aspen Plus®
Xu et al. (2014)	SMR	GA	Aspen Plus®
Yoon et al. (2012)	SMR and EXP	GA	Aspen HYSYS®

The main objective for the optimization of these processes was to minimize the power consumption required for the liquefaction process.

The focus of this project is the optimization of the DMR process alternatives in the Aspen HYSYS simulator, using the SQP algorithm in the built-in optimizer. As a conclusion for the research Austbø (2015) did, most of the optimization work has been carried out for the C3MR and SMR processes, and the most widely used simulator was ASPEN HYSYS. The optimization methods used vary, with more focus on the SQP and GA algorithms. Hence, not so much optimization on the DMR process has been carried out recently.

In his master thesis, Rødstøl (2015) tested the performances of the SQP algorithm for the optimization of different liquefaction processes, one of them being the APCI DMR process. The results presented in his paper, show a reduction in the specific power consumption from 274.10 to 256.18 kWh/ton of LNG, for the dual mixed refrigerant process. Rødstøl (2015) also optimized the model from Kusmaya (2012) (Rødstøl, 2015) with an original objective value for the APCI model of 316.85 kWh/ton of LNG, to a value of 262.11 kWh/ton of LNG, using the SQP algorithm in ASPEN HYSYS. The main difference in this new optimized model, is the lower pressure levels obtained by Rødstøl (2015).

In the specialization project done by Manescu (2015), optimization using the same Hyprotech SQP algorithm in ASPEN HYSYS was conducted for the four different DMR processes. Table 3.4 presents the values obtained for the specific power consumption for the four alternatives considered.

Table 3.0-4 DRM Process Alternatives, (Manescu, 2015)

Alternative	Initial Specific Power Consumption	Optimized Specific Power Consumption	Units of Measure
APCI	282.5	248.2	<i>kWh/ton of LNG</i>
SHELL	252.9	239.7	<i>kWh/ton of LNG</i>
Tealarc	248.5	227.9	<i>kWh/ton of LNG</i>
Liquefin	254.1	237.9	<i>kWh/ton of LNG</i>

The variables used for this optimization problem were the flow rates of the mixed refrigerants and the pressure ratios of the compressors. The composition of the refrigerants as well as their inlet and outlet pressures were not considered.

In the study conducted by Lee et al, (2012), three proposed liquefaction cycles were presented. The specific power values for the three cycles are compared against the SMR, C3MR, and cascade processes. These values are presented in Table 3.5.

Table 3.0-5 Comparison of Specific Power for Several Cycles, Lee et al. (2012)

Cycles	Specific Power (<i>kWh/kg of LNG</i>)	Percent of Specific Power
SMR	0.4760	100%
Cascade	0.4444	93%
C3MR	0.2945	62%
Proposed Cycle-1	0.3204	67%
Proposed Cycle-2	0.3106	65%
Proposed Cycle-3	0.3184	67%

The proposed cycles presented in the study done by Lee et al. (2012) are shown in Figures 3.5, 3.6 and 3.7.

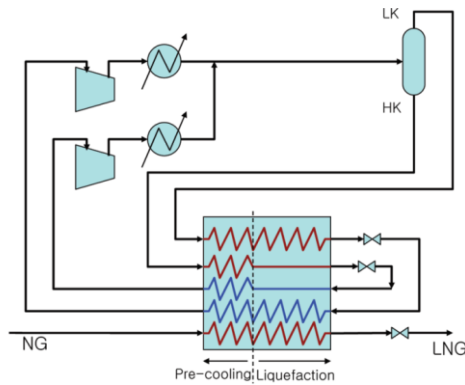


Figure 3.0-5 The proposed Cycle-1

The proposed cycle-1, features the mixed refrigerant which is separated into a liquid stream (heavy key component, HK) and a vapor stream (light key component, LK), in a flash drum. The single mixed refrigerant is separated into two streams, acting like a dual mixed refrigerant process: the heavy liquid stream pre-cools the refrigerant and natural gas streams, while the light vapor stream will be in charge of liquefying the natural gas stream to -150°C , as well as cooling the LK stream (Lee et al. 2012).

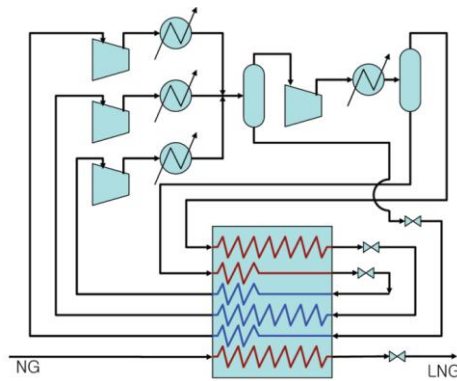


Figure 3.0-6 The proposed Cycle-2

The proposed cycle-2, features a different compression system than the one presented for cycle-1. The new compressor systems contains an LK compressor, an HK compressor and a MK (LK+HK) compressor. A vapor-liquid separator is needed after the mixing point of the

LK and MK and a heavier component is generated (heavier than HK). The new HHK is used as a refrigerant in the cycle, where it is expanded after the vapor liquid separator, right before it enters the LNG heat exchanger.

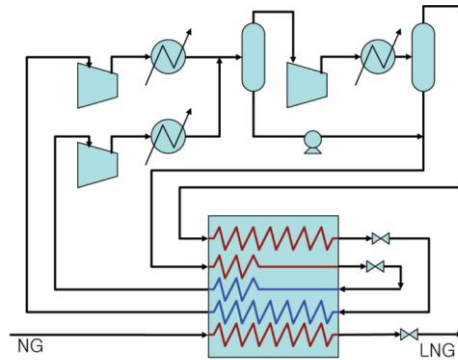


Figure 3.0-7 The proposed Cycle-3

In the proposed cycle-3, the HHK liquid stream goes through a pump before it is mixed with the HK stream. This gives a simplified structure for the proposed cycle 2.

PART TWO: OPTIMIZATION

4. Numerical Optimization

A brief introduction to numerical optimization, as well as a short overview of the non-linear (NLP) and sequential quadratic programming (SQP) used in numerical optimization are presented in this chapter.

4.1 Introduction to Numerical Optimization

Optimization is a key factor in the energy consumption reduction of a plant or an industry. In order to formulate the optimization problem, the objective, the variables and the constraints must be specified. The objective function is a quantitative measure of the performance of a specific equipment or system. The objective function can be either minimized or maximized during optimization. For example, a power consumption of the compressors used in the liquefaction process of the natural gas is subject to minimization, while the exergy efficiency of the same system is subject to maximization. In order to solve the optimization problem and arrive at an acceptable value for the objective function, several variables are considered. These represent the characteristics of the system subject to optimization, and are represented by the flow rates, pressures, temperatures, and different equipment characteristics. They can also be considered the degrees of freedom in a process. The variables need to be adjusted in order to satisfy the process constraints, which are defined in the initial phase of the optimization. (Nocedal and Wright, 1999)

Mathematically, the optimization problem can be formulated as follows:

$$\min_{x \in \mathbb{R}^n} f(x) \quad \text{subject to} \quad \begin{cases} c_i(x) = 0, i \in \mathcal{E}, \\ c_i(x) \geq 0, i \in \mathcal{T}. \end{cases} \quad [4.1]$$

Where,

x is the vector of all variables;

f is the objective function;

c is the vector of the constraints that must be satisfied by the variables;

f and c_i are scalar valued functions of the variables x , while τ, ε are sets of indices of inequality and equality constraints.

Continuous versus Discrete Optimization

Discrete optimization is used to solve problems with integers variables, instead of real, making the problems more difficult to be approached. Continuous optimization is used to find solutions from an infinite set of real components, usually a set of vectors of such components. These types of problems are easier to solve, since the smoothness of the functions allows the use of the objective and constraint functions at a specific point x to obtain information about the function's behavior at the next points closer to x (Biegler, 2010). This project focuses on the use of continuous optimization for solving the optimization problem.

Constrained and Unconstrained Optimization

The optimization problems can be classified based on the variables restrictions, into constrained and unconstrained optimization problems. This project defines a constrained optimization problem. If the constraints and the objective function are linear functions of x , then the problem is named a linear programming problem. If at least some of the constraints or the objective function are nonlinear, then the problem can be classified as a nonlinear programming problem. Nonlinear programming problems are naturally present in engineering sciences, and are more difficult to solve since they may contain several feasible regions for the solution, making it harder to find a global minima (Biegler, 2010).

Global and Local Optimization

While a local minima is defined to be a point where the objective function is minimized in its vicinity, the global minima is defined to be the point where the function is minimized on the whole domain. Global solutions are difficult to identify and locate, and are often used in linear programming. Generally, nonlinear problems process local solutions that are not global solutions (Biegler, 2010).

Optimization Algorithms

The three most important properties that a good optimization algorithm should possess are: robustness, efficiency and accuracy. The algorithms chosen for the optimization problem should perform well on different problems, and for a wide range of values for the initial variables. The algorithm should also be as fast as possible, and be able to find a solution with precision. These properties might be in conflict, so a sensible trade-off between convergence rate and storage time, and robustness and speed, needs to be taken into consideration (Biegler, 2010).

The optimization algorithms can be classified as follows (Nocedal and Wright, 1999):

1. *Linear programming*, where all the constraints and the objective function are linear functions.
2. *Quadratic programming*, with the objective function being quadratic and the constraints linear.
3. *Nonlinear programming*, with some of the constraints being nonlinear functions.
4. *Linearly constrained optimization*, with the constraints linear.
5. *Bound-constrained optimization*, where the constraints include upper and lower bounds.
6. *Convex programming*, with the objective function being convex, the inequality constraints being concave and the equality constraints being linear functions.

4.2 Nonlinear Programming

At an engineering level, different optimization strategies are applied to real processes. The success of optimizing a process consists in relying on the performance of the different methods used. While the mathematicians focus on developing adequate algorithms for solving given optimization problems, the engineers deal with finding the right optimization formulation. Figure 4.1 shows a general classification of optimization problems.

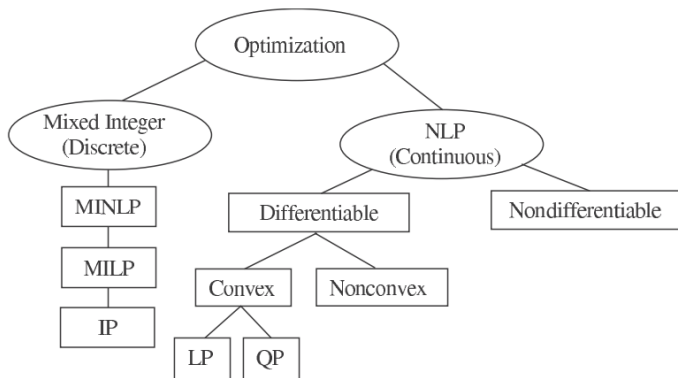


Figure 4.0-1 Optimization Problems Classification (Biegler, 2010)

When classifying an NLP optimization problem, it is important to first determine if it is a differentiable or a non differentiable problem. Differentiable problems have the first and the second derivatives in the continuous form. A differentiable problem then must be defined as convex or non convex.

A function is said to be convex if for any x and y and for any real $0 \leq r \leq 1$ we have that:

$$r \cdot f(x) + (1 - r) \cdot f(y) \geq f(r \cdot x + (1 - r) \cdot y) \quad [4.2]$$

Graphically, the condition is equivalent with the fact that for any two points on the graph, the segment joining those points lies above the function's graph. The advantage of dealing with convex problems is that any local minima is also a global one. However, non convex problems have multiple local solutions, depending on the region found, making it more difficult to be solved.

Nonlinear programming deals with optimization problems where some of the constraints are nonlinear functions (Biegler, 2010). The constraints divide the solutions into two regions: feasible and infeasible regions. If all the constraints are satisfied, then the solution found is located in the feasible region, while, if not, then the optimization problem will give an infeasible solution.

Based on the type of constraints, there are several methods used in nonlinear programming for solving the optimization problem, such as the quadratic programming (QP) and

semidefinite programming (SP). This projects deals with a branch of the quadratic programming, which is the sequential quadratic programming (SQP), discussed in the next subchapter.

4.3 Sequential Quadratic Programming

The sequential quadratic programming is based on Lagrange, Taylor and Newton methods (Boggs, 1996).

Lagrange

The Lagrange Multipliers method is used for finding the local maxima or minima of a function under some equality constraints. The method is based on the fact that when calculating the minimum of a function, a solution is reached when all its partial derivatives are equal to 0.

Let the following function be defined as in Equation 4.3:

$$H(x, y, z) = f(x, y) + z \cdot g(x, y) \quad [4.3]$$

Where:

H, f, g are the functions that need to be solved;

$x, y,$ and z are variables;

z is also known as the Lagrange multiplier.

The solution for this function can be obtained when solving Equation 4.4:

$$\frac{\partial H}{\partial x} = \frac{\partial H}{\partial y} = \frac{\partial H}{\partial z} = 0 \quad [4.4]$$

Taylor

One of the most important results in mathematics is due to Taylor, which states that any function can be written as an infinite sum of terms determined by the function's derivatives at a specific point. As a consequence, a very good approximation of the value of the function can be found at any point by truncating the infinite summation. An example of such an expansion, around 0, is illustrated below:

$$f(x) = f(0) + \frac{x^1}{1!} \cdot f'(0) + \frac{x^2}{2!} \cdot f''(0) + \frac{x^3}{3!} \cdot f'''(0) + \dots \quad [4.5]$$

Newton Method

The Newton method is an iterative method to find a better root approximation of the given function. The method is based on the second order Taylor approximation and it converges quadratically to the solution, but only if the first guess is close to the real root. This method can be easily illustrated graphically, see Figure 4.2.

Let assume x_0 as a first guess, then the next approximation x_1 is set to be the intersection of the x -axis with the tangent of the graph in the point x_0 .

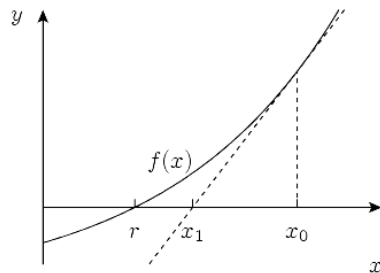


Figure 4.0-2 Solution for Newton Method

The SQP uses a generalization of the methods presented above, and uses a quadratic equation to solve the problem. For every x_k solution found, a quadratic equation is solved in order to find a direction in which the previous solution should go, d_x . In order to compare a new solution with the previous one, a merit function is created.

To answer the question: is x_{k+1} better than x_k , the following inequality should be solved:

$$\emptyset(x_{k+1}) < \emptyset(x_k) \quad [4.6]$$

Where \emptyset is the merit function previously mentioned. If the inequality from Equation 4.6 is satisfied, then x_{k+1} is considered the new solution. Then, a quadratic equation is solved again, in order to find a new direction $d_{x_{k+1}}$, and so on and so forth.

5. Aspen HYSYS Hyprotech SQP Optimizer

In order to achieve the scope of the project defined in the beginning of the report, the optimizer available in Aspen HYSYS is used. The optimizer can work with four different data models: the original model, Hyprotech SQP, MDC Optim and Selection Optimization. The objective of this project is to analyze the Hyprotech SQP model and report on its performance for the DMR process. A detailed description on the Hyprotech SQP optimizer's configuration and its results are presented in this chapter.

5.1 Hyprotech SQP Optimizer Configuration

In order to set up the SQP optimizer, a derivative utility needs to be configured. This utility represents a cluster of the main elements needed for the optimization problem: the variables, constraints and the objective function.

Variables

The elements that are subject to optimization are named variables. Examples of such variables, for the DMR process are: MRs composition and flow rate, pressure levels, temperature levels and pressure ratios in the compressors. The variables are given an initial value, which will be manipulated in order to minimize or maximize the objective function. The lower and upper limits for each variable is also provided in this step.

Figure 5.1 shows a screenshot from the Aspen HYSYS 8.6 simulator, with the variables selected for this project.

Variables	Optimize Flag	Minimum	Current Value	Maximum	Range	Global Min.	Global Max.	Pert. Factor
ICS-WMR	<input checked="" type="checkbox"/>	0.0000	7.8125	2000.0000	<empty>	<empty>	<empty>	<empty>
ICA-CMR	<input checked="" type="checkbox"/>	0.0000	0.0000	2000.0000	<empty>	<empty>	<empty>	<empty>
IC2-CMR	<input checked="" type="checkbox"/>	0.0000	1.5546	2000.0000	<empty>	<empty>	<empty>	<empty>
ICS-CMR	<input checked="" type="checkbox"/>	0.0000	0.0000	2000.0000	<empty>	<empty>	<empty>	<empty>
IC4-WMR	<input type="checkbox"/>	0.0000	0.0000	0.0000	<empty>	<empty>	<empty>	<empty>
IC1-WMR	<input checked="" type="checkbox"/>	4000.0000	5036.5476	6000.0000	<empty>	<empty>	<empty>	<empty>
IC2-WMR	<input checked="" type="checkbox"/>	24000.0000	23654.1312	27000.0000	<empty>	<empty>	<empty>	<empty>
IC3-WMR	<input checked="" type="checkbox"/>	2000.0000	3074.9068	4000.0000	<empty>	<empty>	<empty>	<empty>
IC4-WMR	<input checked="" type="checkbox"/>	1000.0000	1942.7893	3000.0000	<empty>	<empty>	<empty>	<empty>
IC4-WMR	<input checked="" type="checkbox"/>	1000.0000	1777.0860	3000.0000	<empty>	<empty>	<empty>	<empty>
IC2-CMR	<input checked="" type="checkbox"/>	4000.0000	4411.1710	6000.0000	<empty>	<empty>	<empty>	<empty>
IC1-CMR	<input checked="" type="checkbox"/>	11000.0000	12041.1611	13000.0000	<empty>	<empty>	<empty>	<empty>
IC2-CMR	<input checked="" type="checkbox"/>	12500.0000	13355.7869	15000.0000	<empty>	<empty>	<empty>	<empty>
IC3-CMR	<input checked="" type="checkbox"/>	500.0000	1222.9381	3000.0000	<empty>	<empty>	<empty>	<empty>
V1dp	<input checked="" type="checkbox"/>	25.0000	37.9492	40.0000	<empty>	<empty>	<empty>	<empty>
V2dp	<input checked="" type="checkbox"/>	30.0000	49.6974	50.0000	<empty>	<empty>	<empty>	<empty>

Figure 5.0-1 Variables Setup for the Derivative Utility Tab in HYSYS

Constraints

An important element of the constraint optimization problem is represented by the constraints. These are specifications of the process that should be met, when optimizing the process. The values for the constraints are given in the beginning and are not to be changed during optimization. The scale for each constraint added in the derivative utility tab should be specified. The value then of the constraint should be found in the feasible region which is given by the Equation 5.1 (AspenTech, 2011):

$$(minimum - scale) \leq current\ value \leq (maximum + scale) \quad [5.1]$$

The scale is used in order to determine the accuracy of the constraint specified for the optimization.

Figure 5.2 shows a screenshot of the constraints used in the optimization of the DMR process. The current values are taken straight from the process flow sheet and are subject to change once the optimizer runs.

Name	Use Flag	Minimum	Current Value	Maximum	Scale	Min. Chi ² File
LNG2	<input checked="" type="checkbox"/>	2.9000	2.9621	3.2000	0.1000	
LNG3	<input checked="" type="checkbox"/>	2.9000	2.9090	3.2000	0.1000	
SUPERHEAT2	<input checked="" type="checkbox"/>	4.9000	1.1215	5.1000	0.1000	
LNG1	<input checked="" type="checkbox"/>	2.9000	2.9682	3.2000	0.1000	
SUPERHEAT1	<input checked="" type="checkbox"/>	4.9000	16.0468	5.1000	0.1000	

Figure 5.0-2 Constraints Setup for the Derivative Utility Tab in HYSYS

Objective Function

The objective function is represented by a parameter or a function that needs to be minimized or maximized. In this project, the objective function is represented by the specific power consumption of the liquefaction process. The objective function is the ratio between the sum of all compressors work in the process and the flow rate of the LNG obtained.

Figure 5.3 shows a screenshot from the objective value that was used for the optimization of the DMR process. Since the price term has a positive value, it means that a minimization

optimization problem was created. The total consumption power of the compressors has been calculated in a separate spreadsheet and added to the derivative utility tab.

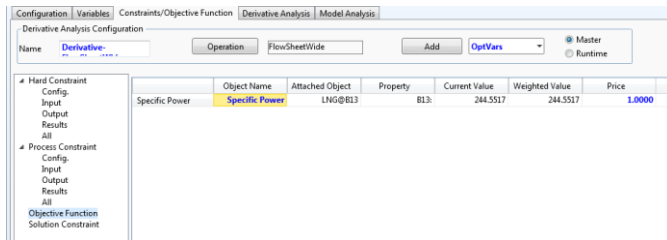


Figure 5.0-3 Objective Function Setup for the Derivative Utility in Aspen HYSYS

5.2 Hyprotech SQP Optimizer Setup

Once the derivative utility is configured, the optimizer can be set up to run the optimization. Figure 5.4 shows a screenshot from the Hyprotech SQP optimizer setup for the DMR process.

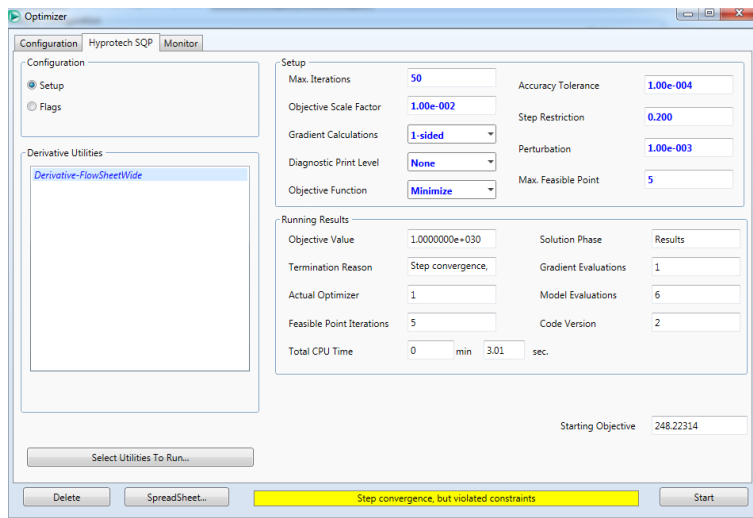


Figure 5.0-4 Aspen HYSYS Optimizer Setup

Setup Section

There are nine parameters that can be manipulated in this section, in order to find the best solution for the optimization problem presented. These parameters are as follows (AspenTech, 2011):

1. *Max. Iterations* - represents the maximum number of the iterations the program will go through in one run. A large number of iterations are required for simulations involving significant noise.
2. *Objective Scale Factor* - this factor is used for scaling the objective function and its gradients. The value of the objective function is multiplied by this factor, in order to get a feasible search when performing an optimization search
3. *Gradient Calculations* - if two-sided gradients are selected, it will take a longer time to arrive at a feasible solution as the process uses twice as many functions to solve the problem. Although it requires longer processing time, the accuracy of the process is higher.
4. *Diagnostic Print Level* - here, None, Partial_1, Partial_2, Partial_3, Full or Excessive can be selected in order to specify the amount of information to be included in the optimizer diagnostic file
5. *Objective Function* - the minimize or maximize functions can be chosen. The SQP optimizer works per default as a minimization problem.
6. *Accuracy Tolerance* - represents the accuracy tolerance for convergence.
7. *Step Restriction* - in order to impose larger restrictions, this parameter is set to lower values.
8. *Perturbation* - smaller values give faster gradient calculations, influencing negatively the accuracy of the gradient if significant noise is present in the simulation
9. *Max. Feasible Point* - specifies the maximum number of iterations for the Hyprotech SQP optimizer. When the maximum number of iterations is reached, the optimizer will end the search and show a message of Step Convergence, meaning that the accuracy defined in the first steps cannot be achieved.

Running Results Section

After running the optimizer, the results are shown in the same screen, under the Running Results section. The most important parameters that need to be analyzed in this section are (AspenTech, 2011):

1. Objective Value - this represents the value of the objective function, which can be compared against the starting objective value at all times during an optimization search. The starting objective value is found on the right down corner of the Optimizer Setup tab, as it can be seen in Figure 5.4.

2. Termination Reason - there are five termination reasons for why an optimization search stops:

OK- it means that a solution has been reached by the program within the boundaries of the constraints.

Step convergence - a step collapse below the step tolerance occurred during the optimization.

Cost convergence - the objective function value for two successive iterations resulted in a difference less than the accuracy tolerance.

Unbounded - the program could not reach a feasible solution within the boundaries given for the variables in the derivative utility function.

Impossible - the program is not able to run under the conditions given.

3. Total CPU Time - represents the time one optimization search needs in order to reach a termination reason.

6 Optimization of DMR Process Alternatives

Chapter six presents the optimization process of the four DMR alternatives that were modeled in the commercial simulator Aspen HYSYS using the information from the patents available. The optimization was done using the Hyprotech SQP optimizer.

6.1 Design Basis

In order to be able to compare the results of the optimization for the chosen alternatives, a design basis has been established for all four models.

The following assumption were considered for the modeling of the DMR alternatives in the commercial simulator Aspen HYSYS (Manescu, 2015):

- *Removal of heavier components from the natural gas stream was outside the scope of the project;*
- *Utility availability was outside the scope of the project;*
- *The pressure drop in all heat exchanger was neglected;*
- *Pressure drop in pipes was neglected;*
- *The air temperature was not relevant;*
- *The heat leak from ambient was negligible.*
- *Flash gas recovery and compression was not part of the scope of the project*

Natural Gas Conditions

The inlet conditions of the natural gas were kept constants for all four models. Table 6.1 presents the values for the inlet conditions as well as the composition of the natural gas stream.

Table 6.0-1 Natural Gas Inlet Conditions

Component/Parameter	Value	Units of Measure
Methane	0.9159	mole fraction
Ethane	0.0493	mole fraction
Propane	0.0171	mole fraction
i-Butane	0.0035	mole fraction
n-Butane	0.0040	mole fraction
i-Pentane	0.0001	mole fraction
Nitrogen	0.0101	mole fraction
Pressure	60	bar
Temperature	22	°C
Flow rate	variable	kmol/h
Vapor Fraction	1	-

LNG Conditions

The outlet conditions for the natural gas stream, were set from the beginning of the project and met by the four models in Aspen HYSYS. Table 6.2 presents the values for the conditions of the LNG stream.

Table 6.0-2 LNG Conditions

Parameter	Value	Unit of Measure
Pressure	1.4	bar
Temperature	-157.6	°C
Higher Heating Value	40.08	MJ/Sm^3
Production	3	MTPA
Liquid Fraction	1	-

Mixed Refrigerants Conditions

The inlet conditions for the mixed refrigerants, as well as their temperature and pressure levels, have been used based on individual patents for each process. These parameters are different for each process, and their values will be presented later in this chapter.

Heat Exchanger Design

Two important parameters were considered in the design of the cryogenic heat exchangers: the minimum approach temperature and the superheating value of the refrigerant stream at the outlet of the cryogenic exchanger. The minimum approach temperature has been chosen as low as possible in order to achieve a higher thermodynamic efficiency, however, a lower limit was established in order to have a reasonable heat transfer area for the heat exchangers. The superheating value of the refrigerant stream leaving the cryogenic exchanger was also set in the beginning of the project, in order to protect the compressor from a potential damage that would result if the refrigerant would condense. Table 6.3 presents the values for those two parameters that were set at the beginning of the Aspen HYSYS modeling for all four DMR alternatives.

Table 6.0-3 Cryogenic Heat Exchangers Conditions

Parameter	Value	Units of Measure
Minimum Approach Temperature	3	K
Superheating	5	K

Coolers and intercoolers are used to cool the refrigerant streams to 20°C, before re-entering the liquefaction cycle. As a cooling agent, sea water is considered to be economical since the project focuses on the potential use of the DMR process on a floating platform. However, sea water is very corrosive if used directly in the process, so a secondary water stream is considered to be used as a cooling agent in the liquefaction process. This secondary water stream exchanges heat with the sea water before it enters the liquefaction process where it will cool the refrigerant streams to 20°C.

Compressors and Pumps Design

Compressors and pumps are needed in the process to increase the refrigerants pressure to the initial values before re-entering the liquefaction process. Table 6.4 presents the values chosen for the efficiencies of both compressors and pumps for all four DMR HYSYS models.

Table 6.0-4 Compressor and Pump Efficiencies

Efficiency, %	Compressor	Pump
Polytropic	78	-
Adiabatic	-	75

Plant Availability

The LNG plant was considered to be working 330 days per year, 24 hours per day, leading to a number of 7920 working hours per year.

Equation of State

Peng-Robinson (PR) equation of state (EoS) was used in all four DMR models in Aspen Hysys. This equation was chosen based on the components present in the natural gas and mixed refrigerants compositions. Most of the previous work done in this area used the same equation of state, although some also used, with good results, the SRK equation. The PR equation of state is used when the water component is not present in the streams analyzed, and when lighter alkanes are present (AspenTech, 2011).

6.2 Optimization Problem Formulation

The optimization problem can be divided into three important steps:

1. Define the objective function for the optimization problem.
2. Choose the constraints that need to be met when running the optimizer;
3. Choose the variables that can be optimized.

Mathematically, the optimization problem can be formulated as per Equation 4.1 from Chapter 4, where all terms were explained:

$$\min_{x \in R^n} f(x) \quad \text{subject to} \quad \begin{cases} c_i(x) = 0, i \in \epsilon, \\ c_i(x) \geq 0, i \in \tau. \end{cases} \quad [4.1]$$

In the first step, the objective function is defined to be the specific power consumption of the DMR process. The work for the pump is also included in the objective function. The scope of

the optimization is to minimize the specific power consumption of the process, so step one can be formulated mathematically as per Equation 6.1:

$$\min_{x \in \mathbb{R}^n} \frac{W_{net}(x)}{m_{LNG}} \quad [6.1]$$

Where, $W_{net}(x)$ represents the compressors power of the DMR process, in kW and m_{LNG} the flow rate of the final LNG stream, in kg/h .

In the second step, the constraints are defined to be the minimum temperature approach in the cryogenic heat exchangers and the superheating of the refrigerant stream that would enter the compression stage. Mathematically, the inequality constraints chosen can be written as per Equations 6.2 and 6.3:

$$dT_i(x) \geq 3 \quad [6.2]$$

$$\Delta T_{superheat_i}(x) \geq 5 \quad [6.3]$$

Where $dT_i(x)$ represents the minimum temperature approach for each cryogenic heat exchanger and $\Delta T_{superheat_i}(x)$ represents the superheating value of the refrigerant stream.

$\Delta T_{superheat_i}(x)$ can be calculated as per Equation 6.4, where $T_{MR\ stream\ dew\ point_i}(x)$ represents the dew point temperature for a specific MR stream, while $T_{MR\ stream_i}(x)$ represents the temperature of the same stream leaving the cryogenic heat exchanger.

$$\Delta T_{superheat_i}(x) = T_{MR\ stream_i}(x) - T_{MR\ stream\ dew\ point_i}(x) \quad [6.4]$$

The DMR process models use between three and six different LNG heat exchangers, so i would vary from three to six. Hence, the total number of constraints for one DMR alternative will be between 6 and 12.

In the third step, the variables that are needed to solve the optimization problem are chosen. The number of variables available for the DMR process that could be optimized are presented in Table 6.5.

Table 6.0-5 Variables Used in Optimization

Variables	Number of variables
MR1 component flow rates	7
MR2 component flow rates	7
MR1 and MR2 inlet temperatures	2
MR1 and MR2 inlet pressures	2
Temperature levels in LNG exchangers	3-4
Pressure levels (depending on the number of throttling valves in the process)	2-5
Pressure ratios	5-6
Total decision variables	28-33

In order to reduce the number of variables that need to be optimized, heuristic rules were introduced. The intermediate pressures for different compressors were calculated using the geometrical mean formula, presented in Equation 6.5. The pressure ratios for the same compressors were calculated as per Equation 6.6.

$$p_{intermediate} = \sqrt{p_{in} \cdot p_{out}} \quad [6.5]$$

Where,

p_{in} is the inlet pressure in the first compressor, in bar;

p_{out} is the outlet pressure of the last compressor, in bar;

$p_{intermediate}$ is the intermediate pressure between the first and the last compressor, in bar.

$$\pi = \frac{p_{in1}}{p_{in2}} \quad [6.6]$$

Where,

π is the pressure ratio between the inlet pressure in the first compressor and the inlet pressure in the second compressor, as per Fig. 6.1. The outlet pressure of the first compressor will be equal with the inlet pressure to the second compressor.

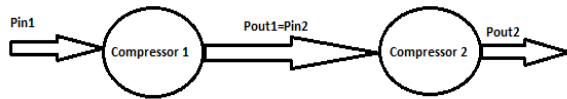


Figure 6.0-1 Compressors Configuration

The inlet temperature of the two mixed refrigerants, as well as the temperature levels in the LNG heat exchangers were kept constant.

After applying these heuristic rules, the total number of variables that were subject to optimization was reduced from 29-33 to 18-22, depending on the configuration of each DMR process alternative.

To sum up, the optimization problem of the DMR process is characterized by:

$$\left\{ \begin{array}{l} \text{one objective function;} \\ 6 - 12 \text{ inequality constraints;} \\ 18 - 22 \text{ variables.} \end{array} \right.$$

Optimization Strategy

One challenging step in setting up the variables in the derivative utility of the simulator, was to determine their starting point and boundaries. As a starting point, the values from a previous work were selected in the first iteration. The boundaries were tight in the beginning, and based on the trend of the results obtained when running the optimizer. They were lowered or increased for every iteration.

Two different optimization strategies were implied in this project:

I: The first strategy implies running the optimizer with tight bounds first and then increasing or decreasing the bounds based on the optimizer results. The new solution found is going to be the starting point for a new iteration. For example, if a variable is at the lower bound in the previous solution, then we will decrease its value and run the optimizer again. However, this approach has a strong disadvantage, because the solution given is a local optimum and the risk of being trapped in this region without being able to find a better local solution is high. In order to reduce this risk, starting points were changed randomly, going further from the initial local region.

II: The second strategy implies going in steps. This means keeping constant some of the variables in the first steps, and optimizing the others and then fixing the optimized variables

while varying the remaining ones. However, this step has also a disadvantage, since variables are quite related between them, and keeping one constant and varying another may influence their values. For example, if the composition of the mixed refrigerants is kept constant, and the pressure levels are allowed to vary, an optimum solution will be found for that specific composition. However, when the composition is allowed to vary, and the pressure levels are kept constant, then the optimizer is somehow restricted to a specific solution which might not be the optimal one.

Both strategies have disadvantages, however, since the scope of the project is to test the optimizer, both options were tested simultaneously in order to get a wider overview on the performance of the Hyprotech SQP optimizer in Aspen HYSYS.

Optimizer Setup

The default values for the setup parameters were changed in order to obtain a minimum value for the objective function. Since the objective of the project was to test the performance of the optimizer, the values for different parameters were varied and the results were considered.

Figure 6.2 presents the default values for the main parameters in the Hyprotech SQP optimizer that were changed during optimization.

Parameter	Value
Max. Iterations	50
Accuracy Tolerance	1.00e-004
Objective Scale Factor	1.00e-002
Step Restriction	0.200
Gradient Calculations	1-sided
Perturbation	1.00e-003
Diagnostic Print Level	None
Max. Feasible Point	5
Objective Function	Minimize

Figure 6.0-2 Optimizer Setup Parameters

The minimization of the objective function is more important than the time to converge, hence, the gradient calculations were chosen to always be 2-sided. The objective function is set to minimize, and it will not be changed during optimization. The diagnostic print level is also out of the scope for this optimization problem. The parameters that were varied when running the optimizer, as well as their ranges, are presented in Table 6.6.

Table 6.0-6 Optimizer Setup Parameters Ranges

Optimizer Parameter	Ranges
Max. Iterations	50-2000
Objective Scale Factor	10^{-8} - 10^0
Accuracy Tolerance	10^{-8} - 10^0
Step Restriction	0.02-0.5
Perturbation	10^{-8} - 10^0
Max. Feasible Point	5-100

6.3 APCI DMR Process Optimization

The optimization of the APCI DMR process started with the configuration of the derivative utility. This is a function in Aspen HYSYS where the variables, constraints and the objective function are defined, and it is needed in order for the optimizer to run. The process flow sheet for the APCI model is found in Appendix A.

Constraints and Objective Function

The objective function has already been defined as being the specific power consumption of the process. The constraints for this alternative are presented in Table 6.7.

Table 6.0-7 APCI DMR Constraints Values

Constraint/Equipment	Minimum Approach	Superheating
LNG 1	3 K	5 K
LNG 2	3 K	5 K
LNG 3	3 K	-

A superheating constraint for the third cryogenic heat exchanger (LNG 3) was not needed, since the stream leaving the exchanger is mixed with another stream before entering the LNG 2 exchanger. The superheating constraint is added to the system to avoid liquid entrance in the compression stage. The APCI process will have then only 5 constraints.

Variables

The number of variables that were used in the optimization problem, are presented in Table 6.8. The total number of variables to work with is 18.

Table 6.0-8 Number of Variables for APCI DMR Process

Variables	Number of variables
MR1 component flow rates	7
MR2 component flow rates	7
MR1 and MR2 inlet pressures	2
Pressure levels	2
Total decision variables	18

Optimization Strategy

The optimization strategy was divided into three steps as follows:

1. Run the optimizer with the starting values for the variables presented in Table 6.9, until reaching an optimal local solution. Change the starting points randomly in order to get out of the "trapped region", and run the optimizer until a feasible optimal local solution is found. The optimizer setup parameters use the default values, except the gradient calculations which are 2-sided.

Table 6.0-9 APCI Variables Starting Points

Component	Units Of Measure	Values MR1	Values MR2
Molar Flow N ₂	kmole/h	0	4,412
Molar Flow C ₁	kmole/h	5,040	12,037
Molar Flow C ₂	kmole/h	25,660	13,356
Molar Flow C ₃	kmole/h	3,079	1,225
Molar Flow iC ₄	kmole/h	1,946	0
Molar Flow nC ₄	kmole/h	1,777	0
Molar Flow iC ₅	kmole/h	0	0
Inlet Pressure	bar	48	55.5
Pressure Level 1	bar	10	-
Pressure Level 2	bar	-	5.8

The boundaries for each variable were set to ± 2000 kmole/h from the initial values for the components flow rates, ± 15 bar for the inlet pressures, and $\pm 2-5$ bar for the pressure levels for both mixed refrigerants. As the optimizer was running and giving acceptable solutions, those ranges were changed accordingly, as presented in step 1. The program was not able to give a solution when running all 18 variables, so the inlet pressure of the two mixed refrigerant was kept constant for the first part of the optimization.

The main challenge was to adjust the boundaries for the variables, so that the optimizer would find a feasible solution. In order to have a better understanding on how the presence and the amount of one component influences the liquefaction process, two diagrams were used. The first one is the heating and cooling composite curves diagram for each LNG heat exchanger present in the process. Every time the optimizer was running and giving a solution based on certain boundaries, the shape of the composite curves diagram was checked. In Figure 6.3, the composite curves for the three heat exchangers at the optimization starting points conditions is presented. Figure 6.4 shows the shape of the composite curves for the same LNG exchangers, after running the optimizer and getting a message of "Step convergence, but violated constraints". This is a random solution found for the APCI process, but it is not the best one.

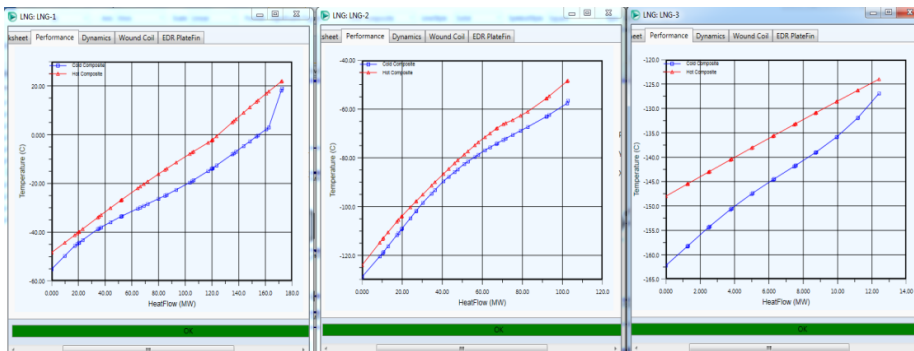


Figure 6.0-3 Initial Composite Curves Diagrams for APCI Model

As it can be seen from the composite curves in Figure 6.3, there is room for heat transfer improvement, especially in the last heat exchanger. The specific power consumption for this alternative is 248.22 kWh/ton of LNG.

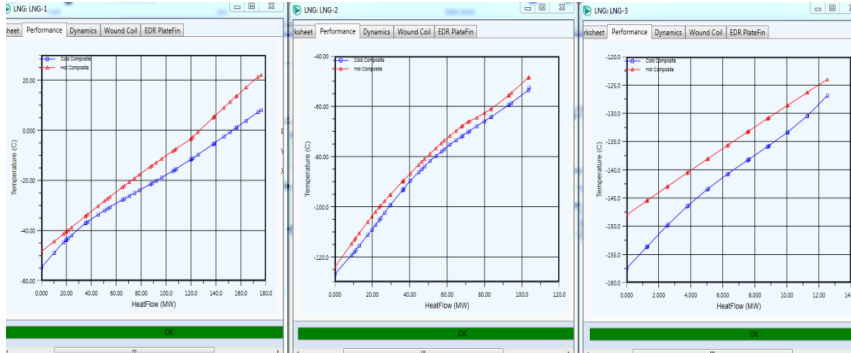


Figure 6.0-4 Composite Curves Diagrams Alternative Solution for APCI Model

In Figure 6.4, the composite curves for the three LNG heat exchangers are somewhat different, especially for the first and the third LNG heat exchanger. Also, the specific power consumption was minimized by 8.75%, giving a value of 226.5 kWh/ton of LNG. Just by looking at composite curves, the following observations were made:

- at the cold end of the first LNG heat exchanger, the heating and cooling curves are closer to each other, which suggests a more efficient heat transfer. This implies that the cold streams contain more heavier components than the initial solution. At the hot end, the curves are further away from each other, suggesting that the cold streams are too cold, so by adding more heavier components, the heat transfer would be more efficient (the temperature difference between the streams will decrease).

- in the third LNG heat exchanger, the curves are getting closer, however, more work can be done in this area as well.

In Table 6.10, the initial values of the variables chosen are compared against the values obtained by this random optimized version.

Table 6.0-10 Comparison of the Initial Variables Values and a Random Solution

Component	Units Of Measure	Values MR1	Optimized Values for MR1	Values MR2	Optimized Values for MR2
Molar Flow N ₂	kmole/h	0	0	4,412	3,868
Molar Flow C ₁	kmole/h	5,040	5,834	12,037	13,647
Molar Flow C ₂	kmole/h	25,660	25,010	13,356	12,501
Molar Flow C ₃	kmole/h	3,079	4,374	1,225	1,378
Molar Flow iC ₄	kmole/h	1,946	2,411	0	0
Molar Flow nC ₄	kmole/h	1,777	1,974	0	0
Molar Flow iC ₅	kmole/h	0	0	0	0
Inlet Pressure	bar	48	48	55.5	55.5
Pressure Level 1	bar	10	10.76	-	-
Pressure Level 2	bar	-	-	5.8	6.93

The values that were increased are marked with yellow, while the values that were decreased are marked with green. Overall, the flow rates for both mixed refrigerants have increased, however, the power consumption of the compressors has decreased.

A second diagram was plotted in order to observe the impact the composition and the pressure have on the minimization of the compressors work. Figures 6.5 and 6.6 show how the molar composition of each component has changed for both MR1 and MR2, versus the specific power consumption. During these iterations, the inlet pressures as well as the pressure levels were varied, however, the optimizer would not be able to converge with so many variables, so the inlet pressure was kept constant in this step.

The reason for plotting the molar fraction versus the specific power consumption, was to notice a trend for the variation of different values for the MRs flow rates. This was used when trying to get out of the "trapped region" where only one local optimal solution was given.

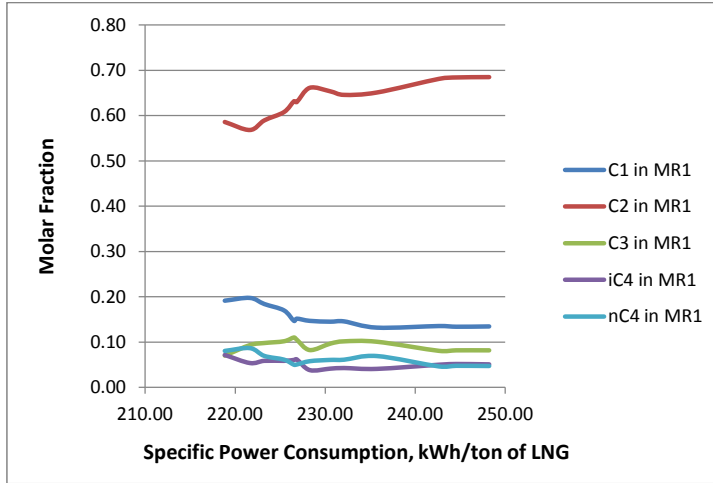


Figure 6.0-5 MR1 Composition Vs. Specific Power Consumption for APCI Model

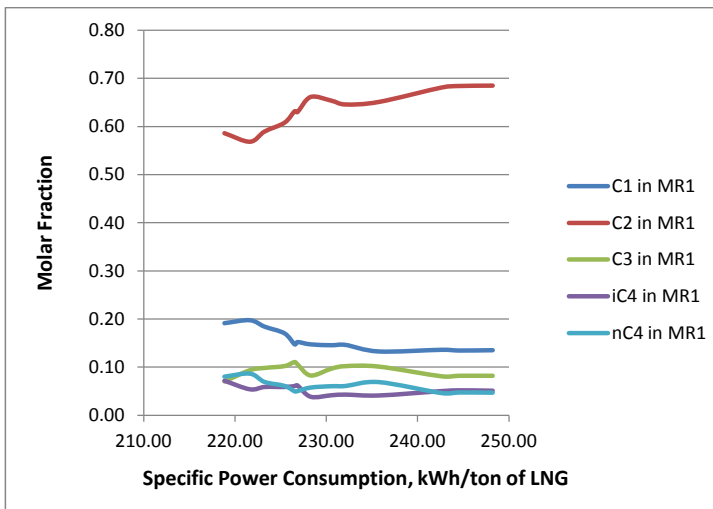


Figure 6.0-6 MR2 Composition Vs. Specific Power Consumption for APCI Model

The final optimized variables values, are presented in Table 6.11, against the initial values. The objective function for this solution is 218.5 kWh/ton of LNG.

Table 6.0-11 Optimized Variables Vs. Initial Values for APCI Model

Component	Units Of Measure	Values MR1	Optimized Values for MR1	Values MR2	Optimized Values for MR2
Molar Flow N2	kmole/h	0	0	4,412	3,842
Molar Flow C1	kmole/h	5,040	7,716	12,037	13,813
Molar Flow C2	kmole/h	25,660	23,615	13,356	12,347
Molar Flow C3	kmole/h	3,079	2,834	1,225	1,373
Molar Flow iC4	kmole/h	1,946	2,897	0	0
Molar Flow nC4	kmole/h	1,777	3,240	0	0
Molar Flow iC5	kmole/h	0	0	0	0
Inlet Pressure	bar	48	48	55.5	55.5
Pressure Level 1	bar	10	12.2	-	-
Pressure Level 2	bar	-	-	5.8	7.23

The constraints are however, not met by the optimizer. Their values are presented in Figure 6.7.

	Use Flag	Minimum	Current Value	Maximum	Scale	Min. Chi^2 Flz
LNG1min	<input checked="" type="checkbox"/>	3.0000	2.9113	<empty>	0.0100	<input type="checkbox"/>
LNG2min	<input checked="" type="checkbox"/>	3.0000	2.3638	<empty>	0.0100	<input type="checkbox"/>
LNG3min	<input checked="" type="checkbox"/>	3.0000	2.9154	<empty>	0.0100	<input type="checkbox"/>
LNG1superheat	<input checked="" type="checkbox"/>	5.0000	1.6712	<empty>	0.0100	<input type="checkbox"/>
LNG2superheat	<input checked="" type="checkbox"/>	5.0000	2.2306	<empty>	0.0100	<input type="checkbox"/>

Figure 6.0-7 Constraints in the Optimizer for the APCI Model Optimized Solution

Throughout the project, it was noticed that the constraints are strongly related to the variables optimized. The superheating of the stream leaving the LNG heat exchanger and entering the compression stage is related to the composition of the mixed refrigerants. This can be

explained by the fact that different components have different dew points, which of course, will influence the new dew point of a specific stream. The minimum approach temperature, however, is strongly related to the pressure level for each liquefaction stage. The minimum approach temperature in the LNG 1 heat exchanger is influenced by the pressure level in the pre-cooling stage, while the minimum approach in both LNG 2 and LNG 3 heat exchangers is related to the pressure level in the liquefaction stage. This can be explained by the fact that different components vaporize at different pressures, so if the pressure level increased or decreases, it will influence also the driving forces in the cryogenic heat exchangers.

2. Run the optimizer with the optimal solution found in step 1 as starting point, and test the optimizer performance by varying the setup parameters from Table 6.6. The inlet pressures for both mixed refrigerants were varied together with the rest of the variables.

Max. Iterations Variation

The first setup parameter of the optimizer that was varied was the maximum number of iterations. The other setup parameters used the default values, except for the gradient calculations which would always be 2-sided.

The results of the optimizer are presented in Figure 6.8. The orange line indicates that the optimizer gave the termination reason "Step convergence, but violated constraints". It can be noticed that after 500 iterations, the objective function remains constant.

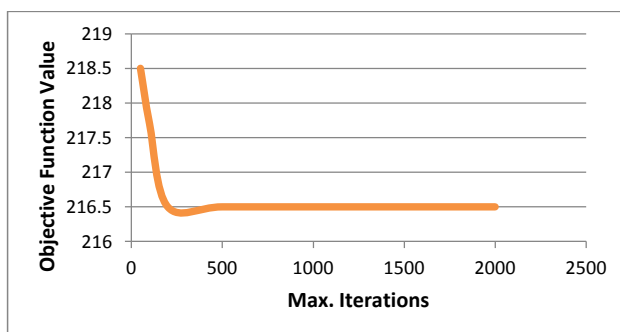


Figure 6.0-8 Maximum Iterations Variation for APCI Model

Objective Scale Factor Variation

The objective scale factor parameter was varied within the range of 10^{-8} - 10^0 . The maximum iterations parameter was kept at a value of 500, since from this value up, the objective function remained constant. All the other parameters used the default settings. By varying the objective scale factor, the objective function value remains constant. The color red in Figure 6.9 indicates the fact that the optimizer was not able to reach a feasible solution.

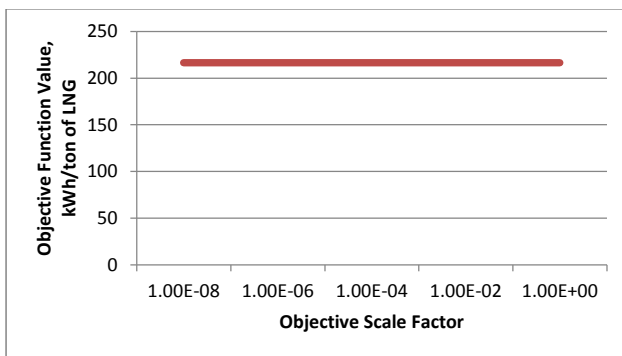


Figure 6.0-9 Objective Scale Factor Variation for APCI Model

Accuracy Tolerance Variation

Next, the accuracy tolerance parameter was varied within the range of 10^{-8} - 10^0 . The objective scale factor was set to 10^{-6} (Eirik,2015). As is can be seen from Figure 6.10, the accuracy tolerance variation does not have any influence on the objective function after the value 10^{-6} .

Comment [I1]:

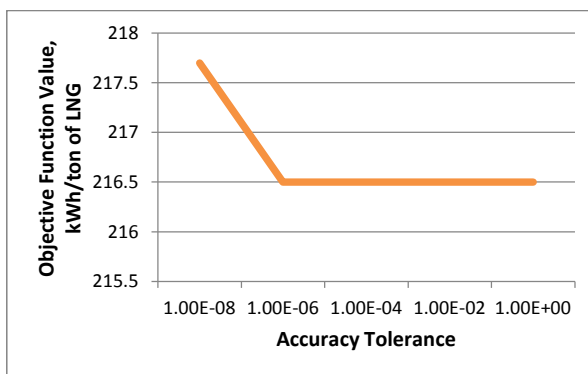


Figure 6.0-10 Accuracy Tolerance Variation for APCI Model

Step Restriction Variation

The step restriction parameter is varied within the range of 0.02-0.5. The accuracy tolerance was set to be 10^{-8} . Figure 6.11 shows the variation of the objective function with the accuracy tolerance. The orange color represents the fact that the optimizer ended the operation giving the "Step convergence, but violated constraints" message.

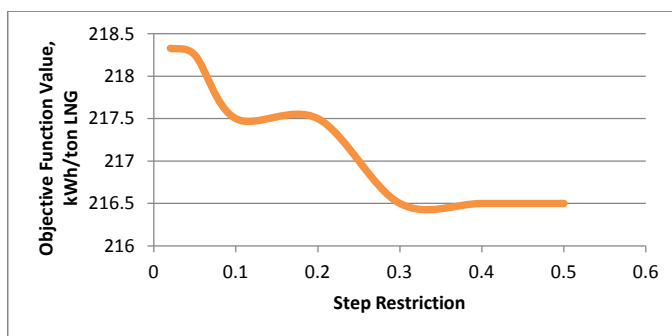


Figure 6.0-11 Step Restriction Variation for APCI Model

Perturbation Variation

Varying the perturbation parameter, the optimizer was not able to perform the optimization, giving the "Stopped" message for all values used, except for the default value, when the "Step convergence, but violated constraints" message showed. The objective function value did not change.

Maximum Feasible Point Variation

When varying the maximum feasible point from 5 to 100, the optimizer was not able to perform the operation. The objective values increased and decreased several times during the optimization itself, however, the operation was not possible to be completed.

3. Compare the results obtained for the objective function against the initial value.

The performance of the optimizer was tested in the first two steps, using different approaches in each step. In the first step, the optimizer ran using the default values as a setup, and the

objective value was able to be reduced from 248.2 to 218.5 kWh/ton of LNG, representing a reduction of 12% from the initial value. In the second step, the variation of the setup parameters of the optimizers did not have a great influence on the objective function. However, the objective function value decreased with 2 kWh/ton LNG, which represents only 0.92% of the optimized value in the first step.

Table 6.12 shows an overview of the variables values for the final optimized version in step two, and the values in the initial APCI model.

Table 6.0-12 Variables Values Comparison for APCI Model

Component	Units Of Measure	Values MR1	Optimized Values for MR1	Values MR2	Optimized Values for MR2
Molar Flow N ₂	kmole/h	0	0	4,412	3,811
Molar Flow C ₁	kmole/h	5,040	7,691	12,037	13,861
Molar Flow C ₂	kmole/h	25,660	23,627	13,356	12,300
Molar Flow C ₃	kmole/h	3,079	2,840	1,225	1,386
Molar Flow iC ₄	kmole/h	1,946	2,887	0	0
Molar Flow nC ₄	kmole/h	1,777	3,204	0	0
Molar Flow iC ₅	kmole/h	0	0	0	0
Inlet Pressure	bar	48	47.9	55.5	55.3
Pressure Level 1	bar	10	12.35	-	-
Pressure Level 2	bar	-	-	5.8	7.3

The constraints values for the final solution are compared against the values from the previous and initial solutions in Table 6.13. As it can be noticed, the optimizer was not able to minimize the objective function without violating the constraints.

Table 6.0-13 Constraints Values Comparison for APCI Model

Constraint	Initial Solution	Optimized Solution Step 1	Optimized Solution Step 2
Min. Approach LNG 1, K	3.0	2.9	2.6
Min. Approach LNG 2, K	3.0	2.4	2.0
Min. Approach LNG 3, K	2.9	2.9	2.9
Superheat LNG 1, K	16	1.7	2.3
Superheat LNG 2, K	1.1	2.2	2.6
Objective Function, kWh/ton of LNG	248.2	218.5	216.5

6.4 Shell DMR Process Optimization

The second alternative that was subject to optimization was the Shell DMR process. The process flow sheet of the HYSYS model can be found in Appendix B.

Constraints and Objective Function

The constraints of the process are presented in Table 6.14. It should be noted that these are inequality constraints, since the optimizer is not able to work accurately with equality constraints. The objective function is the specific power consumption of the process.

Table 6.0-14 Shell DMR Constraints Values

Constraint/Equipment	Minimum Approach	Superheating
LNG 1	3 K	5 K
LNG 2	3 K	5 K
LNG 3	3 K	5 K
LNG 4	3 K	-

The last LNG heat exchanger (LNG 4) does not need a constraint for the superheating value of the cold stream, as it enters LNG 3 before the compression stage, so a constraint on the LNG 3 will suffice to meet the compressors safety. The number of constraints for the Shell process is seven, with two more constraints than the APCI model.

Variables

The variables used in the optimization of the Shell process are the same as for the APCI process, and they are presented in Table 6.15.

Table 6.0-15 Number of Variables for Shell DMR Process

Variables	Number of variables
MR1 component flow rates	7
MR2 component flow rates	7
MR1 and MR2 inlet pressures	2
Pressure levels	3
Total decision variables	19

It can be noted from the table that the Shell model uses 19 variables, instead of 18 as the APCI model did. This is because the Shell process has three pressure levels, two in the pre-cooling stage and one in the liquefaction stage. There is another potential variable that could be optimized in this process, and that is the stream split ratio in the pre-cooling stage, as it can be noticed in Figure 6.12. However, due to the previous bad performance of the optimizer, this variable was not included, and the split ratio was kept constant. After arriving at a satisfying optimal local solution, the optimizer ran only to find the best stream split ratio.

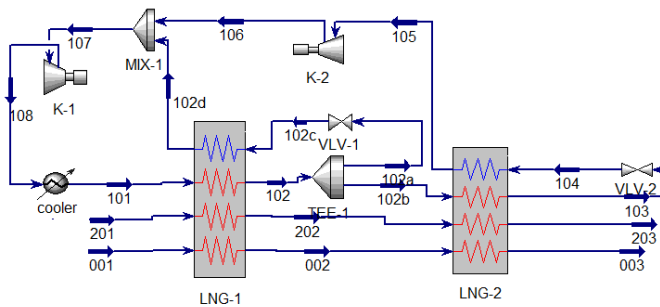


Figure 6.0-12 Pre-cooling Stage for Shell DMR Process

Optimization Strategy

The same steps as for the APCI process optimization were followed:

1. Run the optimizer with the starting values for the variables presented in Table 6.16, until reaching an optimal local solution. The optimizer setup parameters use the default values, except the gradient calculations which are 2-sided.

Table 6.0-16 Variables Starting Points for Shell DMR Process

Component	Units Of Measure	Values MR1	Values MR2
Molar Flow N ₂	kmole/h	0	2,101
Molar Flow C ₁	kmole/h	0	12,547
Molar Flow C ₂	kmole/h	5,886	8,975
Molar Flow C ₃	kmole/h	15,214	6,394
Molar Flow iC ₄	kmole/h	0	0
Molar Flow nC ₄	kmole/h	2,617	0
Molar Flow iC ₅	kmole/h	0	0
Inlet Pressure	bar	18	48.6
Pressure Level 1	bar	7.5	-
Pressure Level 2	bar	2.8	-
Pressure Level 3	bar	-	3

The variables boundaries ranges were set up to be ± 2000 kmole/h for the components flow rates, ± 10 bar for the inlet pressures, and ± 2.5 bar for the pressure levels for both mixed refrigerants. The values are added or subtracted from the initial values.

In order to be able to find the optimal local solution, the same approach as for the APCI alternative was used. The composite curves were checked every time the optimizer ran. The curves behavior when changing the composition of the mixed refrigerants was crucial in understanding how to adjust the boundaries after the first optimizer run. Also, the molar flow of the components was plotted against the specific power consumption of the process, to see how a certain amount of one component influences the objective function. Again, these plots

were used during optimization in order to have an understanding on how to manipulate the boundaries and starting points of the variables used.

Figure 6.13 shows the composite curves for the initial Shell DMR process alternative. The composite curves were plotted for each single LNG heat exchanger in order to notice the impact of the pressure level change on the constraints of the process during optimization. From Figure 6.13 it can be noticed that there is room for optimization in all heat exchangers, with an emphasis on LNG 1, LNG 2 and LNG 4. A good temperature distribution can be observed in LNG 3. This can be explained by the presence of a phase separator for the MR2 stream right before it enters the liquefaction stage, defined by LNG 3. The enthalpy difference of the vapor and liquid streams give a better heat transfer within the LNG heat exchanger.

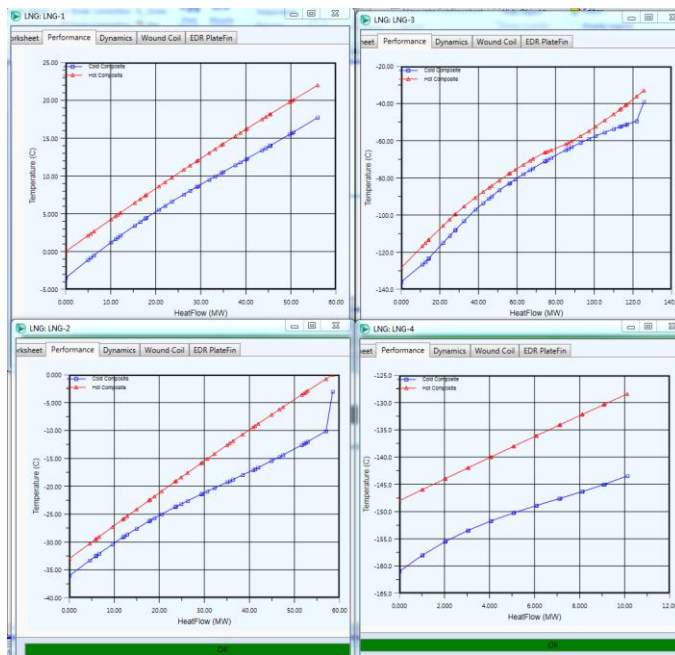


Figure 6.0-13 Initial Composite Curves Diagrams for Shell Model

Figure 6.14 shows the composite curves for the optimal local solution found in this step. This is the solution that was considered for the next step.

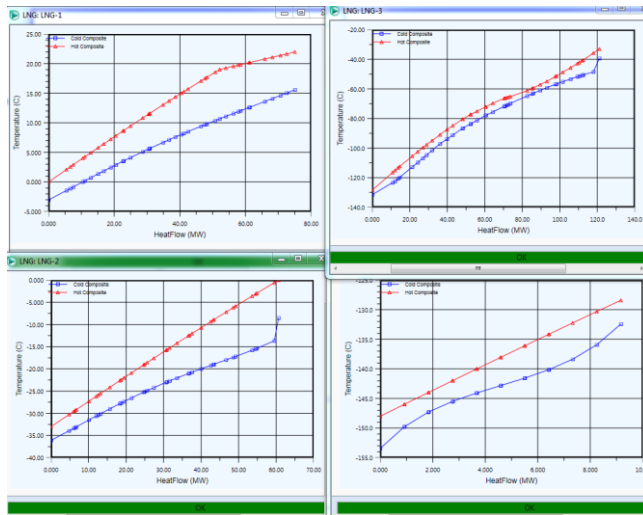


Figure 6.0-14 Composite Curves for the Optimized Solution for Shell Model

From the composite curves diagram for the optimized solution, we can conclude that:

- LNG 1: the shape of the hot composite curve has changed, going "away" from the cold composite curve. This implies that the driving forces within the exchanger are large, and improvement can take place.
- LNG 2: the shapes of the hot and cold composite curves remained the same.
- LNG 3: the composite curves seem to be closer to each other, still meeting the constraints for the driving forces.
- LNG 4: the composite curves came closer to each other, showing a better distribution of the driving forces inside the last heat exchanger.

It can be concluded from the composite curves, that there is plenty of "room" for improvement in the next step of the optimization problem, when the optimizer performance will be challenged.

Figures 6.15 and 6.16 show the variation of the molar flow rate of the components found in the mixed refrigerants, with the specific power consumption, during optimization.

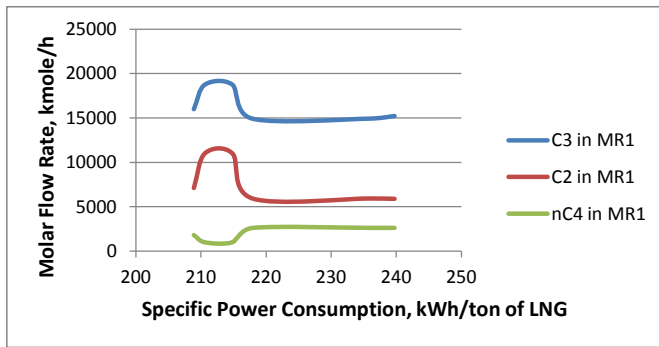


Figure 6.0-15 Molar Flow Variation for MR1 for Shell Model

During optimization, the molar flow rate of the components increased and decreased based on the change in the MRs pressures, and their pressure levels throughout the liquefaction processes.

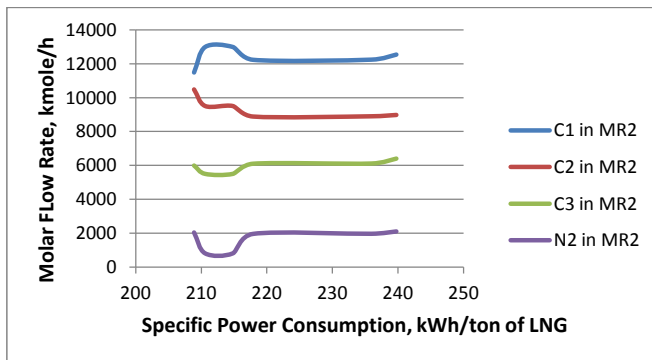


Figure 6.0-16 Molar Flow Variation for MR2 for Shell Model

From these figures it can be noted that several optimal local solution may be found, depending on the other variables and the boundaries used. For example, the amount of N_2 present in MR2 seems to give a lower specific power consumption when it decreases, finding a local optimal solution, however, as the iterations continue, and the starting points are changed, it seems that increasing the flow rate of the N_2 will give an even lower value for the objective function, indicating that a new local solution was found.

In Table 6.17, the values for the optimized solution were compared against the initial values for the Shell DMR process. An overview of the constraints for both solutions is further given in Figure 6.17.

Table 6.0-17 Initial Vs. Optimized Variables Values for Shell Model

Component	Units Of Measure	Values MR1	Optimized Values for MR1	Values MR2	Optimized Values for MR2
Molar Flow N ₂	kmole/h	0	0	2,101	800
Molar Flow C ₁	kmole/h	0	0	12,547	13,000
Molar Flow C ₂	kmole/h	5,886	11,001	8,975	9,500
Molar Flow C ₃	kmole/h	15,214	18,760	6,394	5,500
Molar Flow iC ₄	kmole/h	0	0	0	0
Molar Flow nC ₄	kmole/h	2,617	996	0	0
Molar Flow iC ₅	kmole/h	0	0	0	0
Inlet Pressure	bar	18	16.5	48.6	49
Pressure Level 1	bar	7.5	9.7	-	-
Pressure Level 2	bar	2.8	3.7	-	-
Pressure Level 3	bar	-	-	3	3.4

The values that have decreased are marked with green, while the values that have increased are marked with yellow. The total flow rate of the MR1stream has increased during optimization, while the flow rate of the MR2 stream has decreased. The specific power consumption has decreased from 239.7 kWh/ton of LNG to 214.8 kWh/ton, resulting in 9% efficiency increase.

	Use Flag	Minimum	Current Value	Maximum	Scale	Min. Chi ² Flz
LNG3dT	<input checked="" type="checkbox"/>	2.9000	3.0702	3.5000	0.1000	<input type="checkbox"/>
LNG1dT	<input checked="" type="checkbox"/>	2.9000	3.0235	3.5000	0.1000	<input type="checkbox"/>
LNG2dT	<input checked="" type="checkbox"/>	2.9000	3.0934	3.5000	0.1000	<input type="checkbox"/>
LNG1superheat	<input checked="" type="checkbox"/>	4.9000	-2.8174	<empty>	0.1000	<input type="checkbox"/>
LNG2superheat	<input checked="" type="checkbox"/>	4.9000	2.7455	<empty>	0.1000	<input type="checkbox"/>
LNG3superheat	<input checked="" type="checkbox"/>	4.9000	14.8721	<empty>	0.1000	<input type="checkbox"/>
LNG4dT	<input type="checkbox"/>	<empty>	3.2944	<empty>	<empty>	<input type="checkbox"/>

Figure 6.0-17 Constraints in the Optimizer for Shell Model

The constraints presented in Figure 6.17 are not entirely met by the optimizer. The superheat corresponding to the stream leaving LNG 1 contains 0.04 mole fraction of liquid. However, since the stream is mixed with another stream before going to the compression stage, it does not affect the performance of the HYSYS model. Next step will try to get the optimizer to meet this constraint as well.

2. Run the optimizer with the optimal solution found in step 1 as starting point, and test the optimizer performance by varying the setup parameters from Table 6.6.

Max. Iterations Variation

Figure 6.18 shows the impact the variation of the maximum iterations parameter has on the objective function value. The orange line shows that the optimizer gave the "Step convergence, but violated constraints" message.

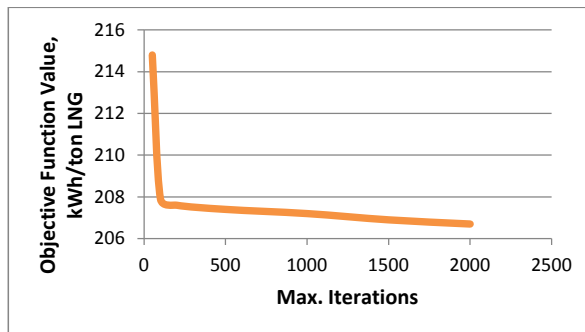


Figure 6.0-18 Maximum Iterations Variation for Shell Model

It can be noticed that the behavior of the optimizer for Shell model is different than the APCI model when varying the maximum number of iterations. Here, the objective function value decreased while increasing the maximum iterations, unlike the APCI model, where after the value of 500, the objective function remained constant. It should be noted that the constraints for the Shell model are more violated.

Objective Scale Factor Variation

When varying the objective scale factor, the maximum iterations parameter was kept at 500, in order to have a fair comparison with the APCI model. The variation of this parameter with the objective function is presented in Figure 6.19.

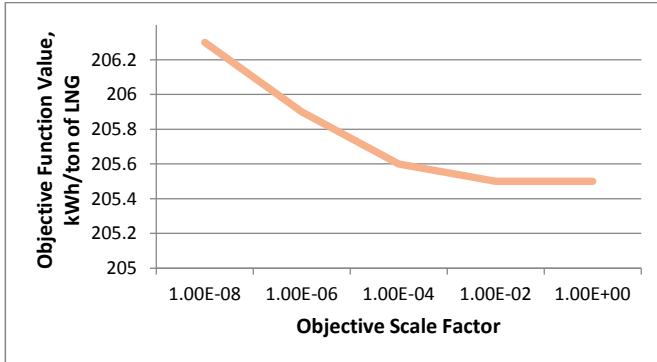


Figure 6.0-19 Objective Scale Factor Variation for Shell Model

From Figure 6.19 it can be observed that the optimizer minimized the objective function until the objective scale factor reached the value of 10^{-4} , receiving the message "Step convergence, but violated constraints". From this value onwards, the optimizer could not arrive to a solution, ending with the message "Stopped".

Accuracy Tolerance Variation

For the variation of the accuracy tolerance parameter, the objective scale factor value was constant at 10^{-4} , while the maximum iterations value was kept constant at 500. Figure 6.20 shows the variation of this parameter with the objective function value.

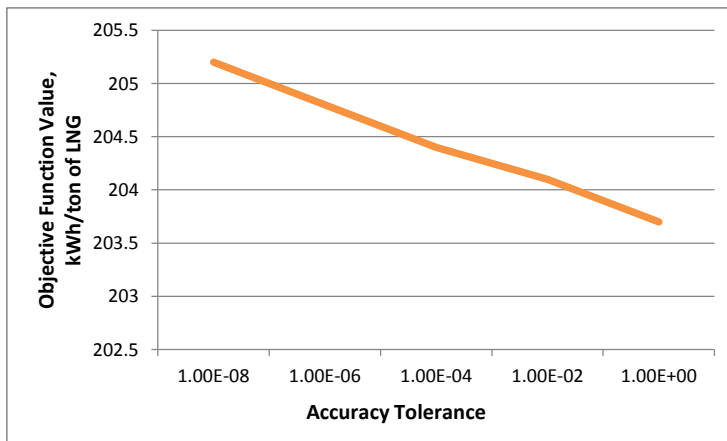


Figure 6.0-20 Accuracy Tolerance Variation for Shell Model

Although the objective function value decreased with the increase of the accuracy tolerance parameter, the constraints were violated more once the accuracy parameter was approaching the value of 1. Therefore, an optimal value for this parameter would be 10^{-8} .

Step Restriction Variation

Figure 6.21 shows the variation of the step restriction factor with the objective function.

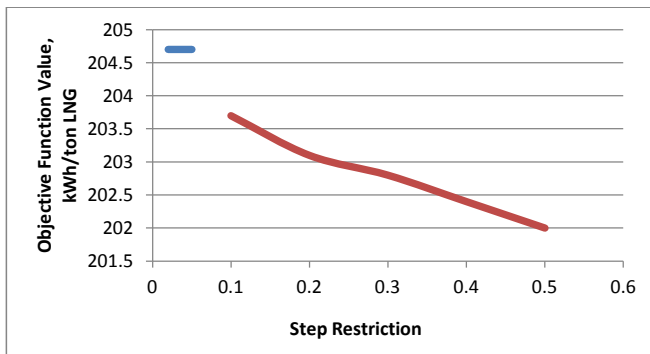


Figure 6.0-21 Step Restriction Variation for Shell Model

The meaning of the blue line is the fact that the optimizer could not arrive to a solution, giving the "Stopped" message. The red line represents the values obtained when the optimizer would arrive at a "Step convergence, but violated constraints" message.

Perturbation Variation

When varying the value of the perturbation parameter, until the parameter reaches 10^{-3} , a "Step convergence, but violated constraints" message is received. However, increasing its value, the optimizer fails, giving the error message "Stopped". Therefore, the optimal value for this parameter is 10^{-3} .

Maximum Feasible Point Variation

When varying this parameter, the optimizer failed to give a solution. Therefore, for further calculations, the maximum feasible point was kept to have the value 5.

3. Compare the results obtained for the objective function against the initial value.

The performance of the optimizer was tested during the first two steps. Although the objective function value decreased from 239.7, the initial value, to 214.7, after the first

optimization step, and to a final value of 200.6 kWh/ton of LNG, in the last step, the constraints were violated each step even more. The constraints violated were related to the second stage of the process, the liquefaction part. Figure 6.22 presents the variation of the two constraints for the liquefaction part for all the iterations from step 2, LNG 3 minimum approach and LNG 4 minimum temperature approach, respectively. The relative error is calculated based on the starting point for step 2, which is 3K for both constraints, and is represented as 0% in the diagram.

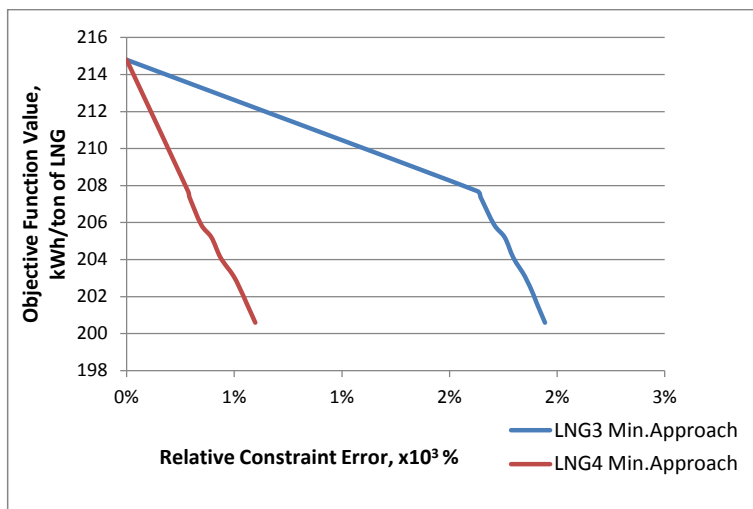


Figure 6.0-22 Relative Constraint Error for Shell Model

However, to have a fair comparison between the solutions, the constraints for the solution found in step 2 were manually changed, and the error in the constraints was reduced. The value for the objective function for this new, manipulated constraints solution, was higher than the solution found in step 1, thus it was not considered.

As a conclusion for the Shell DMR process optimization, the optimizer was not able to perform better when changing the values for the setup parameter. The optimizer worked at its best when default values were used, giving an objective function value of 214.8 kWh/ton of LNG, which represents an efficiency increase of 10.4%.

6.5 Tealarc DMR Process Optimization

The Tealarc process was modeled in Aspen HYSYS and its process flow sheet can be found in Appendix C.

Constraints and Objective Function

The objective function is the minimization of the specific power consumption of the DMR process. The constraints are presented in Table 6.18.

Table 6.0-18 Tealarc DMR Constraints and Objective Function Values

Constraint/Equipment	Minimum Approach	Superheating
LNG 1	3 K	-
LNG 2	3 K	-
LNG 3	3 K	5 K
LNG 4	3 K	5 K
LNG 5	3 K	-
LNG 6	3 K	-
Objective Function	227.9 kWh/ton of LNG	

The streams corresponding to the cryogenic heat exchangers LNG 1, LNG 2, LNG 5 and LNG 6 do not enter directly the compression stage, so the superheating constraint was not selected as a constraint. However, the superheating values for the streams corresponding to these LNG heat exchangers, were monitored throughout the optimization operation, as the streams temperatures should not go below their dew points.

Variables

The variables are presented in Table 6.19. There are four different pressure levels, three in the pre-cooling stage and one in the liquefaction stage of the process, leading to a number of 20 variables.

Table 6.0-19 Number of Variables for Tealarc DMR Model

Variables	Number of variables
MR1 component flow rates	7
MR2 component flow rates	7
MR1 and MR2 inlet pressures	2
Pressure levels	4
Total decision variables	20

Optimization Strategy

The same three steps were conducted for the optimization of the Tealarc process. The same conditions as for APCI and Shell models were implied.

1. Run the optimizer with the starting values for the variables presented in Table 6.20, until reaching an optimal local solution.

Table 6.0-20 Variables Starting Points for Tealarc DMR Model

Component	Units Of Measure	Values MR1	Values MR2
Molar Flow N ₂	kmole/h	0	3,406
Molar Flow C ₁	kmole/h	31	14,629
Molar Flow C ₂	kmole/h	9,927	14,384
Molar Flow C ₃	kmole/h	15,040	352
Molar Flow iC ₄	kmole/h	650	529
Molar Flow nC ₄	kmole/h	0	191
Molar Flow iC ₅	kmole/h	0	0
Inlet Pressure	bar	22	39.95
Pressure Level 1	bar	9.7	-
Pressure Level 2	bar	5.7	-
Pressure Level 3	bar	1.4	-
Pressure Level 4	bar	-	7.2

The variables boundaries ranges were set up to be ± 2000 kmole/h added or subtracted from the initial values of the components flow rates, $\pm 7-15$ bar for the inlet pressures, and $\pm 2-5$ bar for the pressure levels for both mixed refrigerants. These values are used as starting points for the optimization, and are changed later when the composite curves are checked after each iteration.

The Tealarc design is different from the other three DMR alternatives, because of the natural gas stream that enters directly the liquefaction stage of the process, without exchanging heat with the first mixed refrigerant in the pre-cooling stage. It was difficult to get the optimizer to work for this model in particular, since the process was already optimized by the SINTEF Research Group, so a different optimization strategy was employed (Morin et al., 2011). First, the inlet pressures of MRs and their pressure levels were varied in the optimizer, keeping the composition constant for both mixed refrigerants. Then the composition would vary, keeping the pressures and pressure levels constant.

Figure 6.23 gives the variation of the objective function value for different results for the inlet pressures for both mixed refrigerants, when the optimizer is run.

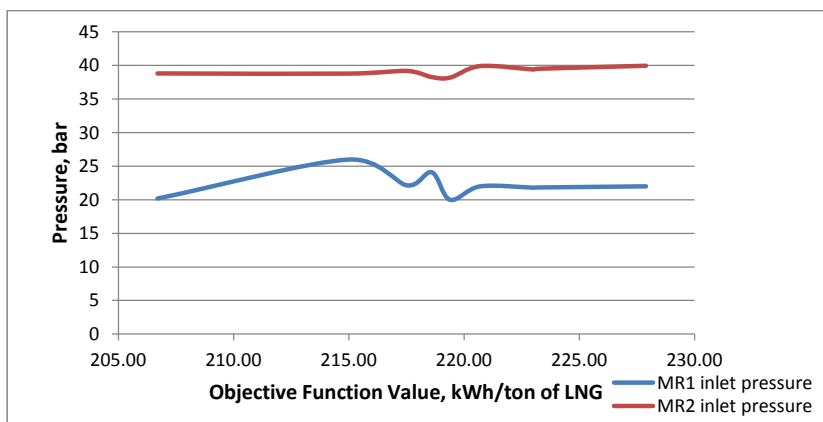


Figure 6.0-23 Pressure Vs. Objective Function for Tealarc Model

The lowest objective function value of 206.7 kWh/ton of LNG, corresponds to a pressure of 20.18 bar for MR1 in the pre-cooling stage, and 38.82 bar for MR2 in the liquefaction stage. The constraints were violated, the optimizer giving the message "Step convergence, but violated constraints". Figure 6.24 gives an overview of the constraints values for the optimal local solution found.

Derivative Analysis Configuration						
Name	Derivative	Operation	FlowSheetWide	Add	OptVars	Mas Run
Hard Constraint		Object Name	Attached Object	Property	Current Value	Use Flag
Config:						
Input	LNG1	LNG1	LNG-1	Minimum Approac	1.4291	<input checked="" type="checkbox"/>
Output	LNG2	LNG2	LNG-2	Minimum Approac	2.7227	<input checked="" type="checkbox"/>
Results	LNG3	LNG3	LNG-3	Minimum Approac	2.8928	<input checked="" type="checkbox"/>
All	LNG4	LNG4	LNG-4	Minimum Approac	5.7993	<input checked="" type="checkbox"/>
Process Constraint						
Config:						
Input	LNG5	LNG5	LNG-5	Minimum Approac	0.9353	<input checked="" type="checkbox"/>
Output	LNG6	LNG6	LNG-6	Minimum Approac	6.2563	<input checked="" type="checkbox"/>
Results	1superheat	1superheat	LNG-1	Spec Calc Value (Ex	7.5108	<input checked="" type="checkbox"/>
All	2superheat	2superheat	LNG-2	Spec Calc Value (Ex	1.5743	<input checked="" type="checkbox"/>
Objective Function	3superheat	3superheat	LNG-3	Spec Calc Value (Ex	9.7740	<input checked="" type="checkbox"/>
Solution Constraint	4superheat	4superheat	LNG-4	Spec Calc Value (Ex	45.0085	<input checked="" type="checkbox"/>

Figure 6.0-24 Constraints Values for Solution 1 for Tealarc Model

Next, the composition for both mixed refrigerants was varied, while keeping their pressures constant. The pressure levels for the two stages were also varied. As a starting point, the optimal local solution found previously was used. It should also be noted that the initial values of the alternative modeled in Aspen HYSYS were used as starting points, however, the optimizer was not able to give a feasible solution, so no results were registered.

The same approach was used when dealing with the boundaries and starting points for the variables: the cold and hot composite curves were always checked and based on their shape, a new starting point or boundary was set in the optimizer. Figures 6.25, 6.26 and 6.27 gives the hot and cold composite curves for the initial alternative, solution 1 and solution 2.

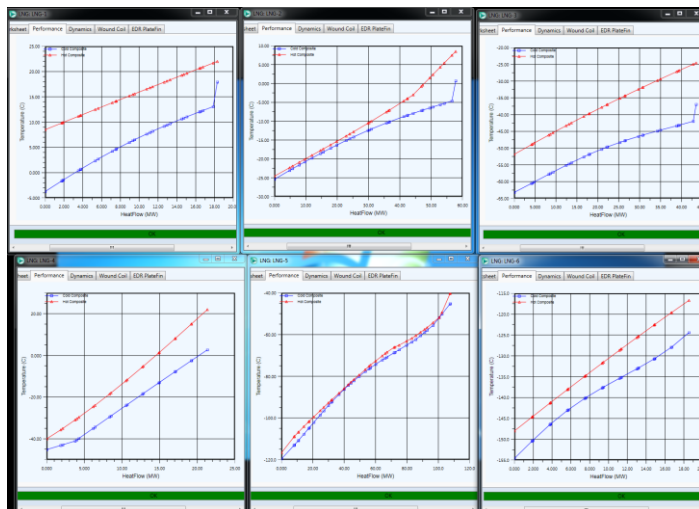


Figure 6.25 Composite Curves Diagrams for Initial Tealarc Model

The aim of the optimization was to get the hot and cold composite curves as close to each other as possible, to minimize the temperature driving forces, however, always checking not to override the two curves. A very good temperature distribution can be noticed in LNG 5 heat exchanger, due to the presence of the phase separator at the entrance to the liquefaction stage.

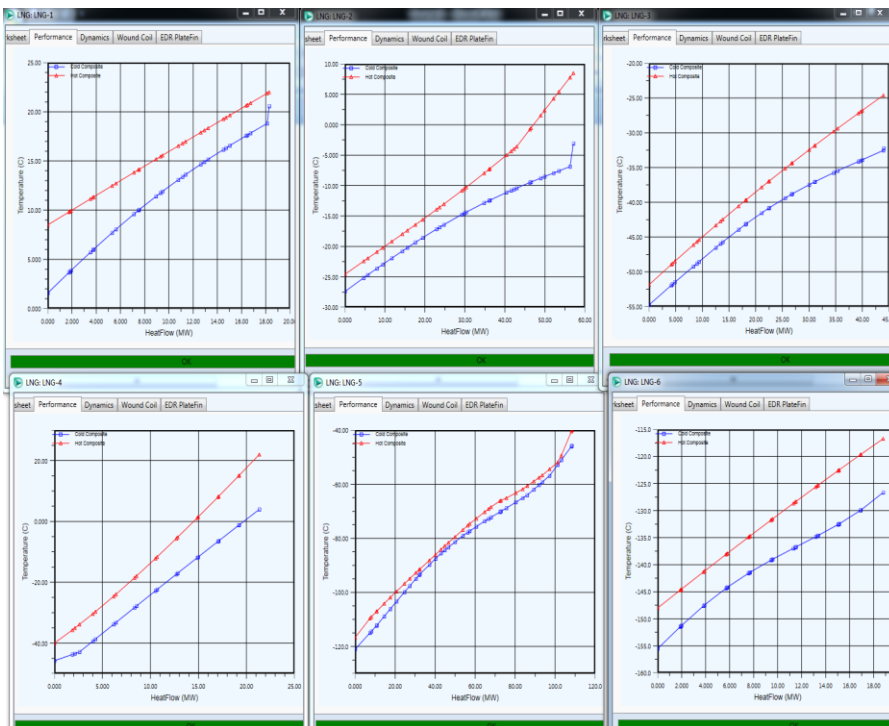


Figure 6.0-25 Composite Curves Diagrams for Solution 1 of the Tealarc Model

Solution 1 gives the hot and cold composite curves of the cryogenic heat exchangers when the pressures and pressure levels are changed. It can be noticed in Figure 6.26 how changing the pressure will definitely influence the temperature levels of the streams and the heat distribution within the cryogenic equipment.

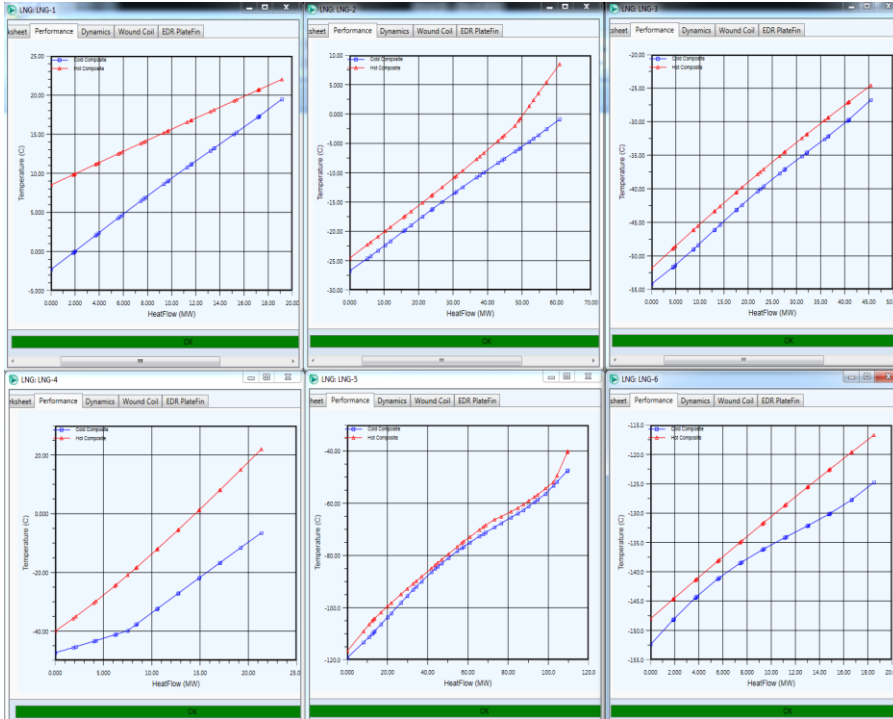


Figure 6.0-26 Composite Curves Diagrams for Solution 2 of the Tealarc Model

A visible improvement can be noticed in LNG 1, LNG 2, LNG 3 and LNG 6 heat exchangers, in the second solution, in Figure 6.26. However, the composite curves for the LNG 4 did not improve. This is the heat exchanger where the natural gas stream enters the liquefaction stage, and the temperature difference between the hot and the cold streams is very high.

The variation of the molar flow rate of the MRs components were also registered and followed throughout the optimization process, in order to have an educated guess for different starting points and boundaries for the variables. Figures 6.27 and 6.28 show how the two MRs molar component flow rates influenced the objective function value.

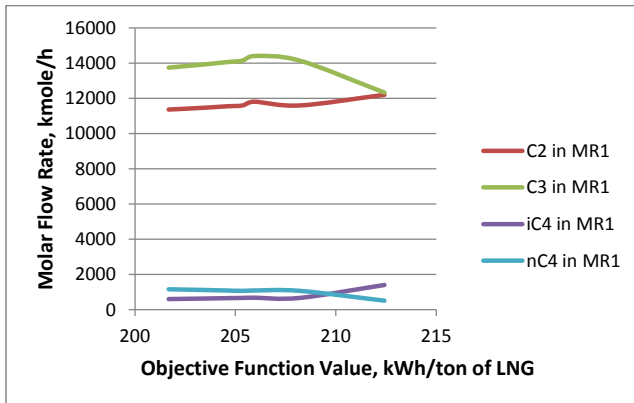


Figure 6.0-27 Molar Flow Rate Variation for MR1 for Tealarc Model

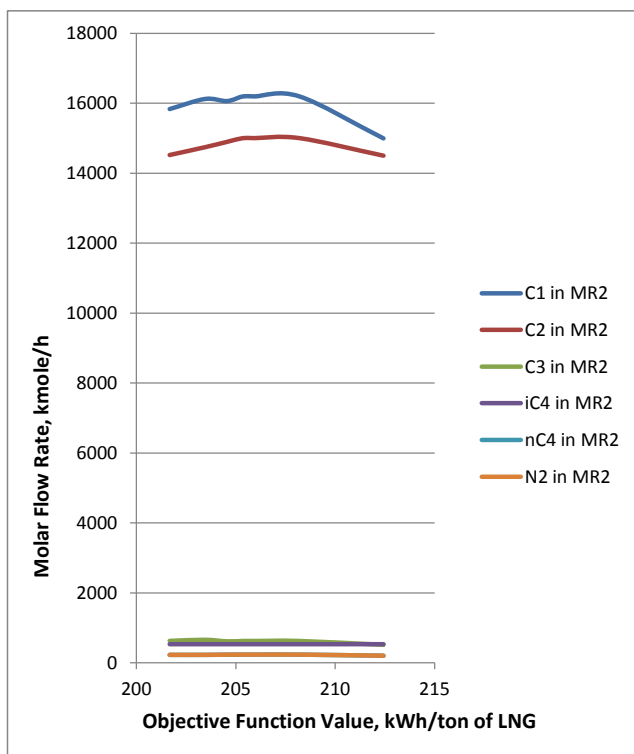


Figure 6.0-28 Molar Flow Rate Variation for MR2 for Tealarc Model

From the two figures it can be observed that the presence of one component influences the amount of the others. For example, the flow rates of the heavier components have a linear

variation, in comparison with the lighter components that increase and decrease several times as the objective function value decreases.

Tables 6.21 and 6.22 give an overview of the variables values for optimal solution found when varying only the pressures (solution 1), and the optimal feasible solution found after varying the composition (solution 2).

Table 6.0-21 Initial Vs. Optimized Solutions MR 1 Values

Parameter	Units Of Measure	Initial Solution	Solution 1	Solution 2
Molar Flow N ₂	kmole/h	0	0	0
Molar Flow C ₁	kmole/h	31	31	0
Molar Flow C ₂	kmole/h	9,927	9,927	11,370
Molar Flow C ₃	kmole/h	15,040	15,040	13,749
Molar Flow iC ₄	kmole/h	650	650	605
Molar Flow nC ₄	kmole/h	0	0	1,163
Molar Flow iC ₅	kmole/h	0	0	0
Inlet Pressure	bar	22	20.18	20.18
Pressure Level 1	bar	9.7	11.38	10.44
Pressure Level 2	bar	5.7	5.3	5.6
Pressure Level 3	bar	1.4	2.1	2.2
Specific Power Consumption	kWh/ton of LNG	227.9	206.7	201.7

The values that have decreased compared to the initial solution are marked with green, while the ones that have increased are marked with yellow.

Table 6.0-22 Initial Vs. Optimized Solutions MR 2 Values

Component	Units Of Measure	Initial Solution	Solution 1	Solution 2
Molar Flow N ₂	kmole/h	3,406	0	0
Molar Flow C ₁	kmole/h	14,629	14,629	15,839
Molar Flow C ₂	kmole/h	14,384	14,384	14,519
Molar Flow C ₃	kmole/h	352	352	623
Molar Flow iC ₄	kmole/h	529	529	528
Molar Flow nC ₄	kmole/h	191	191	225
Molar Flow iC ₅	kmole/h	0	0	0
Inlet Pressure	bar	39.95	38.82	38.82
Pressure Level 1	bar	-	-	-
Pressure Level 2	bar	-	-	-
Pressure Level 3	bar	-	-	-
Pressure Level 4	bar	7.2	6.5	7.1
Specific Power Consumption	kWh/ton of LNG	227.9	206.7	201.7

The constraints however, were violated to a certain extent, and in the next step, when testing the performance of the optimizer, the aim was to meet their setup values.

2. Run the optimizer with the optimal solution found in step 1 as starting point, and test the optimizer performance by varying the setup parameters from Table 6.6. The values obtained in solution 2 from the first step were used as starting points for step 2.

Max. Iterations Variation

When varying the maximum iterations parameter, the objective function decreased from 201.7 to 197.3 kWh/ton of LNG. At the same time, however, the constraints were violated even more, resulting in a minimum approach temperature in LNG 5 of 0.24K, for the lowest value of the objective function, which is not acceptable. It can be concluded that varying this parameter, the optimizer was not able to meet the constraints, but violated them even more. The variation of the objective function when adjusting the maximum iterations parameter is found in Figure 6.29.

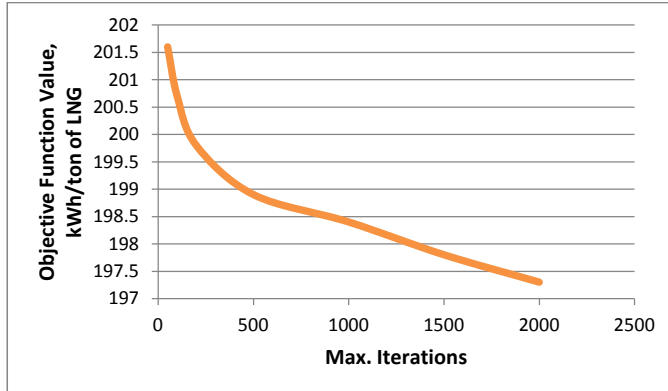


Figure 6.29 Maximum Iterations Variation for Tealarc Model

The performance of the optimizer was, however, better in the Tealarc case than for the Shell model, as the constraints violations were not as high.

Objective Scale Factor Variation

The maximum iterations parameter was kept constant at 500, as it was done for the previous models. Figure 6.30 presents the performance of the optimizer when the objective scale factor is varied.

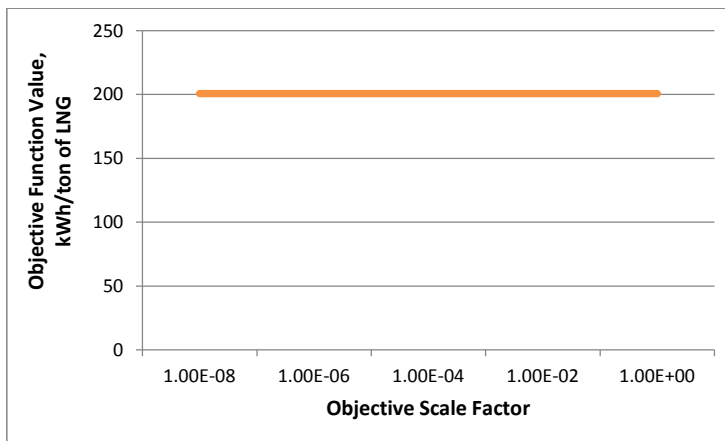


Figure 6.30 Objective Scale Factor Variation for Tealarc Model

Changing the objective scale factor, the objective function value decreased to 200.7 kWh/ton of LNG in the first iteration, and then remained constant. The constraints were violated in this case as well. Thus, it can be concluded that varying the objective scale factor, there was no improvement in meeting the constraints, although the objective function was minimized.

Accuracy Tolerance Variation

The objective scale factor was kept constant and set up to be 10^{-4} , as for the other DMR processes. Figure 6.31 shows the impact the accuracy tolerance variation has on the objective function, for the Tealarc process.

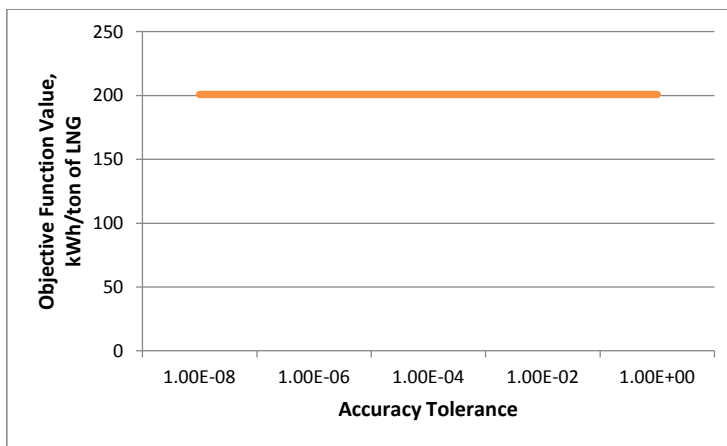


Figure 6.31 Accuracy Tolerance Variation for Tealarc Model

The accuracy tolerance parameter variation had no impact on the objective functions value, nor on the improvement of meeting the constraints values.

Step Restriction Variation

Figure 6.32 presents the impact the step restriction variation had on the objective function of the process.

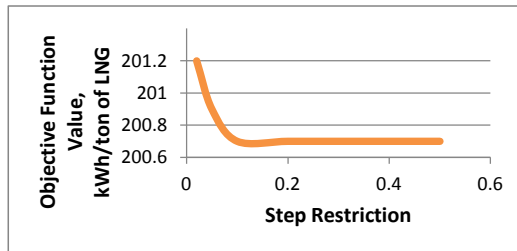


Figure 6.32 Step Restriction Variation for Tealarc Model

The objective function decreased until it reached the value 200.7 kWh/ton of LNG, corresponding to a step restriction value of 0.2. From there on, the value remained constant. However, the optimizer was not able to meet the constraints values.

Perturbation Variation

Figure 6.33 shows the behavior of the objective function when the perturbation parameter is varied. For lower values, the optimizer shows the "Stopped" message, meaning the system was not able to find a feasible solution. When the perturbation parameter reaches the value of 10^{-3} , the optimizer is able to run the operation, ending with the message "Step convergence, but violated constraints". When the perturbation is equal to 1, the objective function starts to increase again.

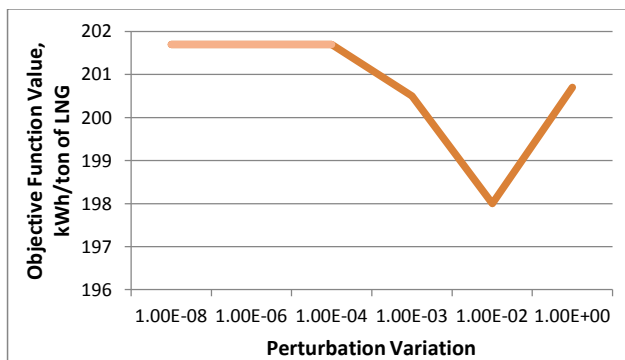


Figure 6.33 Perturbation Variation for Tealarc Model

Maximum Feasible Point Variation

The optimizer failed to give a feasible solution, the operation ending every time with the message "Stopped", except for the default value, 5, when the objective function had the value 201.7 kWh/ton of LNG.

3. Compare the results obtained for the objective function against the initial value.

During the first two steps of the optimization process, the objective function was reduced from 227.9 to 201.7 kWh/ton of LNG in the first step, and to 196.3 kWh/ton of LNG in the second step. However, the optimizer behaved badly when trying to meet the selected constraints in the second step, so the value of 196.3 kWh/ton of LNG is not a realistic value that should be used further. Table 6.23 shows the constraints values for the initial model, solution 1 and solution 2 developed in first step, and solution 3 obtained in the second step.

Table 6.0-23 Constraints Values Comparison for the Tealarc Model

Parameter	Initial Model	Solution 1	Solution 2	Solution 3
Min. Approach. LNG 1, K	3	1.4	2.5	2.4
Min. Approach. LNG 2, K	3	2.7	2.2	2.1
Min. Approach. LNG 3, K	3	2.9	2.2	2
Min. Approach. LNG 4, K	7.8	5.7	7.4	5.9
Min. Approach. LNG 5, K	3	1	1.3	0.03
Min. Approach. LNG 6, K	7.2	6.2	3	2.3
Superheating LNG 3, K	4	9.7	0.5	0.7
Superheating LNG 4, K	46	45	34	37
Objective Function, kWh/ton of LNG	227.9	206.7	201.7	196.3

As a conclusion for the optimization of the Tealarc process, it is safe to say that the optimizer did not have a good performance. Although the objective function was minimized from 227.9 to 196.3 kWh/ton of LNG, the optimizer violated the constraints.

6.6 Liquefin DMR Process Optimization

The last DMR process alternative that was optimized is the Liquefin process, which was modeled in Aspen HYSYS, and the process flow sheet of the model is found in Appendix D.

Constraints and Objective Function

Table 6.24 presents the constraints of the process set up in the Hyprotech SQP optimizer in Aspen HYSYS. The objective function is the minimization of the specific power consumption of the process.

Table 6.0-24 Liquefin DMR Constraints Values

Constraint/Equipment	Minimum Approach	Superheating
LNG 1	3 K	-
LNG 2	3 K	-
LNG 3	3 K	5 K
LNG 4	3 K	5 K

The streams leaving the first two LNG heat exchangers do not enter directly the compressors, so there was no need for a superheating constraint in the optimizer. However, the superheating values of those two streams were checked, so that their temperature will not go below their dew point temperature.

Variables

The number of the variables that were set up in the optimizer is 21, and those variables are presented in Table 6.25. Since more variables are subject to optimization, the optimization operation is expected to be more complicated.

Table 6.25 Number of Variables for Liquefin DMR Process

Variables	Number of variables
MR1 component flow rates	7
MR2 component flow rates	7
MR1 and MR2 inlet pressures	2
Pressure levels	5
Total decision variables	21

The number of pressure levels is the highest between the four alternatives discussed in this project. The Liquefin process, has three pressure levels in the pre-cooling stage and two pressure levels in the liquefactions stage.

Optimization Strategy

The same strategy as for the other alternatives was implemented.

1. Run the optimizer with the starting values for the variables presented in Table 6.26, until reaching an optimal local solution. The optimizer setup parameters use the default values, except the gradient calculations which is 2-sided.

Table 6.26 Variables Starting Points for Liquefin DMR Process

Component	Units Of Measure	Values MR1	Values MR2
Molar Flow N ₂	kmole/h	0	1,353
Molar Flow C ₁	kmole/h	0	11,455
Molar Flow C ₂	kmole/h	23,191	10,875
Molar Flow C ₃	kmole/h	23,191	483
Molar Flow iC ₄	kmole/h	0	0
Molar Flow nC ₄	kmole/h	0	0
Molar Flow iC ₅	kmole/h	0	0
Inlet Pressure	bar	20	55.5
Pressure Level 1	bar	12.3	-
Pressure Level 2	bar	5.2	-
Pressure Level 3	bar	1.7	-
Pressure Level 4	bar	-	5.7
Pressure Level 5	bar	-	2.7

The variables boundaries ranges were set up to be ± 2000 kmole/h added or subtracted from the initial values for the components flow rates, ± 10 bar for the inlet pressures, and $\pm 2-5$ bar for the pressure levels for both mixed refrigerants. The boundaries are, however, changed during optimization, based on the feedback from the hot and cold composite curves. The

starting points for the first optimization run were set up to be the initial values from the model in Aspen HYSYS. After the first run, the values of the optimal local solution found were used as the new starting points. The hot and cold composite curves were used as guidance to understand in which direction should the variables boundaries move in order to escape from the "trapped" region and find another optimal local solution.

Figure 6.34 shows the hot and cold composite curves for the four LNG heat exchangers for the initial alternative. The first three LNG heat exchangers correspond to the pre-cooling part of the process, while LNG 4 corresponds to the liquefaction stage. As it can be noticed from the figure, there is room for improvement in the first part of the process, while the last part is quite optimized as it is. Changing the pressure and composition of the MR1 would be the first step to consider in the optimization process.

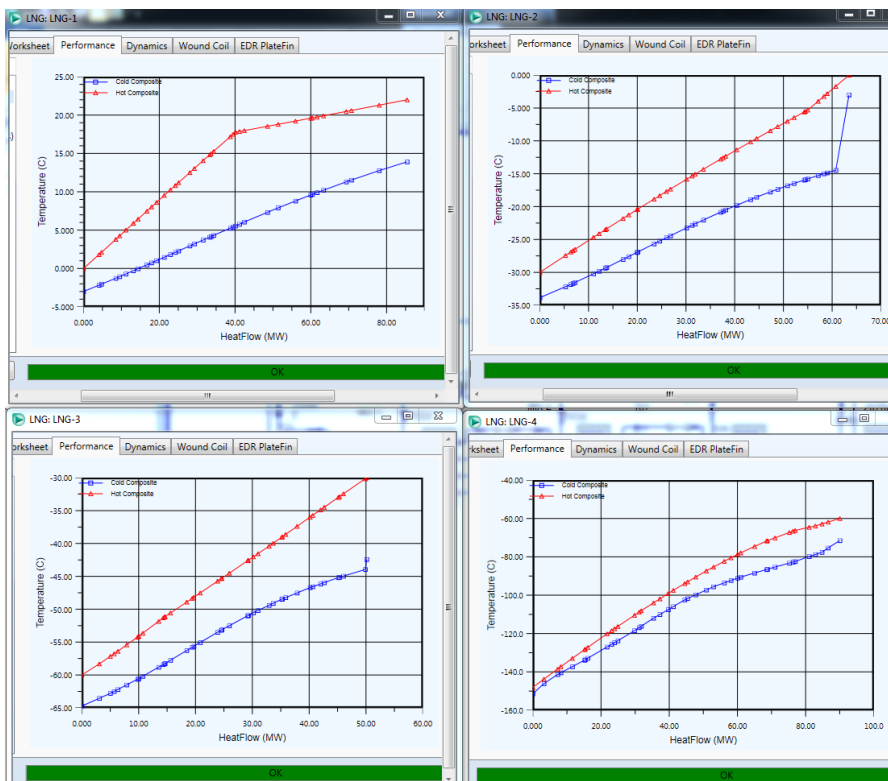


Figure 6.34 Composite Curves Diagrams for Initial Solution for the Liquefin Model

Figure 6.35 shows the composite curve for the best local solution found while the optimizer ran using the default values for its setup parameters. There is a visible improvement in all of the heat exchangers, and this is due to several factors, such as the presence of new components in the MR1 stream, as well as the change in the inlet pressures for both mixed refrigerants. A discussion on how the pressure and different components affect the performance of the system is presented in Chapter 8.

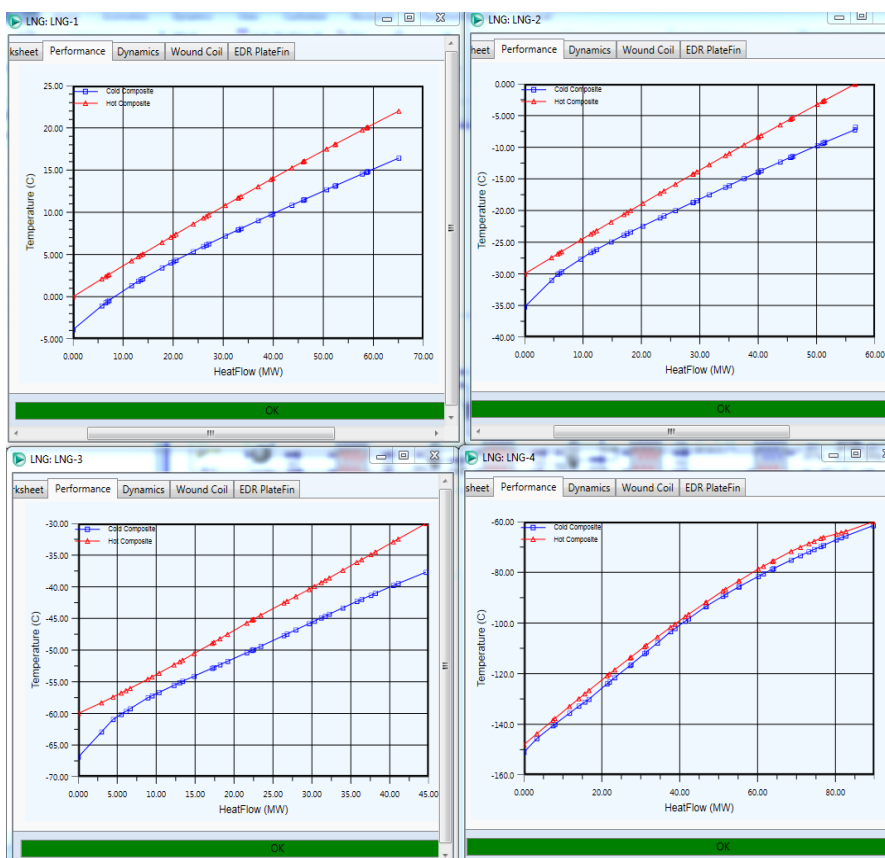


Figure 6.35 Composite Curves Diagrams for Optimized Solution for the Liquefin Model

The best solution found in the first step of the optimization gives an objective function value of 216.5 kWh/ton of LNG, which is 9% lower than the initial starting value. The constraints were, however, violated for the last LNG heat exchanger.

Figures 6.36 and 6.37 show the variation of the molar flow rate of the components of the two MRs, when the specific power consumption was minimized during the optimization process. The variation of the component flow rates was followed in order to have an understanding on how the composition influences the objective function.

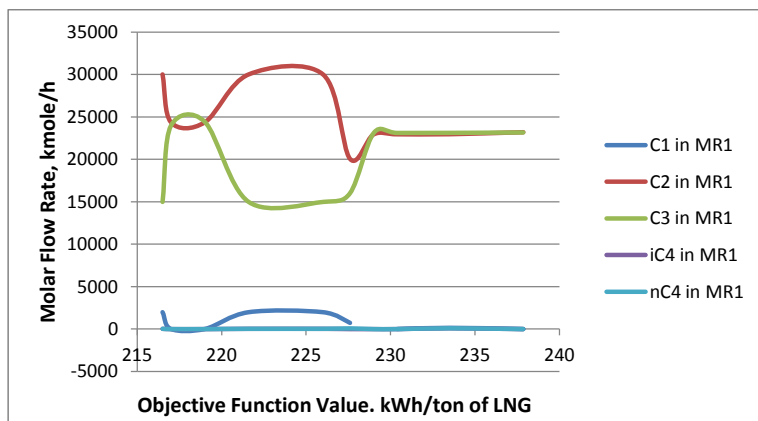


Figure 6.36 MR1 Flow Rate Variation for Liquefin Model

The variation of the molar flow rates is quite different from the previous processes presented. The strong contrast is due to the strong variation of the pressure in the same time as the variation of the composition. For the Liquefin process, the optimizer worked better, varying the pressure in the same time with the molar flow rates of the components.

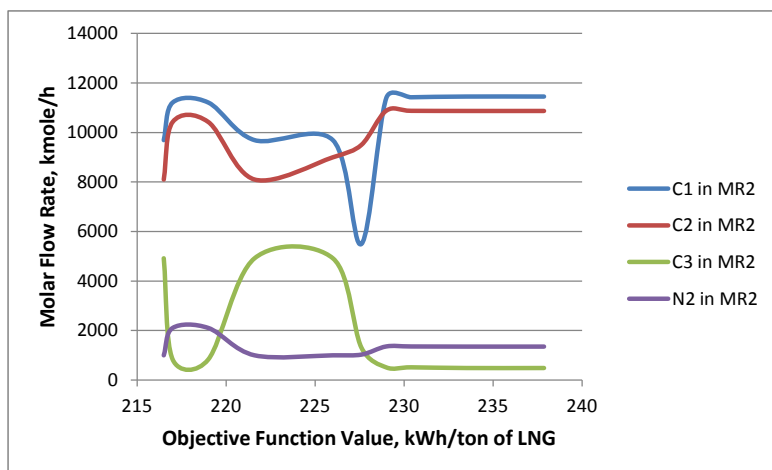


Figure 6.37 MR2 Flow Rate Variation for Liquefin Model

Figure 6.38 gives the variation of the pressure for the two mixed refrigerants with the objective function.

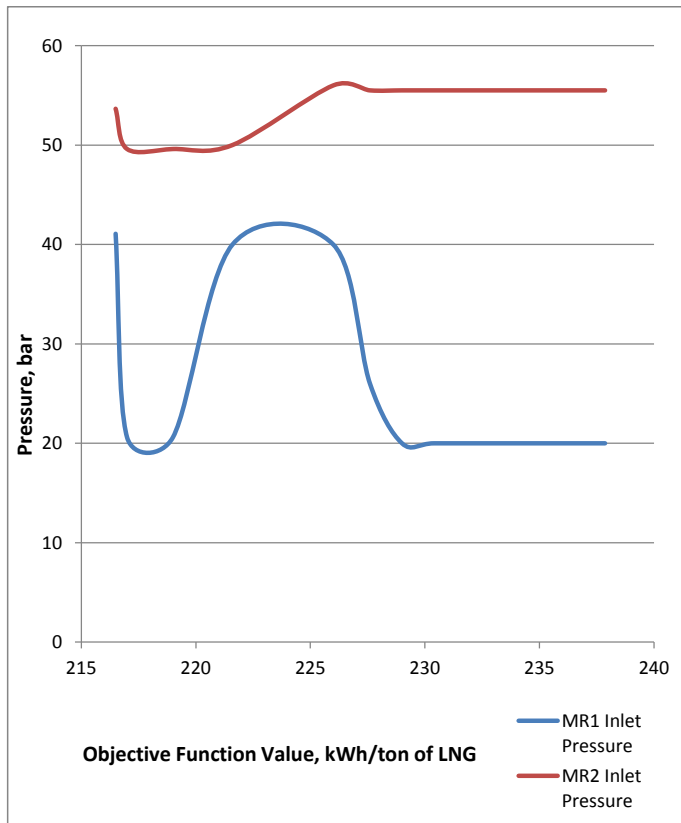


Figure 6.38 Inlet Pressure Variation for the Liquefin Model

There was a strong variation in the inlet pressure for the first mixed refrigerant. At a higher value, the heavier hydrocarbon were present as well, while at lower values, only ethane and propane were found. The behavior of the MR1 stream at different pressure levels is discussed further in Chapter 8.

Table 6.27 presents an overview on the values for the variables changed during optimization for the initial model and the best local solution found.

Table 6.27 Initial Vs. Optimized Variables Values for Liquefin Process

Component	Units Of Measure	Values MR1	Optimized Values for MR1	Values MR2	Optimized Values for MR2
Molar Flow N ₂	kmole/h	0	0	1,353	1,000
Molar Flow C ₁	kmole/h	0	2,000	11,455	9,695
Molar Flow C ₂	kmole/h	23,191	30,000	10,875	8,100
Molar Flow C ₃	kmole/h	23,191	15,000	483	4,914
Molar Flow iC ₄	kmole/h	0	34	0	0
Molar Flow nC ₄	kmole/h	0	34	0	0
Molar Flow iC ₅	kmole/h	0	0	0	0
Inlet Pressure	bar	20	41.1	55.5	53.6
Pressure Level 1	bar	12.3	19.4	-	-
Pressure Level 2	bar	5.2	8.9	-	-
Pressure Level 3	bar	1.7	3.2	-	-
Pressure Level 4	bar	-	-	5.7	5.5
Pressure Level 5	bar	-	-	2.7	2.2

The inlet pressure of the first mixed refrigerant has doubled, while its total flow rate increased with only 1.4%. It can be observed the presence of C₁, iC₄ and nC₄ in the optimal solution. For the second mixed refrigerant the amount decreased for C₁ and C₂ can be found in the flow rate increase of the C₃ component.

2. Run the optimizer with the optimal solution found in step 1 as starting point, and test the optimizer performance by varying the setup parameters from Table 6.6.

Max. Iterations Variation

The variation of the maximum iteration parameter with the objective function is presented in Figure 6.39.

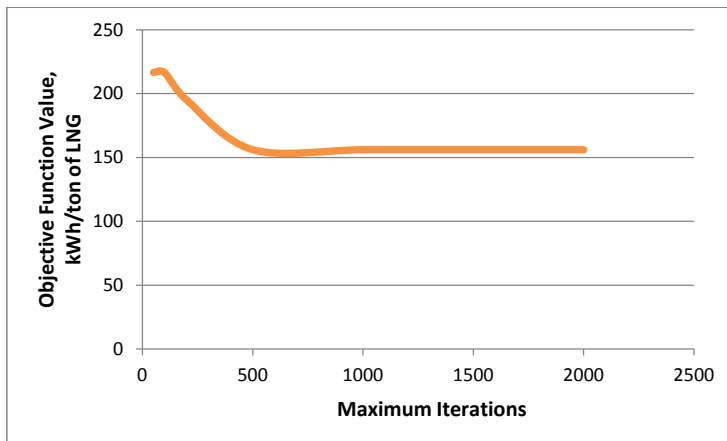


Figure 6.39 Maximum Iterations Variation for the Liquefin Model

Although the results show that the objective function would decrease with the increase of the maximum iterations, the constraints in the optimizer are not met, so the solutions found cannot be considered as a new optimal local solution.

Objective Scale Factor Variation

The maximum iterations parameter was kept constant at a value of 500. The results of the optimizer when the objective scale factor is varied, are presented in Figure 6.40. For a value of 10^{-8} for the objective scale factor, the objective function value decreased from 216.5 to 191.6 kWh/ton of LNG. The constraints, however, were not met. For the value 10^{-6} , the optimizer gave a better solution, as the constraints were violated, but not as much as in the first iteration. This time the objective function value decreased from 216.5 to 205.6 kWh/ton of LNG. For a value of 1 for the objective scale factor, the program was not able to give a feasible solution at all.

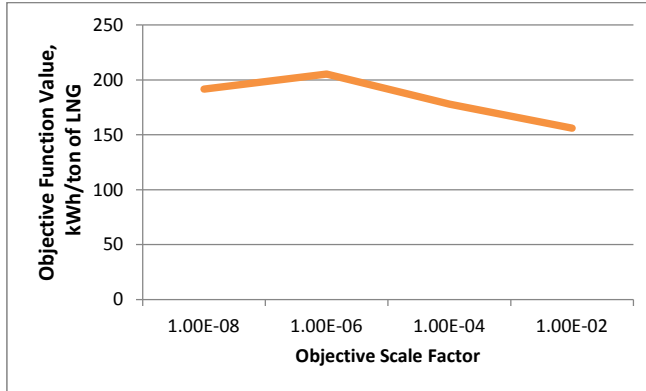


Figure 6.40 Objective Scale Factor Variation for the Liquefin Model

When the objective scale factor value is set to be higher, the focus is on solving the optimization function, but when the value is set to be lower, the focus is on meeting the constraints. This was noticed also from the results of the optimizer. The lower the objective scale factor was selected, the constraints were violated with a lower error, while when a higher value was selected, the objective function decreased, but the constraints errors increased.

Accuracy Tolerance Variation

The accuracy tolerance was varied next, while keeping the objective scale factor at a value of 10^{-4} . Figure 6.41 gives the objective function value when the accuracy tolerance parameter is varied from 10^{-8} to 1.

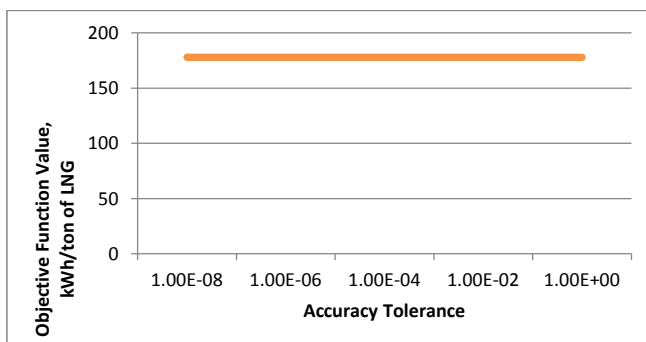


Figure 6.41 Accuracy Tolerance Variation for the Liquefin Model

The objective function decreased in value to 176 kWh/ton of LNG when the accuracy tolerance was set to 10^{-8} , however the optimizer was not able to meet the constraints. The objective function value remained constant for the rest of the iterations, the optimizer not being able to give a feasible solution.

Step Restriction Variation

Figure 6.42 shows the variation of objective function when the step restriction is varied within the interval [0.02, 05].

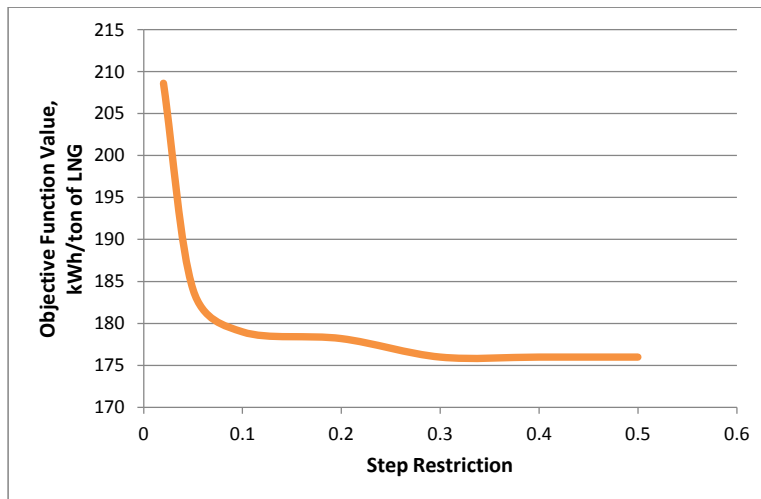


Figure 6.42 Step Restriction Variation for the Liquefin Model

The objective function value is decreasing as the step restriction parameter is increasing. After the step restriction reaches the value of 0.3, the objective function remains constant and independent of how much the step restriction increases. However, the optimizer was not able to meet the constraints, so no feasible solution was registered.

Perturbation Variation

The perturbation parameter was varied next, while keeping the others parameters of the optimizer constant. The step restriction factor was kept constant at a value of 0.2 for all iterations. The optimizer was not able to find a feasible solution while adjusting this parameter, so no results were registered.

Maximum Feasible Point Variation

The maximum feasible point is the last setup parameter of the optimizer that was varied. Figure 6.43 shows how the objective function value decreased at 25 feasible points, and then remained constant as the maximum feasible point parameter value increased. However, the constraints were not met, so a feasible solution was not registered.

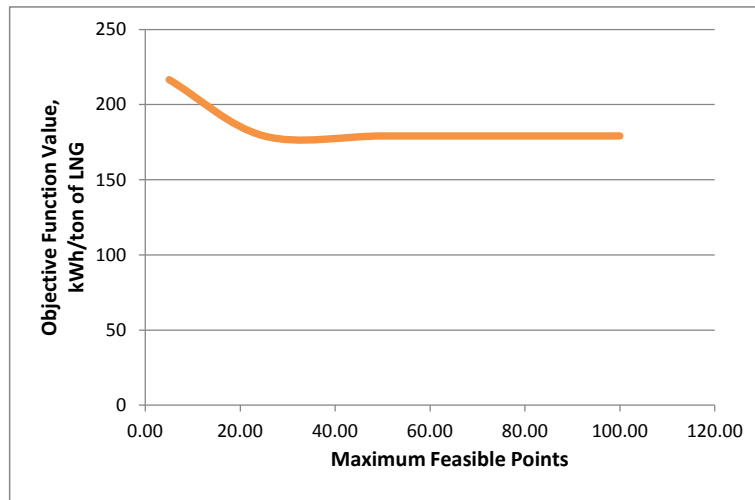


Figure 6.43 Maximum Feasible Points Variation for the Liquefin Model

3. Compare the results obtained for the objective function against the initial value.

In the second step, the setup parameters of the optimizer were varied in order to improve the performance of the program. Although the objective function was minimized to a certain value, the constraints were highly violated, so the solutions the optimizer gave, could not be taken into consideration as final optimal local solutions. However, the solution obtained from the first step of the optimization strategy, gave an acceptable solution to work with, having less violated constraints.

Table 6.28 shows the constraints and the objective function values of the initial model and the feasible solution found from step 1 of the optimization strategy.

Table 6.28 Constraints and Objective Value Comparison for the Liquefin Model

Parameter	Initial Model	Solution 1
Min. Approach. LNG 1, K	3	2.9
Min. Approach. LNG 2, K	3	2.9
Min. Approach. LNG 3, K	4	2.9
Min. Approach. LNG 4, K	2.5	2.1
Superheating LNG 3, K	1.5	6
Superheating LNG 4, K	3.3	19
Objective Function, kWh/ton of LNG	237.9	216.5

In conclusion, varying the setup parameters of the optimizer, was not possible to improve either the constraints nor the objective function values more than already was done with the default values.

6.7 Hyprotech SQP Optimizer Results

The running results of the optimizer when using the Hyprotech SQP method were analyzed for each DMR process alternative.

Objective Value

The objective function was selected to be the specific power consumption which was represented by the ratio between the total power consumption of the liquefaction process in kW, and the mass flow rate of the LNG produced in ton/h. Tabel 6.29 contains the objective values for the four alternatives optimized.

Table 6.29 Objective Values Comparison

DMR Alternative	Objective Value, kWh/ton of LNG	Improvement from the Initial Value, %
APCI	218.5	11
Shell	214.8	10
Tealarc	201.7	12
Liquefin	216.5	9

Termination Reason

For all the feasible solutions the optimizer found, the termination reason was always "Step convergence, but violated constraints". When the boundaries needed to be changed, the "Unbounded" termination reason occurred. The optimizer would give the "Stopped" termination reason when it was not able to calculate a solution based on the new values for the setup parameter.

Actual Optimizer

The actual optimizer result gives the number of major iterations during the optimization operation. Table 6.30 presents the average actual optimizer value for all four optimized alternatives.

Table 6.30 Actual Optimizer Values

DMR Alternative	Average Value
APCI	17
Shell	11
Tealarc	9
Liquefin	7

The higher the number of the major iterations, the more likely it was that the optimizer would give a better solution.

Feasible Point Iterations

The feasible point iterations results shows how many minor iterations took place since the last major iterations. This number is related directly with the setup parameter maximum feasible point, which it was set to 5 in most iterations, as the optimizer was not able to give feasible solutions for higher values. So, the feasible point iterations result for all four DMR alternatives was 5.

Total CPU Time

The CPU time displays the time the optimizer has taken to solve the optimization problem. Table 6.31 contains the average time in seconds, the optimizer needed to finalize an optimization problem for each DMR process alternative. A number of 1003 simulations were conducted during the project, when testing the performance of the optimizer. Table 6.31 also gives the number of simulations for each alternative optimized.

Table 6.31 CPU Time and Number of Simulations

DMR Alternative	Average CPU Time	Number of Simulations
APCI	173.1	222
Shell	133.7	268
Tealarc	124.9	280
Liquefin	111.3	233

Gradient and Model Evaluations

Those two results show how many gradient, respectively model evaluations were performed during one optimization operation. The longer the CPU time, the higher the number of the gradient and model evaluations. The average values for the four DMR alternatives optimized are presented in Table 6.32.

Table 6.32 Gradient and Model Evaluations

DMR Alternative	Average Gradient Evaluations	Average Model Evaluations
APCI	23	47
Shell	19	38
Tealarc	15	27
Liquefin	9	21

PART THREE: EVALUATION

7. Thermodynamic Analysis

A thermodynamic analysis was conducted in order to better understand how the properties of the fluids influence the efficiency and the performance of the liquefaction process. Also, a comparison between the four processes modeled in Aspen HYSYS has been based on the results from the exergy analysis that has been conducted. Exergy represents the maximum work that can be achieved from a certain amount of energy (Querol et al., 2013). Thus, an exergy analysis was needed to find the losses in the system, in order to further optimize the process.

Exergy Loss

As a general definition, the exergy loss of a system represents the difference between the exergy in and out of the system (Querol et al., 2013).

Table 7.1 presents the formulas for calculating the exergy loss in the equipment needed in the liquefaction of natural gas.

Table 7.0-1 Exergy Loss Formulas [Venkatarathnam, 2008]

Equipment	Formula, kW
Compressor	$\Delta ex_{loss} = \dot{m}(e_{in} - e_{out}) - \dot{W}_c$
Pump	$\Delta ex_{loss} = \dot{m}(e_{in} - e_{out}) - \dot{W}_p$
Throttling Valve	$\Delta ex_{loss} = \dot{m}(e_{in} - e_{out})$
LNG Heat Exchanger	$\Delta ex_{loss} = \sum_{i=1}^n \dot{m}_i(e_{i_{in}} - e_{i_{out}})$
Cooler	$\Delta ex_{loss} = \dot{m}(e_{in} - e_{out})$
Mixer	$\Delta ex_{loss} = \sum_{i=1}^n \dot{m}_{i_{in}} e_{i_{in}} - \dot{m}_{out} e_{out}$
Phase Separator	$\Delta ex_{loss} = \dot{m}_{in} e_{in} - \sum_{i=1}^n \dot{m}_{i_{out}} e_{i_{out}}$

Where,

\dot{m} is the flowrate of the stream in kg/s ;

e_{in} is the exergy of the stream that enters the equipment in kJ/kg ;

e_{out} is the exergy of the stream that leaves the equipment in kJ/kg ;

\dot{W}_c is the compressor work in kW ;

\dot{W}_p is the power of the pump in kW ;

i, n are the number of the streams entering or leaving the equipment.

Exergy Efficiency

The exergy efficiency of a process is defined as the ratio between the amount of exergy that leaves the system and the exergy that enters the system, and it can be written as equation 2 (Venkatarathnam, 2008).

$$\eta_{ex} = 1 - \frac{\sum \text{exergy loss in each component}}{\text{actual power supplied}} \quad (2)$$

7.1 Physical Exergy

Physical exergy is the maximum work achieved by taking a mass from certain conditions, T, P to environmental conditions, T_o, P_o , through physical processes. During liquefaction, most of the processes take place without changing the composition of the stream, thus they are physical processes. When calculating the exergy loss and exergy efficiency of the process, the physical exergy of the streams were used for the compressors, pumps, throttling valves, LNG heat exchangers, coolers and heaters.

The physical exergy can be calculating using entropy and enthalpy values of the streams at different conditions using equations from the specific literature. However, in this project, the values for physical exergy were taken directly from the HYSYS simulation of the DMR

process for all alternatives, and used in the calculation of the exergy loss and exergy efficiency.

7.2 Chemical Exergy

The chemical exergy is the maximum useful energy that can be achieved when taking a mass from environmental state to dead state through chemical processes. During liquefaction, mixers and phase separator change the composition of the streams, and that is why it is important to also include the chemical exergy into the calculation of the exergy of a stream.

The chemical exergy of a stream was calculated using equation 3 (Querol et al., 2013).

$$b_{ch} = \sum (x_i b_{ch_i}) + RT_o \sum (x_i \ln x_i) \quad (3)$$

Where,

b_{ch} is the chemical exergy of the stream in kJ/kmole ;

x_i is the molar fraction of each component in the stream;

R is the universal gas constant, with a value of $8.13446 \text{ kJ}/\text{kgmoleK}$;

b_{ch_i} is the chemical exergy of each component in kJ ;

T_o is the ambient temperature of 288.15 K .

The term $RT_o \sum (x_i \ln x_i)$ represents the destroyed exergy due to mixing of the streams, and it is also called the *mixture exergy* [10]. When calculating the chemical exergy loss for different mixers and phase separators, the first part of the equation (3) can be ignored and we can use only the mixture exergy. The equation used for the calculation of the chemical exergy loss in mixers and separators is therefore:

$$\Delta b_{ch} = RT_o \left(n_{in} \sum (x_i \ln x_i)_{in} - n_{out} \sum (x_i \ln x_i)_{out} \right) \quad (4)$$

Where n_{in} and n_{out} are the flow rates of the streams entering and leaving the mixers and phase separators, in $kgmole/h$.

The total exergy loss of a mixer or a phase separator is thus the sum of the physical and chemical exergy losses.

7.3 Results

The results from the exergy analysis of the four optimized DMR process alternatives were compared against each other, as well as against the initial alternative models, for a better visualization of the improvement achieved regarding the specific power consumption of the process.

The exergy losses for the compressors, pumps, coolers and the cold box of the processes are presented in Figure 7.1.

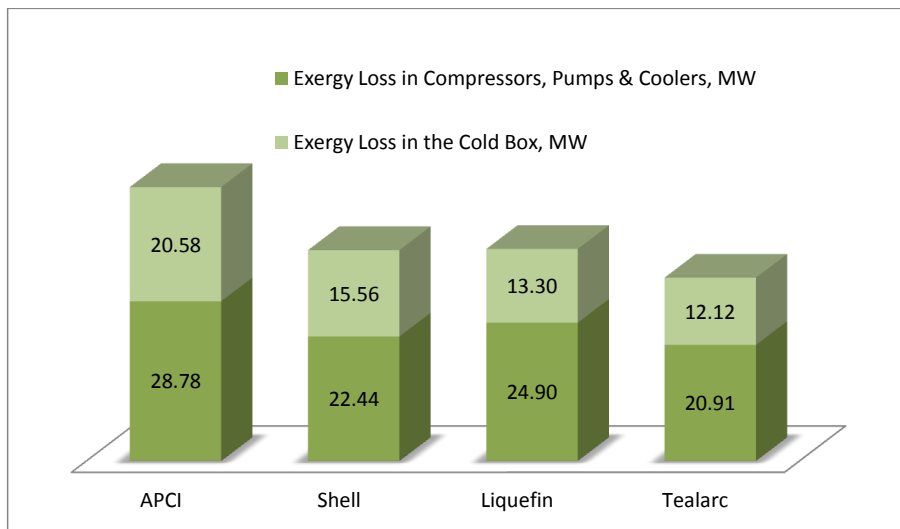


Figure 7.0-1 Exergy Loss Comparison

The APCI model has the highest exergy losses in the cold box and the compressors, pumps and coolers part. Tealarc model has the lowest exergy losses, which will lead to the highest exergy efficiency. The reason for having the highest efficiency is the presence of three pressure levels, as well as the presence of a phase separator for the second mixed refrigerant

in the beginning of the liquefaction stage. For having such an advantage, the exergy loss in compressors, pumps and coolers is quite high, although still the lowest from the proposed alternatives. The reason is that the inlet temperature of the stream entering the compression stage in the liquefaction stage is higher than for the other three processes. The temperature is higher because the second mixed refrigerant enters the liquefaction stage at the cold end of the liquefier, where it will warm up, and then later exchanges heat with the warm natural gas stream that enters directly the liquefaction stage, skipping the pre-cooling part.

Figure 7.2 presents a comparison between the total exergy loss for the optimized alternatives and the initial models.

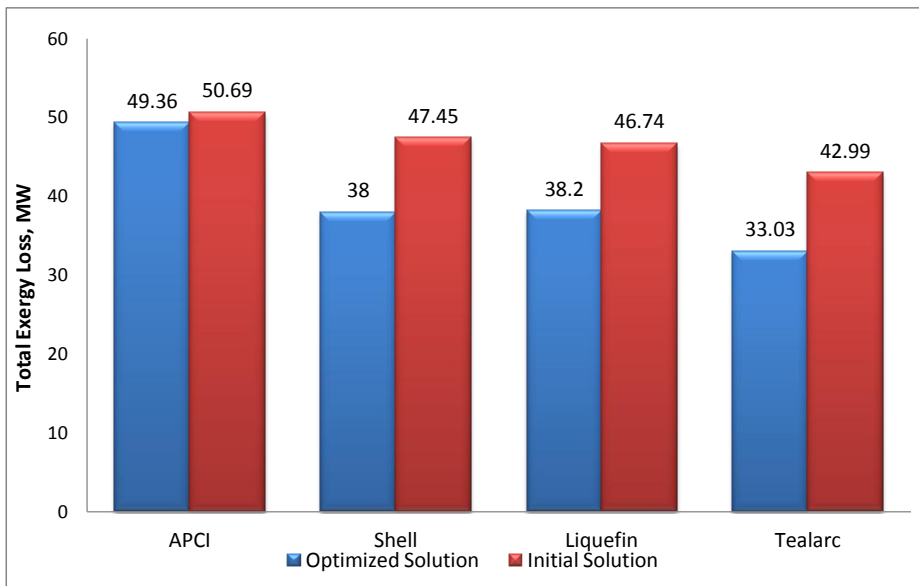


Figure 7.0-2 Total Exergy Loss Initial Vs. Optimized Solution

From Figure 7.2 it can be noticed that the highest improvement was done for the Shell process, where the exergy loss decreased by 20%, after optimization. The APCI model had the lowest improvement, in correlation with exergy losses. The Shell model has a phase separator in the liquefaction stage, which increased its efficiency.

Figures 7.3 and 7.4 show the exergy efficiencies of the four optimized alternatives for the compressors, pumps and coolers and the cold box.

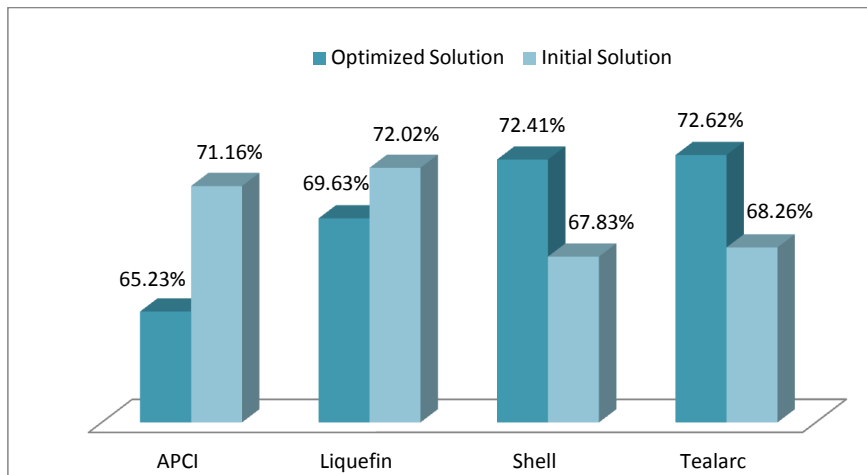


Figure 7.0-3 Compressors, Pumps and Coolers Exergy Efficiencies

APCI and Liquefin models have lower exergy efficiencies for the compressors, pumps and coolers, for the optimized version than for the initial alternative. The two processes have in common the absence of a phase separator in the liquefaction stage, and they both operate at higher inlet pressures than the other remaining processes.

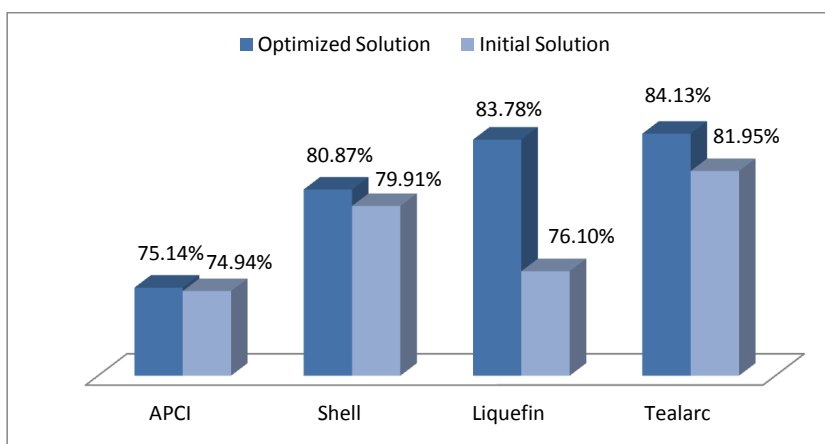


Figure 7.0-4 Cold Box Exergy Efficiencies

The APCI optimized solution is not very different from the initial model, however, the Liquefin process shows a most significant improvement in exergy efficiency for the cold box,

an improvement of 10% from the initial solution. This improvement is due to a high increase of the inlet pressure for the first mixed refrigerant which gave better temperature distribution within the cryogenic heat exchangers. Also, the composition has suffered changes, and iC4 and nC4 components were added in the first mixed refrigerant. How the composition affected the process will be discussed in the next chapter.

Figure 7.5 gives the overall exergy efficiencies for the optimized DMR processes, as well as the corresponding overall exergy efficiencies for the initial models.

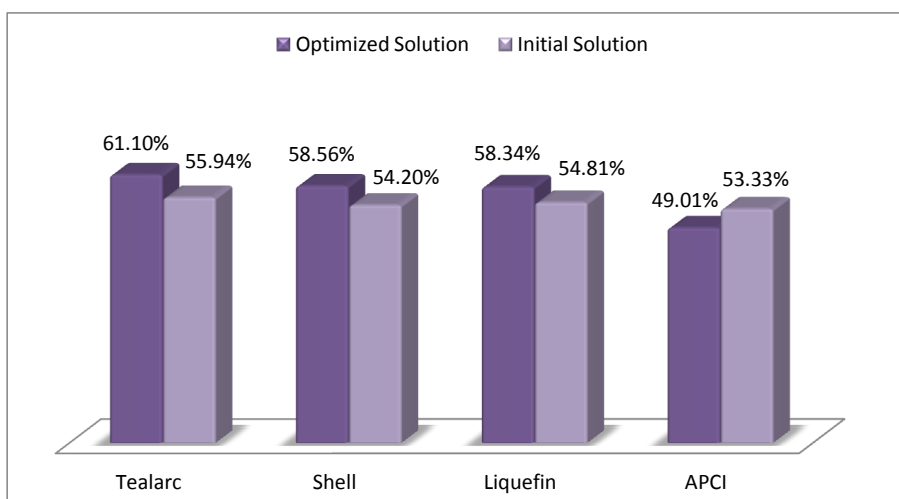


Figure 7.0-5 Overall Exergy Efficiencies

Tealarc optimized model has the highest overall exergy efficiency, and also the highest improvement with an increase in its efficiency of 9%. However, the overall exergy efficiency for the APCI model decreased by 8% of the value for the initial model. Although the optimizer provided a solution that minimized the objective function, the exergy loss was higher than for the initial solution. This can be also explained by the fact that the optimizer was not able to meet the constraints.

For a further optimization of the process, an overview of the losses for each equipment of the liquefaction process was calculated and presented in order to understand where improvements can be conducted. Figures 7.6, 7.7, 7.8 and 7.9 show the split of the exergy losses and the useful effect in the overall DMR process for the all DMR alternatives considered.

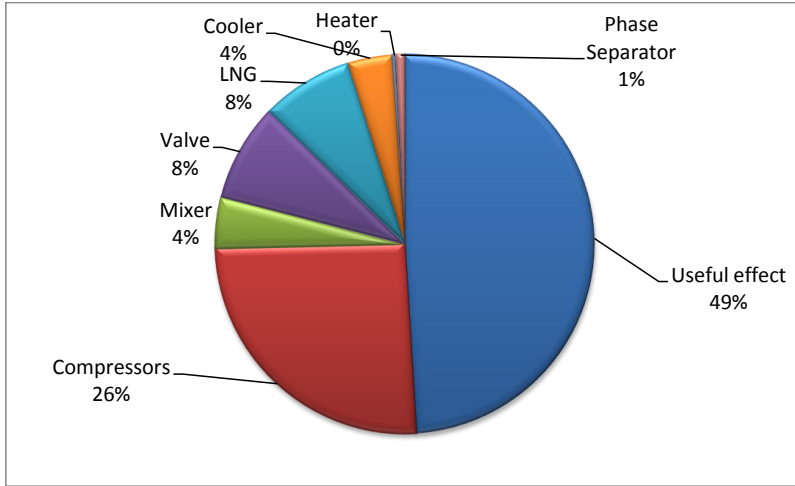


Figure 7.0-6 Exergy Losses for APCI Model

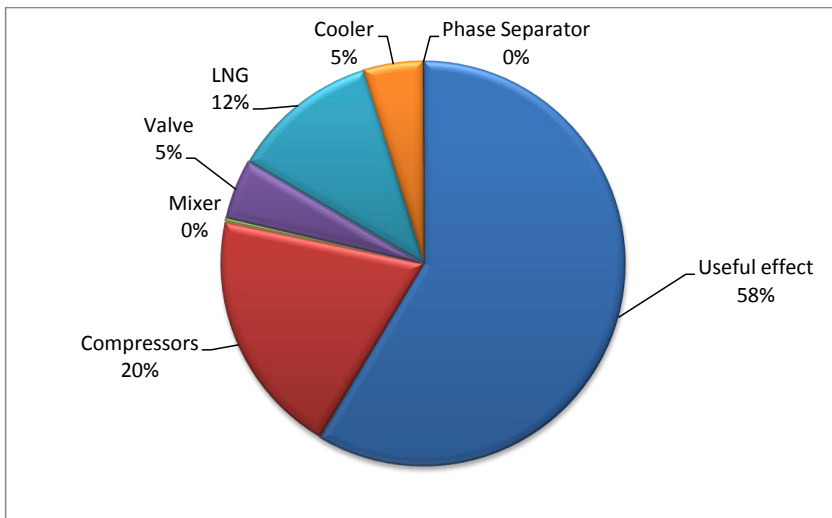


Figure 7.0-7 Exergy Losses for Shell Model

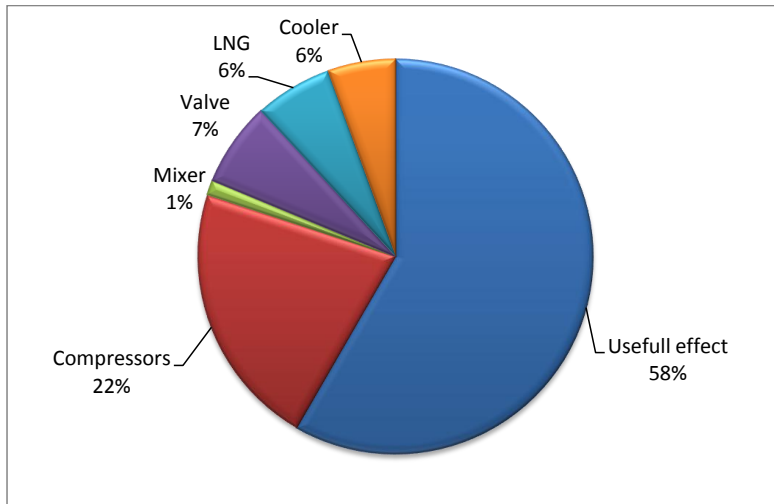


Figure 7.0-8 Exergy Losses for Liquefin Model

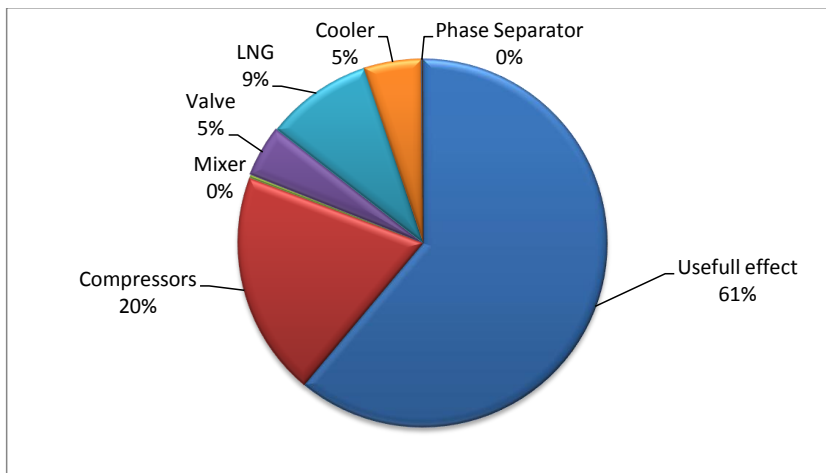


Figure 7.0-9 Exergy Losses for Tealarc Model

The compressors have the highest impact on the exergy losses, followed by the LNG heat exchangers and coolers and mixers. Particular attention should be paid to the APCI model, that has not only the lowest useful effect percentage, but also a result which is lower than the useful effect of the initial model.

8. Discussions

This chapter consists of a discussion of the performance of the Hyprotech SQP optimizer that was used for solving the optimization problem for the four DMR process alternatives. A comparison between the optimized solution and the initial solution, together with a thermodynamic analysis discussion is included as well.

8.1 Hyprotech SQP Performance

The performance of the optimizer using the SQP method was studied when aiming to minimize the objective function, and adjust the variables in order to meet the constraints. The output results of the optimizer were also analyzed.

Objective Function

The aim of the optimization problem was to minimize the objective function. Figure 8.1 shows how much the objective function was minimized during the optimization operation for the four DMR process alternative studies. The initial values are compared with the optimized values. It can be noted that the APCI process was the best optimized alternative with a 12% decrease in the objective function, while the specific power consumption of the Liquefin process was minimized by 9% of its original value.

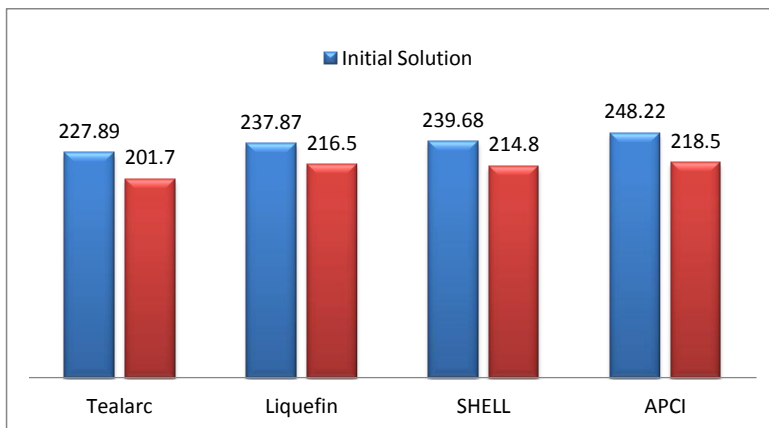


Figure 8.0-1 Objective Function Values, kWh/ton of LNG

Constraints

The best way to study the performance of the optimizer was to look at the constraints values after the optimization operation. A good optimization algorithm would be able to meet the constraints and minimize the objective function at the same time. However, this was not the case for the Hyprotech SQP method that was used in the HYSYS optimizer. Although the program was able to minimize the objective function to a certain extent, the constraints were violated. Table 8.1 shows how much the constraints were violated for each optimized alternative.

Table 8.0-1 Constraints Values Comparison Table

Constraints	Setup Value	APCI		Shell		Tealarc		Liquefin	
		Value	Error	Value	Error	Value	Error	Value	Error
LNG1	3 K	2.9 K	3%	3 K	0%	2.5 K	17%	2.9 K	3%
LNG2	3 K	2.4 K	20%	3 K	0%	2.2 K	27%	2.9 K	3%
LNG3	3 K	2.9 K	3%	3 K	0%	2.2 K	27%	2.9 K	3%
LNG4	3 K	-	-	3.3 K	0%	7.4 K	0%	2.1 K	30%
LNG5	3 K	-	-	-	-	1.3 K	57%	-	-
LNG6	3 K	-	-	-	-	3 K	0%	-	-
Superheating 1	5 K	1.7 K	66%	2.7 K	46%	0.5 K	90%	6 K	0%
Superheating 2	5 K	2.2 K	56%	14.8 K	0%	34 K	0%	19 K	0%

The constraints were set as inequality constraints, so the values obtained should have been more or equal to the setup values. The errors in yellow represent in percentage, how much the constraints were violated for each process. If a constraint value was higher than the setup value, then the error was selected to be 0. It can be noticed that the Shell model managed to meet all the minimum approach temperature constraints in the heat exchangers, while in the Liquefin process the optimizer managed to meet all the superheating values. There seems to be a trade-off between either meeting the minimum temperature approach in the LNG heat exchangers, violating the superheating values of the streams going to the compression stage, or meeting the superheating constraints and violating the minimum temperature approach in

the cryogenic exchangers. Unfortunately, the optimizer was not able to meet all the constraints in the same time. However, the constraints in the Shell model are the least violated, making it the most successful optimization solution from the four options.

CPU Time

The average CPU time for one optimization problem is the most relevant result from the optimizers running results, besides the objective value. Figure 8.2 shows the average CPU time in minutes for each alternative optimized.

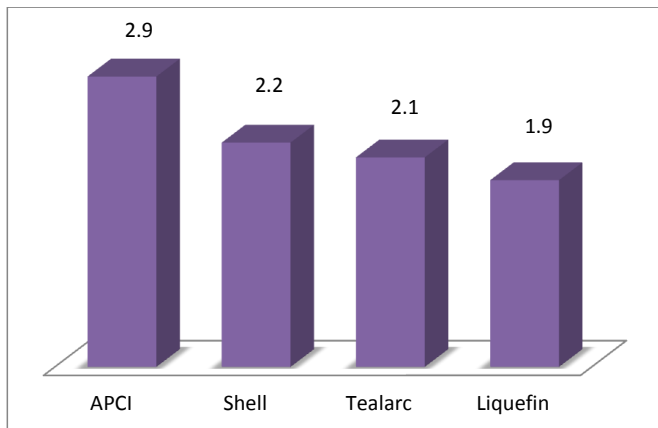


Figure 8.0-2 Average CPU Time Comparison

The longer the time taken to solve one optimization problem, the higher the chances to obtain the best local solution. However, depending on the design of each process and its constraints, it was sometimes difficult to get the optimizer to run for longer periods of time. When the setup parameters of the optimizer were varied in the second step of the optimization strategy, the CPU times of one iteration would last a few seconds until the optimizer would give the termination reason as "Stopped" or "Unbounded". The Liquefin process was the most challenging alternative to optimize as it was difficult to find good boundaries within which the variables would be adjusted. Surprisingly, the APCI model took the most time to run an optimization problem, however, the program was not able to meet any of the constraints. On the contrary, the Liquefin process took the shortest period of time to solve an optimization problem, and the program managed to meet the superheating results.

8.2 Power Consumption

The specific power consumption of the liquefaction process is determined mainly by the power of the compressors. Figure 8.3 shows the values of the total power consumption for all four DMR process optimized alternatives, comparing them with the values from the initial solution. For the calculation of the power consumption for the APCI model, the power of the pump was also taken into consideration. Although the Tealarc process has the lowest compression power, it is the APCI model that decreased the most in value, from 93.27 MW to 82.76 MW. However, as it was noticed previously, the Shell model was the one able to meet the most process constraints during the optimization.

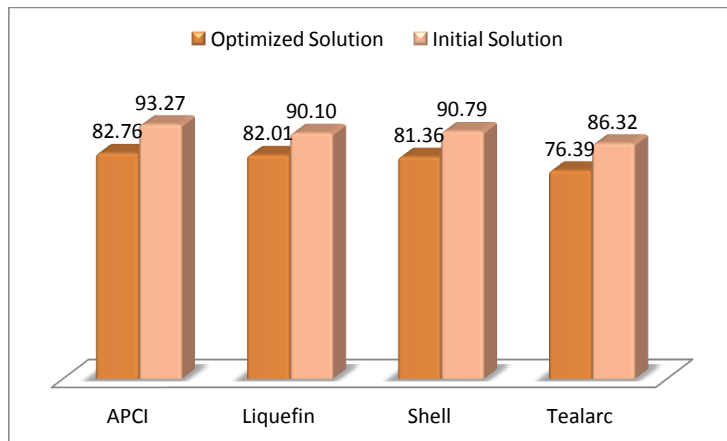


Figure 8.0-3 Total Power Consumption, MW

In order to understand why the compressors power was reduced, a closer look is taken at the variables that were adjusted during the optimization: the MRs component molar flow rates and their inlet pressures, as well as the corresponding pressure levels.

Mixed Refrigerants Component Molar Flow Rates

The compressors power is influenced by the flow rate of the mixed refrigerants and by the suction temperature. Increasing the flow rate of the MRs, will increase the compressors work. A lower compressor suction temperature will give a lower compressor work. In order to achieve lower suction temperatures, the MR streams need to contain lighter components, such as nitrogen or methane. If the molar flow rate of methane is increased then the dew point

temperature of the stream is decreased, thus decreasing the compressor suction temperature, which should be 5K above the dew point, as stated in the process constraints. However, if heavier hydrocarbons are added to the new optimized mixture, then the dew point of the stream may increase again.

Figures 8.4 and 8.5 show the phase envelopes for the two mixed refrigerants for the APCI process alternative, that were modeled in PROII. For a better understanding on how the composition has changed, they were plotted together with the phase envelope of the same stream for the initial solution. The green lines represent the boiling point curves of the initial and optimized solution, while the violet lines represent the dew point curves of the same streams.

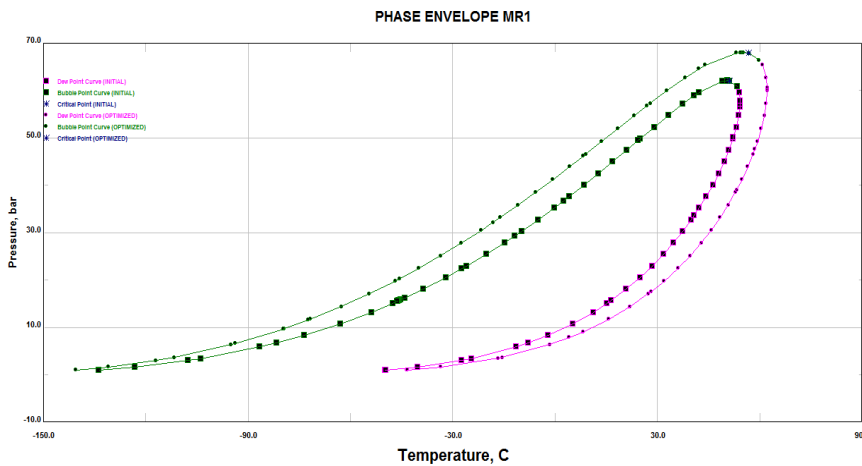


Figure 8.0-4 MR1 Stream Phase Envelope APCI

For the first mixed refrigerant, the dew point curve shifted to the right, while the boiling point curve shifted to the left. The phase envelope of the optimized MR1 composition is wider, with a higher dew point than the initial solution. This might be surprising considering the fact that the compressor work for the pre-cooling stage decreased after optimization. Also, the total flow rate of MR1 increased after optimization.

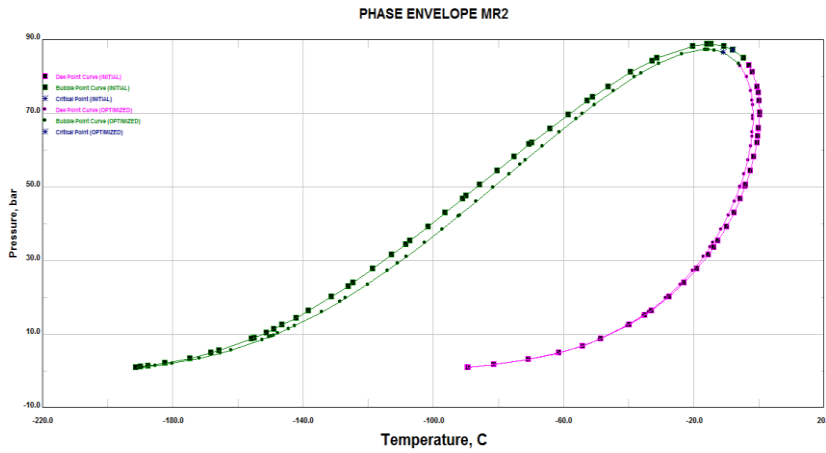


Figure 8.0-5 MR2 Stream Phase Envelope APCI

For the second mixed refrigerant, the dew point curve slightly shifted to the left, resulting in a lower dew point temperature for the stream entering the liquefaction process. The boiling point curve shifted to the right, resulting in a higher boiling point temperature.

Figures 8.6 and 8.7 show the phase envelopes for the Shell process alternative. Here, the phase envelope for the first mixed refrigerant is moved entirely to the right. The flow rates of ethane and propane have increased, while the flow rate of a heavier hydrocarbon, the i-butane, has decreased.

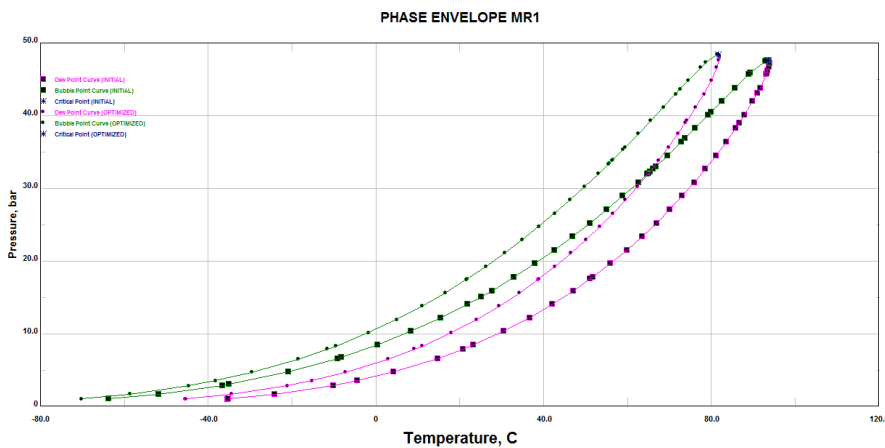


Figure 8.0-6 MR1 Stream Phase Envelope Shell

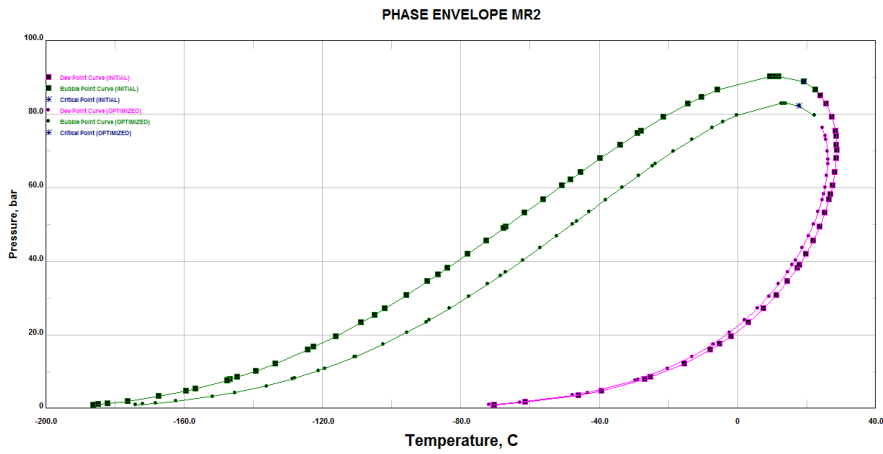


Figure 8.0-7 MR2 Stream Phase Envelope Shell

For the optimized version of the second mixed refrigerant, the phase envelope shifted to the left for the dew point curve and to the right for the boiling point curve. The dew point temperature of the optimized MR2 stream is lower now, due to the increase of the methane and ethane flow rates.

Figures 8.8 and 8.9 show the behavior of the phase envelope for the Tealarc process alternative, when the composition of the two mixed refrigerants is optimized.

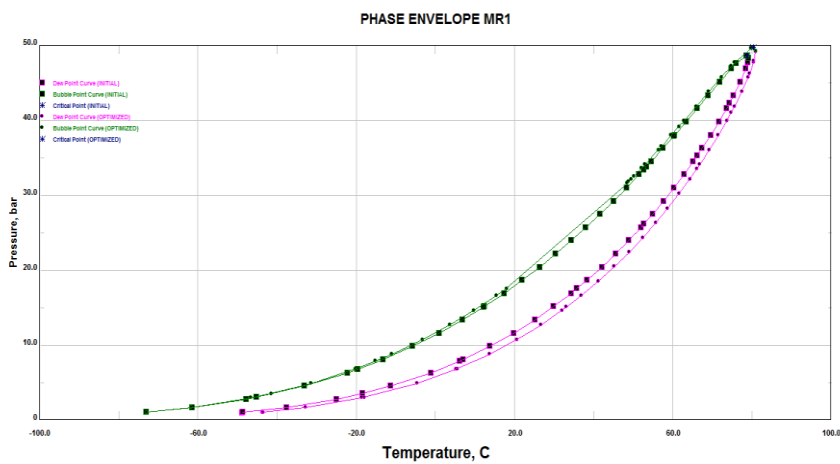


Figure 8.8 MR1 Phase Envelope Tealarc

Here, the dew point curve for the optimized MR1 has moved to the right, while the boiling point curve has slightly moved to the left. The difference is very small, since the increase of the lighter component, ethane, was balanced by an increase of the heavier component, the n-butane, as well as a decrease of propane.

Although the phase envelope shape for the MR1 stream did not change too much, there was a 3.7 MW reduction in the compression stage.

For the second mixed refrigerant, the variation in the composition between the initial and the optimized solutions can be observed more easily, in Figure 8.9. Here, the optimized MR2 phase envelope moved to the right, reducing the boiling point temperature and increasing the dew point temperature of the MR2 stream. However, it can also be observed that the cricondebar, which is the pressure critical point, has a lower value. This means that the higher pressure limit has been lowered.

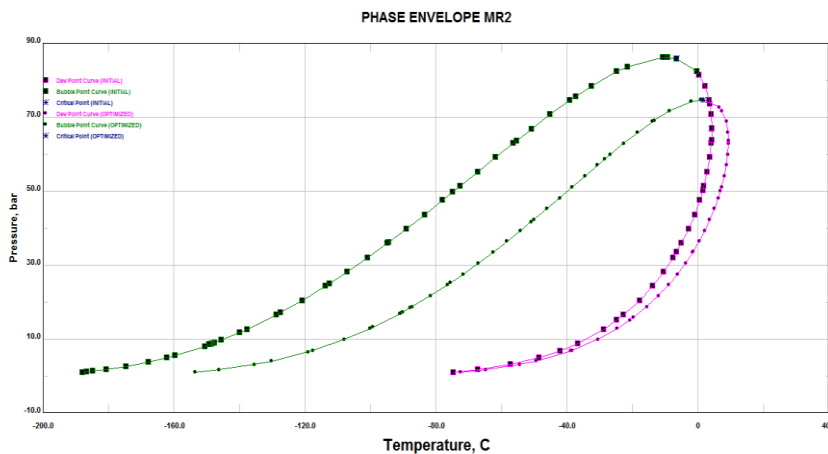


Figure 8.9 MR2 Phase Envelope Tealarc

Figures 8.10 and 8.11 show the phase envelope behavior of the MRs streams for the Liquefin process alternative.

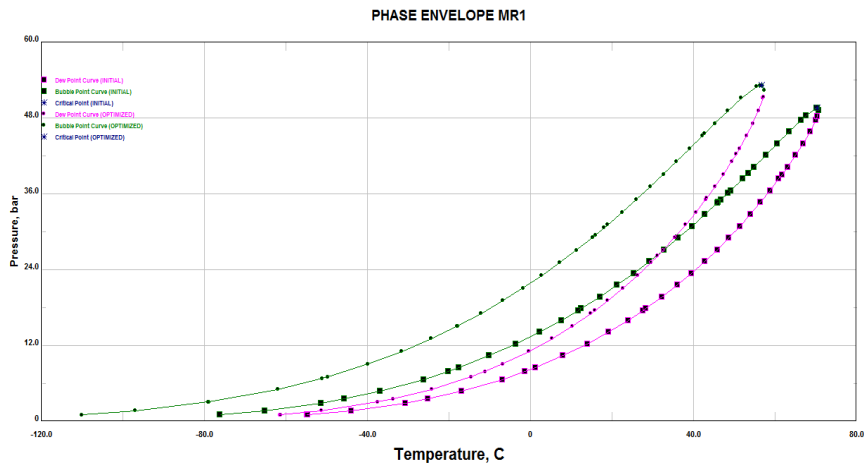


Figure 8.9 MR1 Phase Envelope Liquefin

The dew and boiling point curves for MR1 have both shifted to the left, decreasing their dew point and boiling point temperatures for the same pressure levels. The change in the dew point curve is due to the presence of methane in the optimized solution, and the increase of ethane, while decreasing the propane molar flow rate. However, the inlet pressure of MR1 increased from 20 to 41.1 bar, increasing the stream dew point temperature over the initial value.

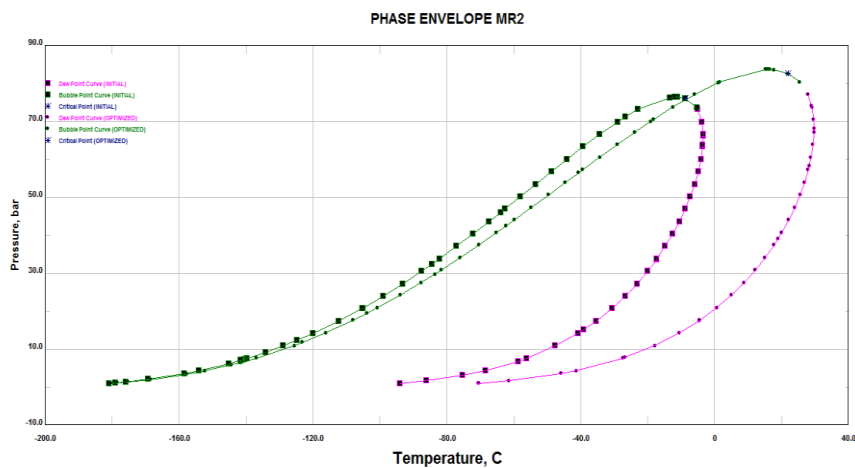


Figure 8.10 MR2 Phase Envelope Liquefin

In the second mixed refrigerant, the molar flow rate of the most volatile component decreased. For that reason the dew point curve shifted to the right, increasing its dew point temperature, while the boiling point curve shifted a little to the right as well, due to the increase of the propane molar flow rate. An increase in the dew point temperature requires an increase in the flow rate of the mixed refrigerant in order to be able to reach the temperatures required by the liquefaction process.

Inlet Pressures and Pressure Levels

The higher the difference between the inlet pressure and the pressure level, the lower the compressors power is. When looking at the phase envelope for MR1 for the Liquefin process, for example, there can be noticed a higher temperature drop in the dew point at the inlet pressure, and the dew point at the first pressure level, for the optimized solution than for the initial solution. This gives a better heat distribution within the heat exchanger, which will lead to a higher vapor density of the lead to a lower volume flow, which will, of course, decrease the compressor work. Figures 8.11 and 8.12 show the vapor density versus temperature for the same MR1 stream in the first LNG heat exchanger for both optimized and initial solutions.

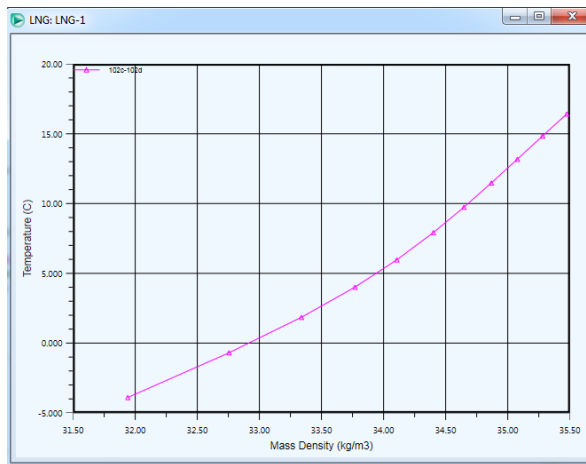


Figure 8.11 Vapor Density Vs. Temperature Optimized Solution

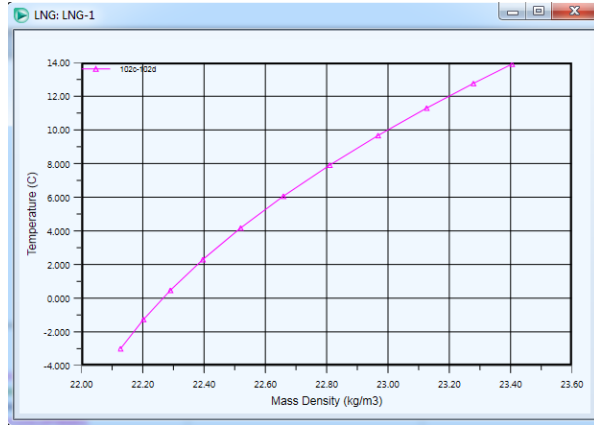


Figure 8.12 Vapor Density Vs. Temperature Initial Solution

The higher vapor density of the optimized solution gives an actual volume flow rate for the stream that enters the compression stage of $1.82 \times 10^4 \text{ m}^3/\text{h}$, while the initial solution had an actual volume flow rate of $3.48 \times 10^4 \text{ m}^3/\text{h}$. The compressor work in the pre-cooling stage is reduced in the optimized solution from 40.4 MW to 38.6 MW, and in the liquefaction stage from 49.7 MW to 43.3 MW.

The number of pressure levels also influences the compressor work. The higher the number of pressure levels, the lower the compressors work is. Liquefin model is, again, considered as an example. In the pre-cooling stage, natural gas is cooled to a temperature of -30°C . The cooling is done using three LNG heat exchangers at three different pressure levels. In the first heat exchanger, the natural gas stream is cooled to 0°C . A fraction of the mixed refrigerant is expanded to a pressure that gives the necessary temperature to achieve the 0°C in the natural gas stream. The rest of the mixed refrigerant flow is sent to the second LNG heat exchanger, where again, a fraction of it is expanded to a different pressure enough to meet the specifications for the natural gas outlet temperature. The last fraction of the MR1 flow rate is then expanded to the lowest pressure in order to achieve -30°C in the natural gas stream leaving the pre-cooling stage. Now, a smaller volume of gas is going to be compressed from the lowest pressure to the initial value, leading to a lower compressor work. The process flow schemes of the four DMR alternatives are found in the Appendixes A to D, and they can be consulted to see different pressure levels for different alternatives.

8.3 Heat Transfer in Cryogenic Heat Exchangers

The heat transfer within the cryogenic heat exchangers was analyzed through the composite curves of the hot and cold streams involved in the process. The composite curves for the optimized solution were compared with the ones from the initial solution.

Figures 8.13, 8.14, 8.15, 8.16 and 8.17 present the plotted composite curves for both initial and optimized solution for all four DMR process alternatives. For the Tealarc DMR process, the natural gas stream is not present in the pre-cooling stage, and the MR1 stream is not present in the liquefaction stage, so two different charts were plotted to show how the hot and cold streams vary with the heat flow throughout the heat exchangers. The composite curves can be found in the Appendixes E to N at a larger resolution.

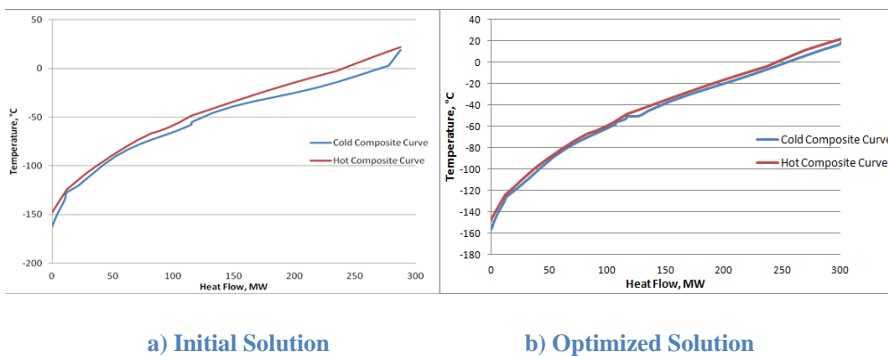


Figure 8.13 Composite Curves for APCI

The hot and cold composite curves for the APCI model are closer to each other, giving a better heat transfer within the cryogenic heat exchangers. The Pinch points are determined by the inlet temperature of the three LNG heat exchangers. The shape of the curves is determined by the temperature distribution within the exchangers, and the temperature distribution is influenced by the composition of the streams. The optimizer was able to find a better solution of the composition of the mixed refrigerants, and this was expected, as the variables boundaries were manipulated always after consulting the composite curves for each LNG heat exchanger.

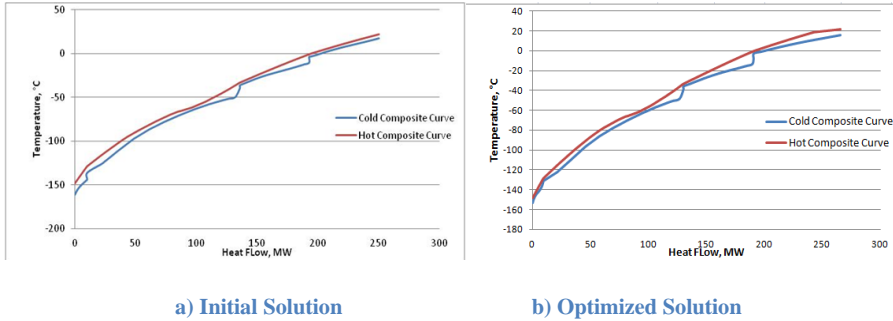


Figure 8.14 Composite Curves for Shell

The shape of the hot and composite curves for the Shell model in the optimized solution looks similar to the one in the initial solution. The only exception is at the cold end of the curves, where there can be noticed a better heat distribution. However, the optimizer was not able to find a better solution for the rest of the cooling curve. The minimum approach in all heat exchangers met the inequality constraint of $\geq 3K$.

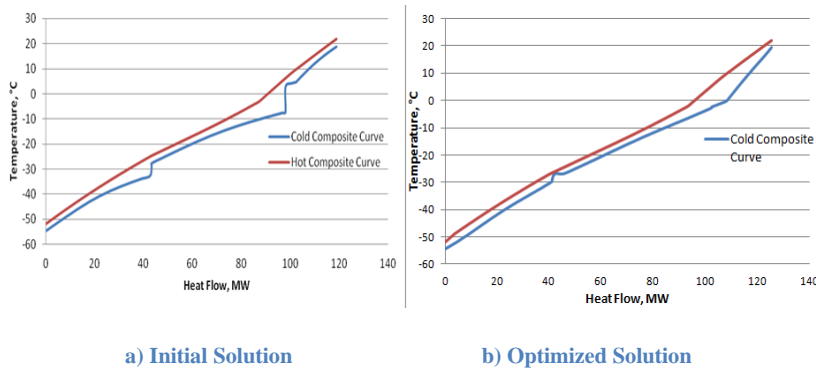
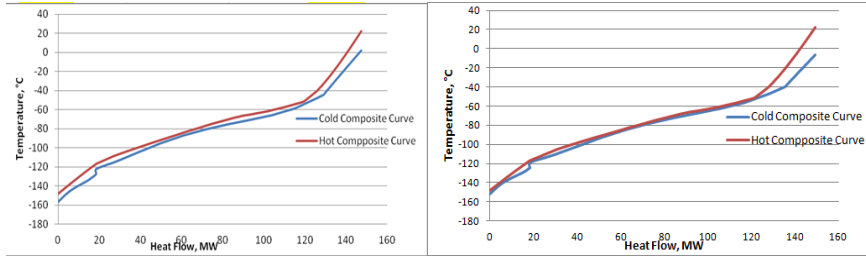


Figure 8.15 Composite Curves for the Pre-Cooling Stage Tealarc

For the Tealarc model, it can be seen an improvement in the shape of the cold composite curve for the pre-cooling stage. The composition of the mixed refrigerants was manipulated in order to achieve a better temperature distribution within the cryogenic heat exchangers. However, the minimum temperature approach constraint was not entirely fulfilled by the optimizer.

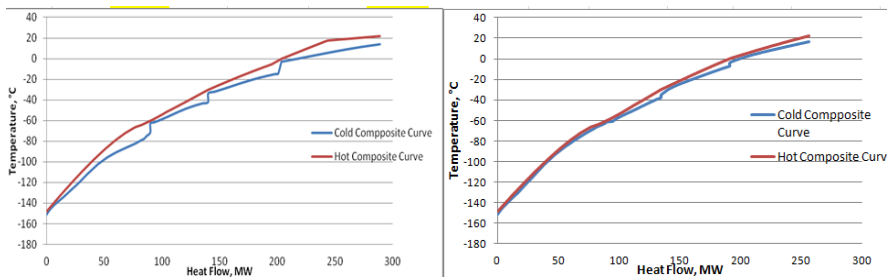


a) Initial Solution

b) Optimized Solution

Figure 8.16 Composite Curves for the Liquefaction Stage Tealarc

In the liquefaction stage, however, the optimizer was not able to manipulate the composition of the second mixed refrigerant so that a better temperature distribution would take place within the LNG heat exchangers. Also, the minimum temperature approach constraint was not entirely fulfilled by the optimizer.



a) Initial Solution

b) Optimized Solution

Figure 8.16 Composite Curves for the Liquefaction Stage Liquefin

The shape of the cold composite curve for the Liquefin model suggests a better temperature distribution within all four heat exchangers present in the DMR process. However, the minimum approach temperature constraint was as well violated by the optimizer.

8.4 Compactness

For the design of a LNG plant, the compactness of the system is important, especially for floating platforms, where space is one of the parameters that is taken into consideration when choosing the right liquefaction process. Therefore, the compactness of the four alternatives has been calculated to a certain extent, only from the liquefaction process point of view. The size of the cryogenic heat exchangers and the size or the compressors, as well as the number of equipment were considered.

Cryogenic Heat Exchangers

Tables 8.2 and 8.3 present the duty, UA, LMTD, and the f_T values from the Aspen HYSYS models for the cryogenic heat exchangers in all four DMR process alternatives, for both initial and optimized solutions.

Q stands for the duty, in MW and was calculated as the sum of the duties of all LNG exchangers.

UA represents the product between the overall heat transfer coefficient (U) and the heat transfer area (A), in $MW/^\circ C$ and was calculated as the sum of the UA values for all LNG exchangers in the process. Counter-current flow was assumed in all heat exchangers.

LMTD stands for the logarithmic mean temperature difference, in $^\circ C$ and was calculated as an average value for all the LNG heat exchangers in the liquefaction process.

F_T is a correction factor, used to correct the logarithmic mean temperature. The correction factor depends on the geometry of the heat exchangers, as well as the inlet and outlet temperatures of the hot and cold streams.

Table 8.0-2 Cryogenic Heat Exchangers Design Initial Solution

Process/Parameter	APCI	Shell	Tealarc	Liquefin
Q, MW	287.5	250.2	266.4	289
UA, MW/°C	43.4	50.2	56.6	40.3
LMTD, °C	7.1	6.7	6.4	7.1
f_T	0.9	0.75	0.74	1

Table 8.0-3 Cryogenic Heat Exchangers Design Optimized Solution

Process/Parameter	APCI	Shell	Tealarc	Liquefin
Q, MW	300.4	266.0	274.82	256.03
UA, MW/°C	82.9	46.0	92.89	77.85
LMTD, °C	4.0	5.6	5.91	3.77
f_T	0.9	1	0.5	0.9

A low correction factor indicates a non-reasonable close temperatures between cold and hot streams. The correction factor for the Tealarc process is very low, which actually confirms the violated constraints from the optimization operation, were the minimum approach temperature for the fifth LNG heat exchangers is 1.3 K.

Based on the values from the initial and optimized solutions, Liquefin is the only process that has lowered its heat exchangers duty. However, its UA value is higher, because of the lower LMTD, which will imply a higher heat transfer area. From the optimized solution, Shell model is the best alternative for a floating LNG platform.

Compressor Suction Volume

The suction volume is one of the parameters that dictate the size of the compressors. Tables 8.4 and 8.5 present the values for the compressor suction volume for both mixed refrigerants for the DMR alternatives, for the initial and optimized solutions.

Table 8.0-4 Compressor Suction Volume for the Initial Solution

Compressor Suction Volume, m^3/h	APCI	Shell	Tealarc	Liquefin
MR1	81,825	80,850	80,241	105,630
MR2	90,352	187,209	122,756	93,913
Total	172,177	268,059	202,997	199,543

Table 8.5 Compressor Suction Volume for the Optimized Solution

Compressor Suction Volume, m^3/h	APCI	Shell	Tealarc	Liquefin
MR1	69,804	67,275	82,068	58,445
MR2	74,338	158,099	102,565	111,294
Total	144,142	225,374	184,632	169,739

In the initial solution, the APCI model requires the lowest compressor suction volume. After optimization, APCI process still requires the lowest compressor suction volume, however, all the other processes have reduced their compressor volume substantially. Liquefin process has reduced in half the compressor suction volume in the pre-cooling stage.

Figure 8.17 shows better the combined suction volume improvement for each alternative for the overall liquefaction process. The best improvement can be seen in the Shell process, where the suction volume has decreased with 16% from its initial value.

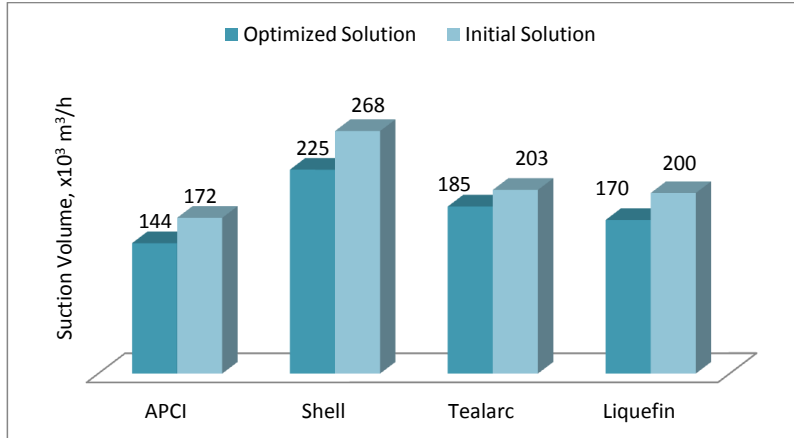


Figure 8.17 Compressor Suction Volume Comparison

Number of Equipment

The complexity of the process also has an impact on the compactness of the system, and Table 8.6 presents the number of the most important pieces of equipment for each alternative considered. The valves, mixers, splitters and flash gas separator were not included when counting the main equipment pieces. The number of equipment is the same for the optimized solution as for the initial alternative, since neither the composition, nor the pressure change had an impact on the design of the process.

Table 8.6 Number of Equipment in DMR Process Alternatives

Alternative/ Equipment	APCI	Shell	Liquefin	Tealarc
Compressor	5	5	6	5
Pump	1	0	0	0
Cooler	5	4	4	5
LNG	3	4	4	6
Phase separator	3	1	0	1
TOTAL	17	14	14	17

Although Shell and Liquefin alternatives have both the smallest number of equipment pieces; the size of the equipment will also have to be taken into consideration when deciding for the compactness of the system.

8.5 Safety

Safety is crucial in any type of plant, be it onshore or offshore. Offshore platforms have a limited escape routes, so before choosing the right liquefaction process for a floating device, a safety analysis should be done. Some of the important parameters used to measure the safety level for a liquefaction process are the flammability of the components used, the flow rate of the refrigerants as well as their phase state.

Flammability of Refrigerants

The hydrocarbons components are flammable. However, some of them are more flammable than others, so it is good practice to look into the composition of the refrigerants used in the liquefaction cycle, in order to determine their flammability rate. Since all DMR processes use hydrocarbons, all four alternatives are considered to be highly flammable. Propane is one of the hydrocarbons which is extremely flammable, so special attention is paid to its presence in the MR mixtures.

Figure 8.18 and 8.19 show the total molar flow rate of propane found in the two mixed refrigerants for both initial and optimized solution.

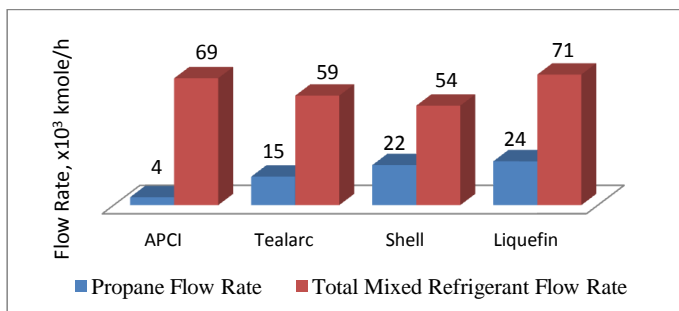


Figure 8.18 Propane and Mixed Refrigerant Flow Rates Initial Solution

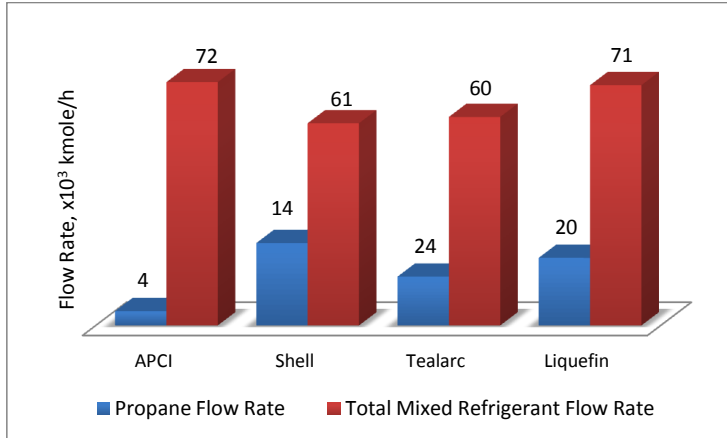


Figure 8.19 Propane and Mixed Refrigerant Flow Rates Optimized Solution

The APCI process is by far the best option, containing the lowest amount of propane in the mixed refrigerant mixtures for both initial and optimized solution. There is little variation in the amount of mixed refrigerants and propane in the optimized solution compared to the initial solution.

Mixed Refrigerants Flow Rate

Figure 8.20 shows how much have the molar flow rates of the mixed refrigerants increased after optimization.

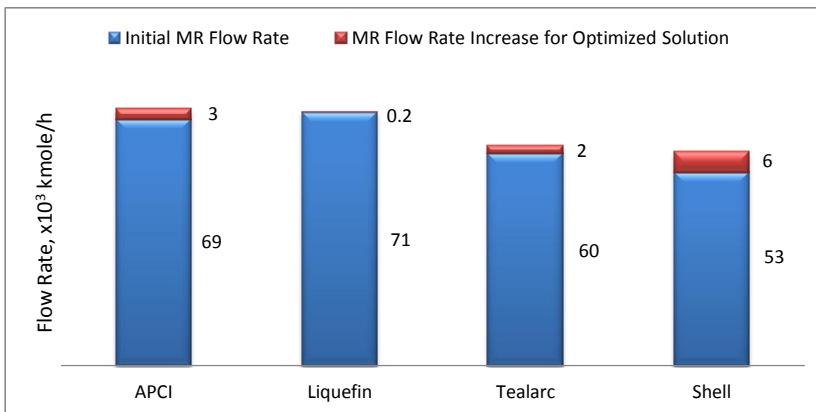


Figure 8.20 Mixed Refrigerants Flow Rate Increase for the Optimized Solution

Shell DMR process alternative uses the lowest amount of mixed refrigerants, while the APCI process uses 20% more MRs for the liquefaction of the same amount of natural gas flow rate.

Refrigerant Phases

Refrigerants in the DMR processes are circulating in both liquid and vapor form throughout the system. A certain amount of refrigerant will be stored on the plant, to complete the cycle, when needed, so attention should be paid when choosing the storage tanks. Since liquid has a higher energy density, in case of leakage, the fire would be more intense. However, in case of leakage in the gas form, above a certain percentage, hydrocarbons are toxic and affect the central nervous system.

9. Conclusions

The main objective of the master thesis was to test the performance of the Hyprotech SQP optimizer in the commercial simulator Aspen HYSYS on four different DMR process alternatives. The results from the optimization problem were used to compare the efficiencies of the four alternatives. For a better comparison, an exergy analysis was conducted for each process, in order to find which process operates with the least exergy losses, and to be able to spot a potential improvement in the existing process configuration.

Tables 9.1 and 9.1 give an overview of the main parameters that were considered for the comparison of the four DMR alternatives, for the initial and the optimized solutions.

Table 9.0-1 Summary of Parameters for the Initial DMR Alternatives

Parameter	Shell	APCI	Liquefin	Tealarc
Specific Power Consumption, kWh/ton	239.68	248.24	237.87	227.90
Exergy Efficiency, %	54.20	53.33	54.81	55.94
UA, $MW/°C$	50.24	43.44	40.26	56.64
Total Suction Volume, m^3/h	268,059	172,177	199,543	202,997
Total Mixed Refrigerant Flow Rate, $kgmole/h$	53,735	68,537	70,548	59,139
Propane Flow Rate, $kgmole/h$	21,608	4,305	23,674	15,391
Number of Equipment	14	17	14	17

The best value for each parameter considered is highlighted in green. By comparing the values for the initial and the optimized solution, we can observe that, while the specific power consumption has decreased after optimization, the values for the other parameters have increased.

Table 9.0-2 Summary of Parameters for the Optimized DMR Alternatives

Parameter	Shell	APCI	Liquefin	Tealarc
Specific Power Consumption, kWh/ton	214.8	218.5	216.5	201.7
Exergy Efficiency, %	53.3	52.4	52.9	56.8
UA, $MW/°C$	46.0	82.9	77.85	92.89
Total Suction Volume, m^3/h	225,374	144,142	169,739	184,632
Total Mixed Refrigerant Flow Rate, $kgmole/h$	59,557	71,678	70,777	61,418
Propane Flow Rate, $kgmole/h$	24,260	4,207	19,914	14,372
Number of Equipment	14	17	14	17

When designing a liquefaction process for a floating platform, not all the parameters will be of the same importance. The compactness of the system has an impact on the investment costs and on the space availability on the floating device; however, the energy that needs to be delivered in the system, the specific power consumption, has a high impact on the energy costs. The flow rate of the mixed refrigerants has an impact on safety when deciding which process to choose for an offshore platform. In order to be able to make a fair comparison between the solutions, each parameter was given a score, according to its importance, which can be found in Table 9.3.

Table 9.0-3 Assessment of the Main Parameters

Parameter	Score
Specific Power Consumption, kWh/ton	3
Exergy Efficiency, %	3
UA, $MW/°C$	2
Total Suction Volume, m^3/h	2
Total Mixed Refrigerant Flow Rate, $kgmole/h$	2
Propane Flow Rate, $kgmole/h$	3
Number of Equipment	1

A parameter that receives a score of 3 is of the utmost importance, 2 - very important and 1- important. Further, each process has been given a grade from 1 to 4, based on the parameters values. For example, for the specific power consumption parameter, the lowest value will receives grade 4, while the highest value will receive grade 1. On the contrary, for the exergy efficiency parameter, the lowest value will receive grade 1, while the highest value will receive grade 4. The grades have been given as per Tables 9.4 and 9.5.

Table 9.0-4 Grading Assessment of the Initial DMR Alternatives

Parameter	Shell	APCI	Liquefin	Tealarc
Specific Power Consumption, kWh/ton	2	1	3	4
Exergy Efficiency, %	2	1	3	4
UA, $MW/°C$	2	3	4	1
Total Suction Volume, m^3/h	1	4	3	2
Total Mixed Refrigerant Flow Rate, $kgmole/h$	4	2	1	3
Propane Flow Rate, $kgmole/h$	2	4	1	3
Number of Equipment	4	3	4	3

Table 9.0-5 Grading Assessment of the Optimized DMR Alternatives

Parameter	Shell	APCI	Liquefin	Tealarc
Specific Power Consumption, kWh/ton	3	1	2	4
Exergy Efficiency, %	3	1	2	4
UA, $MW/°C$	4	2	3	1
Total Suction Volume, m^3/h	1	4	3	2
Total Mixed Refrigerant Flow Rate, $kgmole/h$	4	1	2	3
Propane Flow Rate, $kgmole/h$	1	4	2	3
Number of Equipment	4	3	4	3

Finally, the total score for each alternative has been calculated with the formula from Equation 9.1:

$$final\ score = \sum score * grade \quad [9.1]$$

For the optimized solution, a correction factor is introduced, to compensate for the fact that the optimizer was not able to meet the constraints. For the alternatives that were able to fulfill the constraints to 100%, the final score will be multiplied with a correction factor of 1. Table 9.6 shows the values of the correction factor applied to the DMR alternatives.

Table 9.0-6 Correction Factor for the Optimized Alternatives

DMR Alternatives	Correction Factor, <i>f</i>
Shell	0.9
Liquefin	0.8
APCI	0.7
Tealarc	0.5

Thus, the final scores for the initial and optimized alternatives are presented in Table 9.7.

Table 9.7 Final Assessment of the Initial and Optimized Solutions

DMR Alternative	Initial Solution	Optimized Solution
Shell	36	38.7
APCI	39	24.5
Liquefin	41	30.4
Tealarc	48	24

From Table 9.7 it can be seen that the best DMR alternative for an offshore platform would be the Tealarc process, where models are build on the initial MR composition and pressures. After optimization, the Shell process turns out to be the best alternative, based on the optimized conditions. However, this table actually shows the performance of the optimizer: how much it was able to minimize the objective function while meeting the constraints. Although the specific power consumption of the optimized alternatives are lower, the surface area of the cold box has increased, so a sensible trade-off between the maintenance costs and investment cost should be taken into consideration when choosing the right alternative.

Based on the results from this project, the optimized Shell DMR process is considered to be the best solution for an offshore LNG platform, with a power consumption of 214.8 kWh/ton of LNG. For a further optimization of the process, a different optimization method is recommended, as the performance of the Hyprotech SQP optimizer in Aspen HYSYS was not considered to be adequate.

10. Further Work

There are several aspects that were considered out of scope for this project and further work can involve dealing with the following steps:

- A sensitivity analysis could be performed for understanding the flexibility of the process; by varying the sea water temperature and the natural gas feed composition, pressure and temperature to see what impact it will have on the specific power consumption;
- Optimization of the configuration of the process, perhaps substituting the throttling valves for expanders where possible or changing the configuration of the compressors;
- Test the Hyprotech SQP optimizer for different variables, such as temperature levels throughout the cryogenic heat exchangers, or the phase of the mixed refrigerants at the inlet conditions;
- Further study on the exergy losses in order to minimize them, and increase the exergy efficiency;
- Further study for reducing the amount of propane in the mixed refrigerants;
- In-depth study on the compactness, weight and complexity of the system and how it would fit on a FLNG vessel;
- Study of the impact the sea motion has on the equipment on FLNG vessel;
- Develop a new nonlinear programming method that would give better results for the optimization problem.

References

- Andersen, M.N. (2012). Energy Solution for Floating LNG Production System, *Master Thesis*, NTNU, Trondheim, Norway.
- Aravind, P.V. Lecture Notes on Exergy Analysis, Munich, Technical University Munich.
- Aspelund et al., (2010). *An optimization-simulation model for a simple LNG process*, Computers and Chemical Engineering 34 Journal, p.1606-1617.
- AspenTech, (2011). *Aspen HYSYS Tutorials and Application*, Version Number: V8.6, Aspen Technology, Inc.USA.
- Austbø, B., (2015). *Use of Optimization in Evaluation and Design of Liquefaction Processes for Natural Gas*, NTNU, Doctoral Theses Trondheim, Norway.
- Austbø et al., (2013). *Constraint handling in stochastic optimization algorithms for natural gas liquefaction processes*, European Symposium on Computer Aided Process Engineering, June 9-12, Lappeenranta, Finland.
- Austbø, B., Gundersen, T., (2014). *Using Thermodynamic Insight in the Optimization of LNG Processes*, European Symposium on Computer Aided Process Engineering, June 15-18, Budapest, Hungary.
- Austbø, B., Løvseth, S.W., Gundersen, T., (2014). *Annotated bibliography—Use of optimization in LNG process design and operation*, Computers and Chemical Engineering 71 Journal, 391-414.
- Biegler, L., (2010). *Nonlinear Programming: concepts, algorithms, and applications to chemical processes*, SIAM, Philadelphia, US.
- Biegler, L., Grossmann, I., (2004). *Retrospective on optimization*, Computers & Chemical Engineering 28 Journal, 1169-1192.
- Boggs, P., Tolle, J. (1996). *Sequential Quadratic Programming*, Acta Numerica, pp. 1-000.
- Fredheim, A., Solbraa, E., Pettersen, J., & Bolland, O. (2013). *TEP 4185 Natural Gas Technology Compendium*, Trondheim: Department of Energy and Process Engineering, NTNU.

Gharagheizi et al., (2014). A Group Contribution Method for Determination of the Standard Molar Chemical Exergy of Organic Compounds, *Journal of Energy*, p. 1-10.

Grootjans et al., (2002). US Patent Shell US 6,370,910 B1.

Grossman, I., Biegler, L., (2004). *Part II. Future perspective on optimization*, Computers & Chemical Engineering 28 Journal, 1193-1218.

Khan et al., (2016). *Evolution and optimization of the dual mixed refrigerant process of natural gas liquefaction*, Applied Thermal Engineering 96, p. 320-329.

Kim, D., (2013). Comparison of New Liquefaction Processes for FLNG, *Specialization Project*, NTNU, Trondheim.

Lee et al., (2012). *Design and optimization of natural gas liquefaction and recovery processes for offshore floating liquefied natural gas plants*, Industrial and Engineering Chemistry Research, 51(30):10021-10030.

Lim et al., (2013). *Current Status and Perspectives of Liquefied Natural Gas (LNG) Plant Design*, Industrial & Engineering Chemistry Research Review.

Manescu, I. (2015). *The Dual Mixed Refrigerant Process for Natural Gas Liquefaction*, Specialization Project, NTNU, Trondheim, Norway.

Marmolejo-Correa, D., Gundersen, T., (2012). *New Graphical Representation of Exergy Applied to Low Temperature Process Design*, Industrial & Engineering Chemistry Research Review.

Morin et al., (2011). Using evolutionary Search to Optimize the Energy Consumption for Natural Gas Liquefaction, *Journal of Chemical Engineering Research and Design*, p. 2428–2441.

Nocedal, J., Wright, S.J., (1999). *Numerical Optimization*, Springer Science Business Media, LLC.

Paradowski et al., (2000). US Patent Liquefin 6,105,389.

Querol et al., (2011). *Novel Application for Exergy and Thermo-economic Analysis of Processes Simulated with Aspen Plus®*, Energy 36:964–974.

Querol et al., (2013). *Practical Approach to Exergy and Thermo-economic Analyses of Industrial Processes*, Springer.

Rivero R, Garfias M (2006) Standard chemical exergy of elements updated. *Energy* 31:3310–3326.

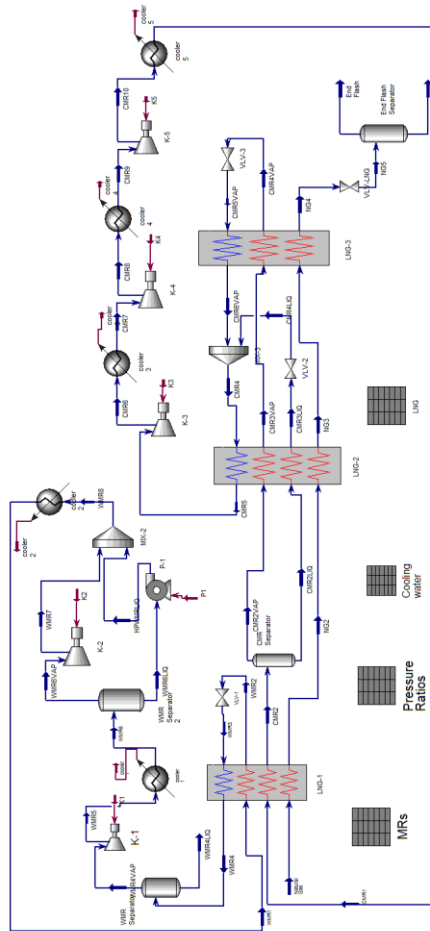
Roberts et al., (2000). US Patent APCI 6,119,479.

Rødstøl, E., (2015). *Optimization of FLNG Liquefaction Processes, Master Thesis*, NTNU, Trondheim, Norway

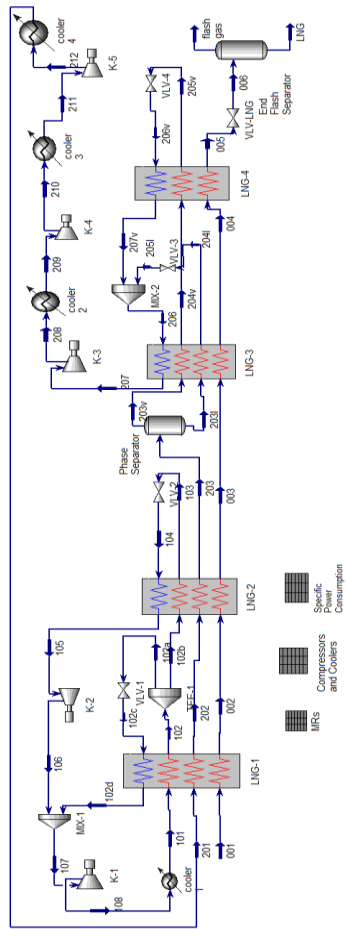
Venkatarathnam, G. (2008). *Cryogenic Mixed Refrigerant Processes*, Springer Science Business Media, LLC.

Wahl, P.E., Løvseth, S.W., Mølnvik, M., (2013). *Optimization of a simple LNG process using sequential quadratic programming*, *Computers and Chemical Engineering* 56 Journal, 27-36.

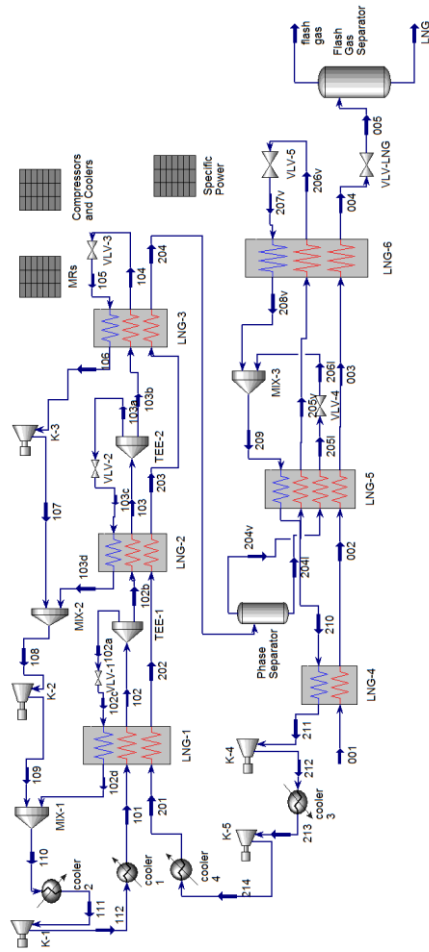
Appendix A: APCI DMR Process Flow Sheet



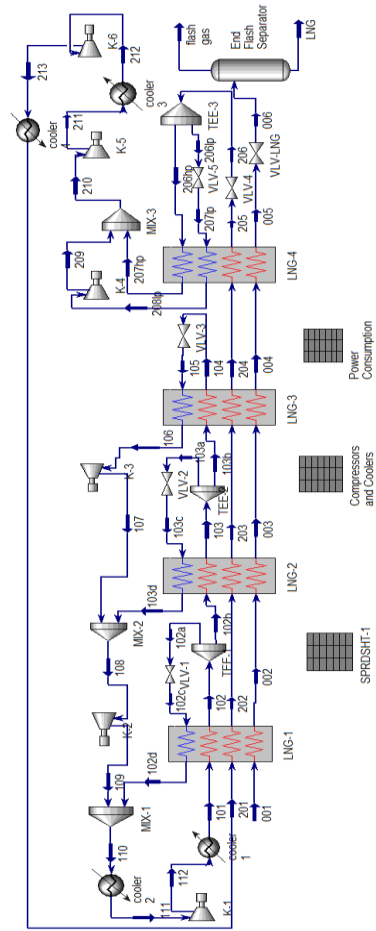
Appendix B Shell DMR Process Flow Sheet



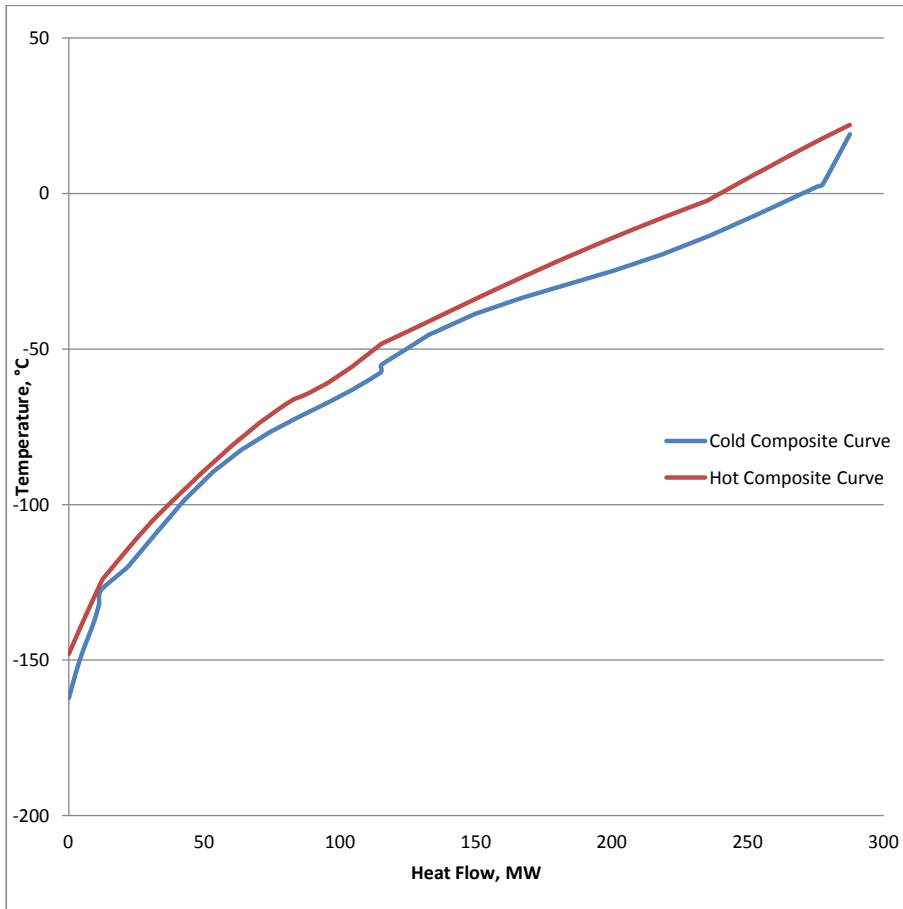
Appendix C Tealarc Process Flow Sheet



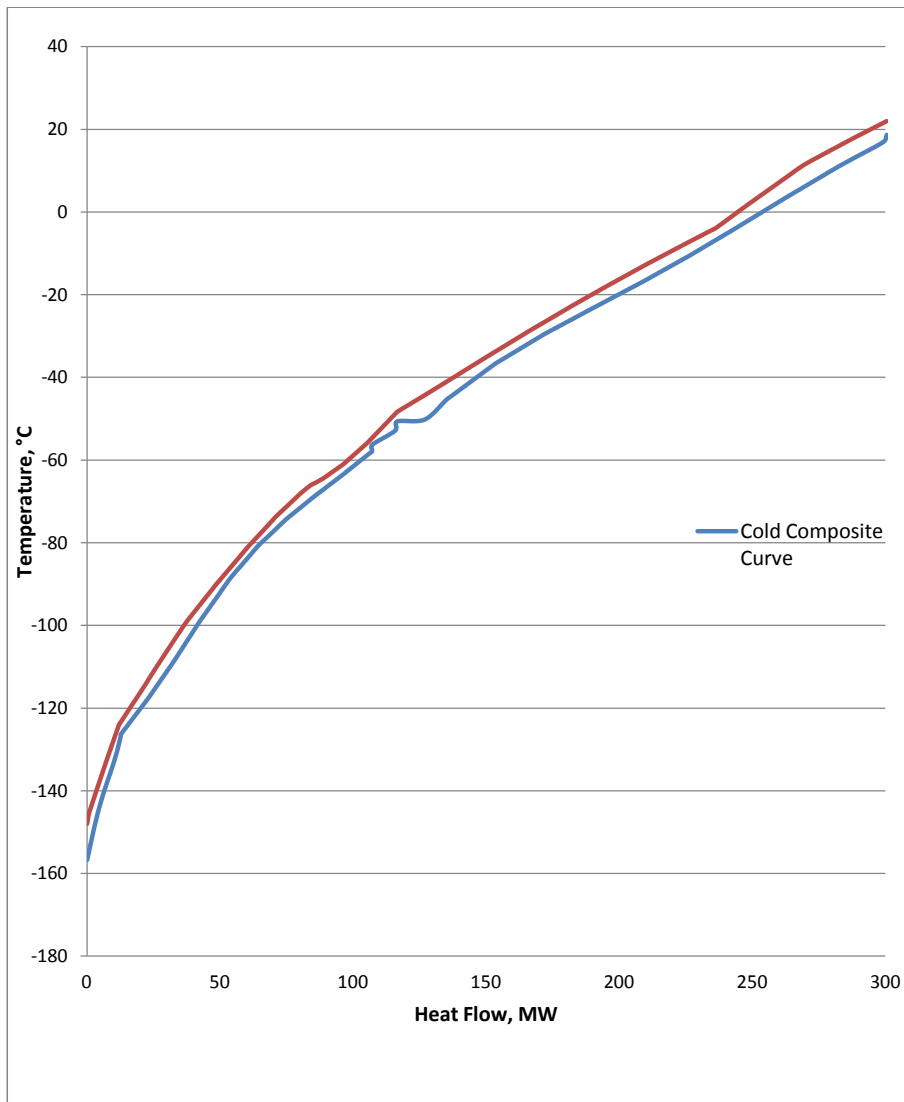
Appendix D Liquefin Process Flow Sheet



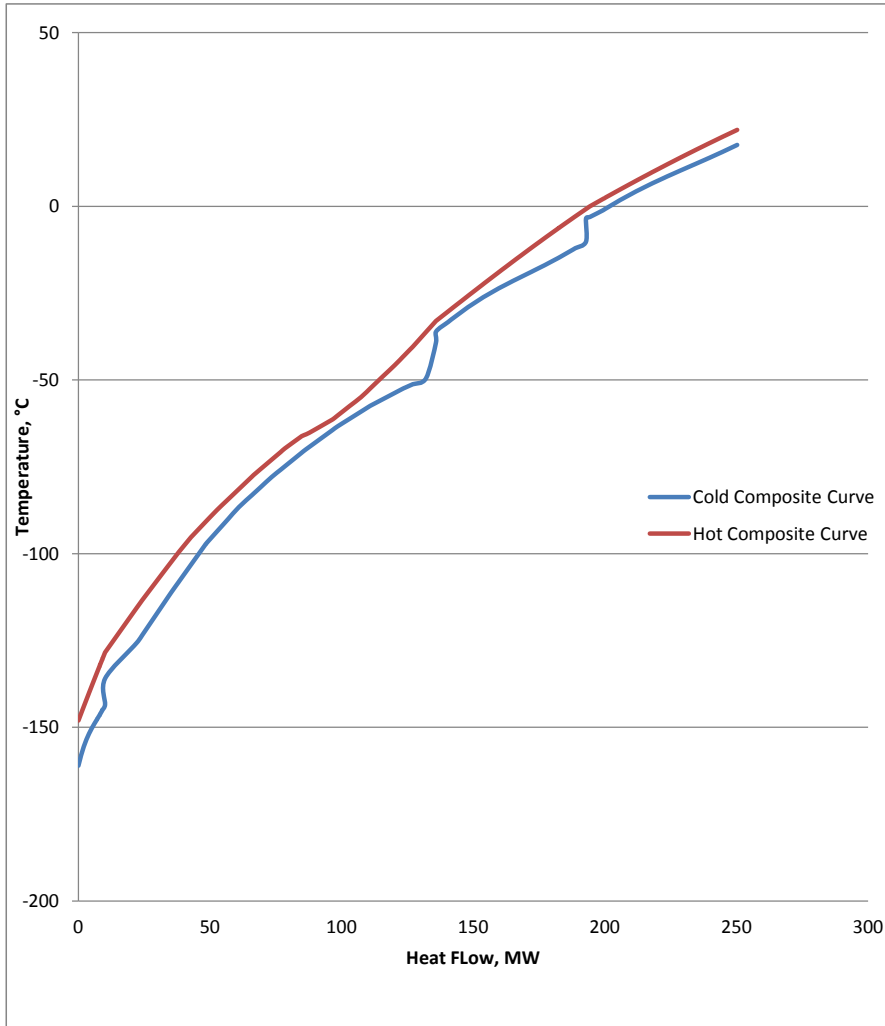
Appendix E Composite Curves Diagram for Initial APCI Alternative



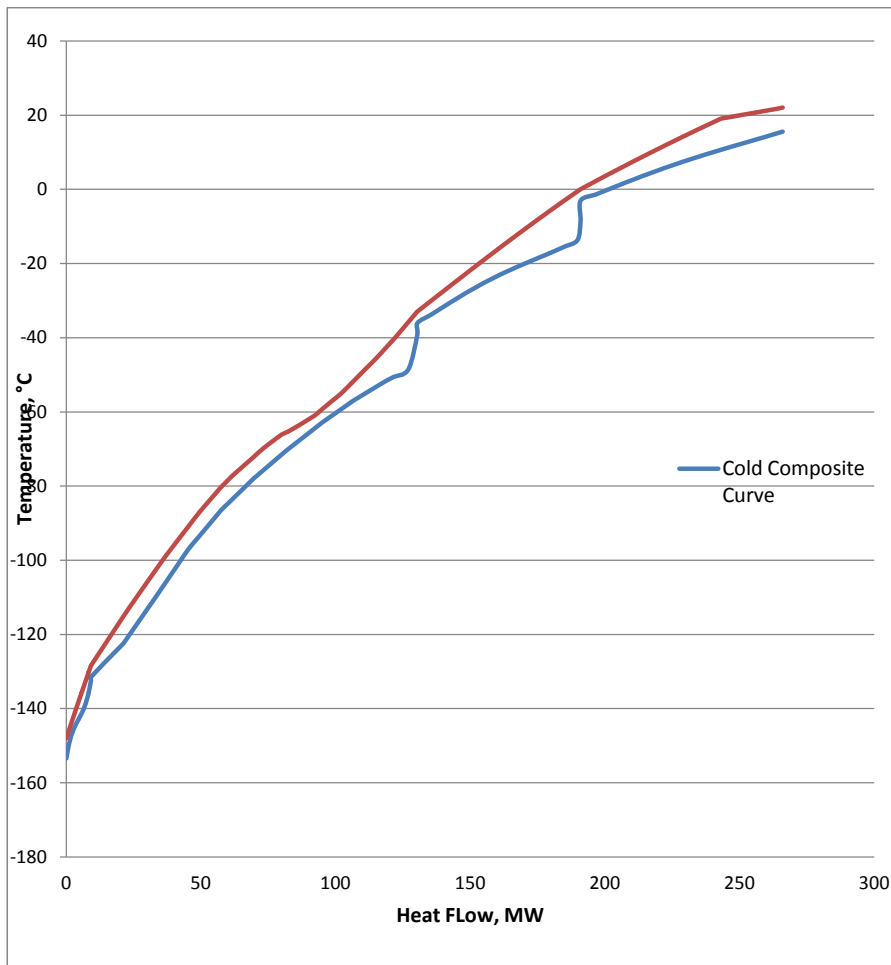
Appendix F Composite Curves Diagram for Optimized APCI Alternative



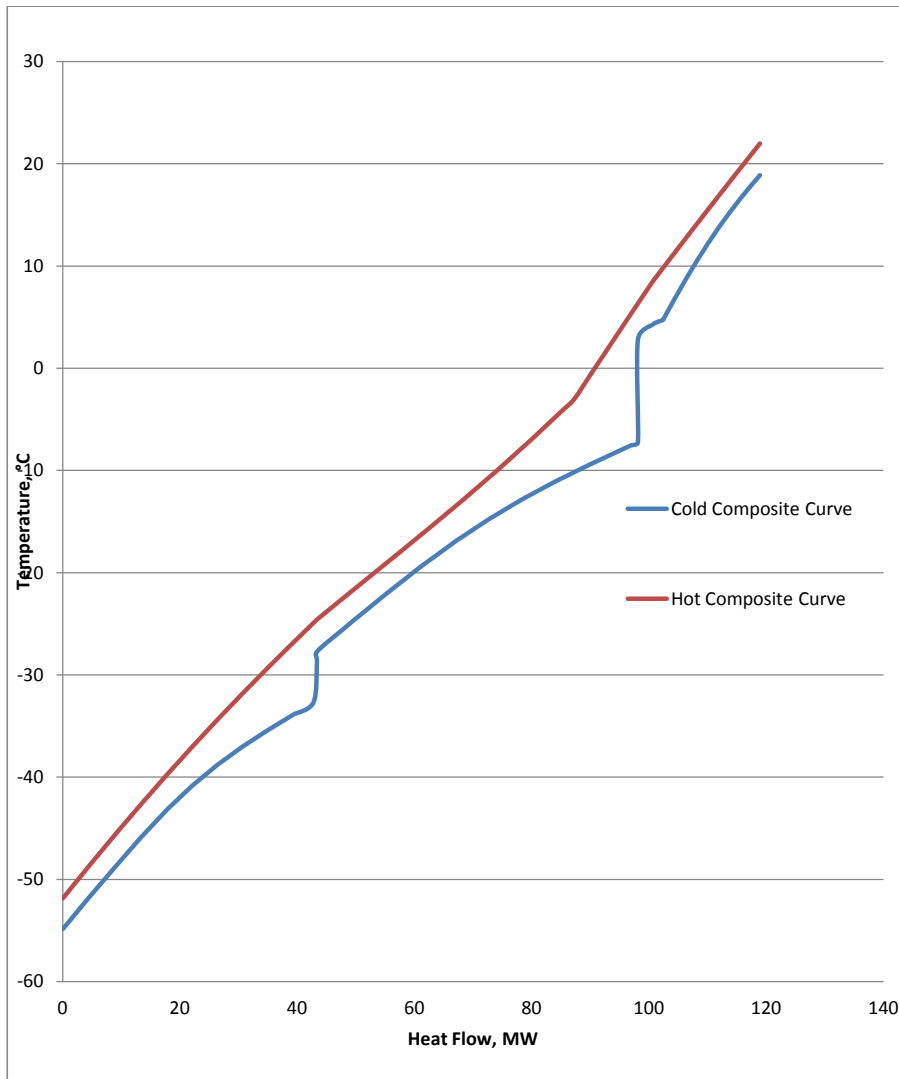
Appendix G Composite Curves Diagram for Initial Shell Alternative



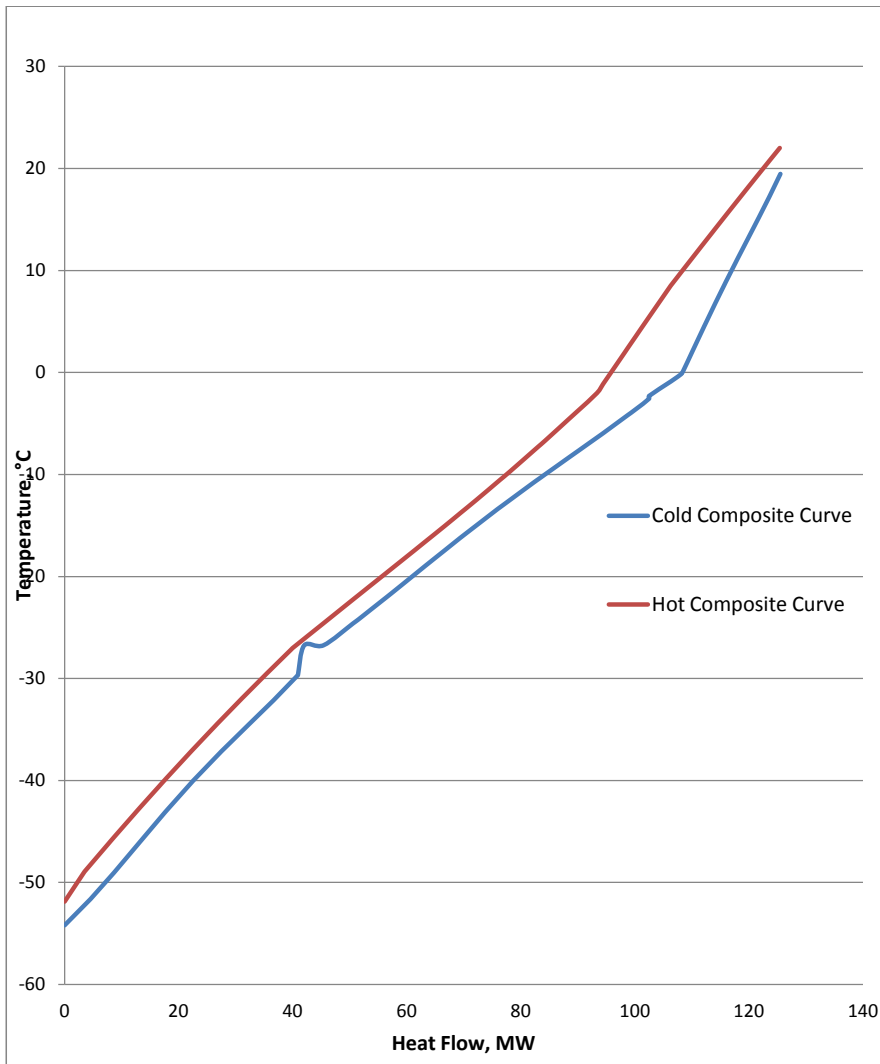
Appendix H Composite Curves Diagram for Optimized Shell Alternative



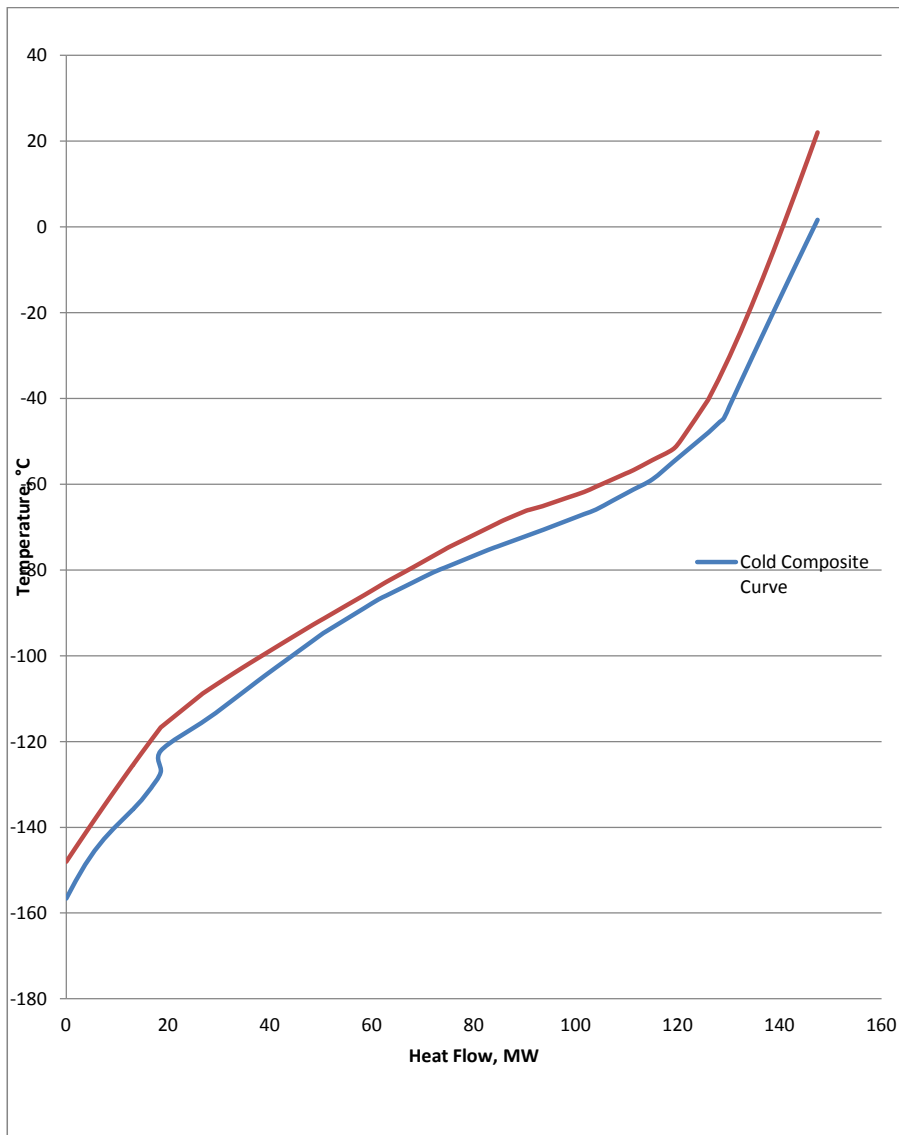
Appendix I Composite Curves Diagram for Initial Tealarc Alternative Pre-Cooling



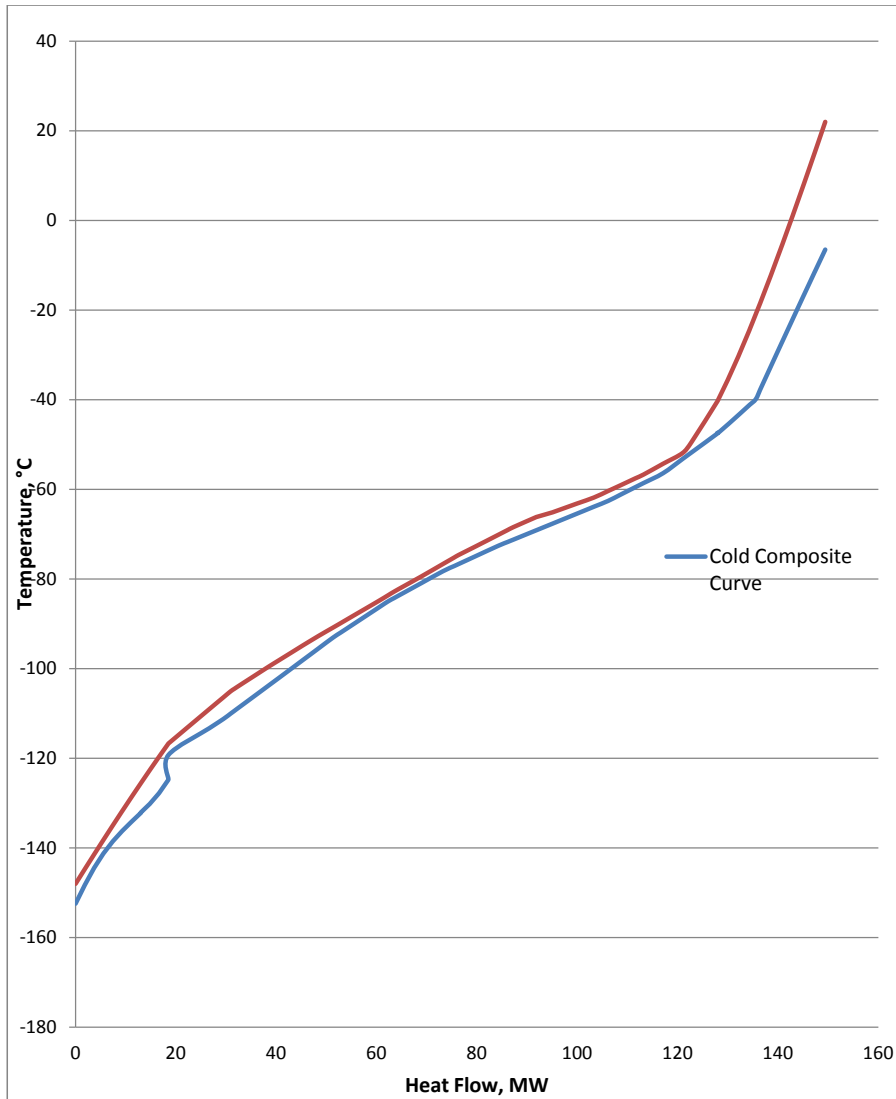
Appendix J Composite Curves Diagram for Optimized Tealarc Alternative Pre-Cooling



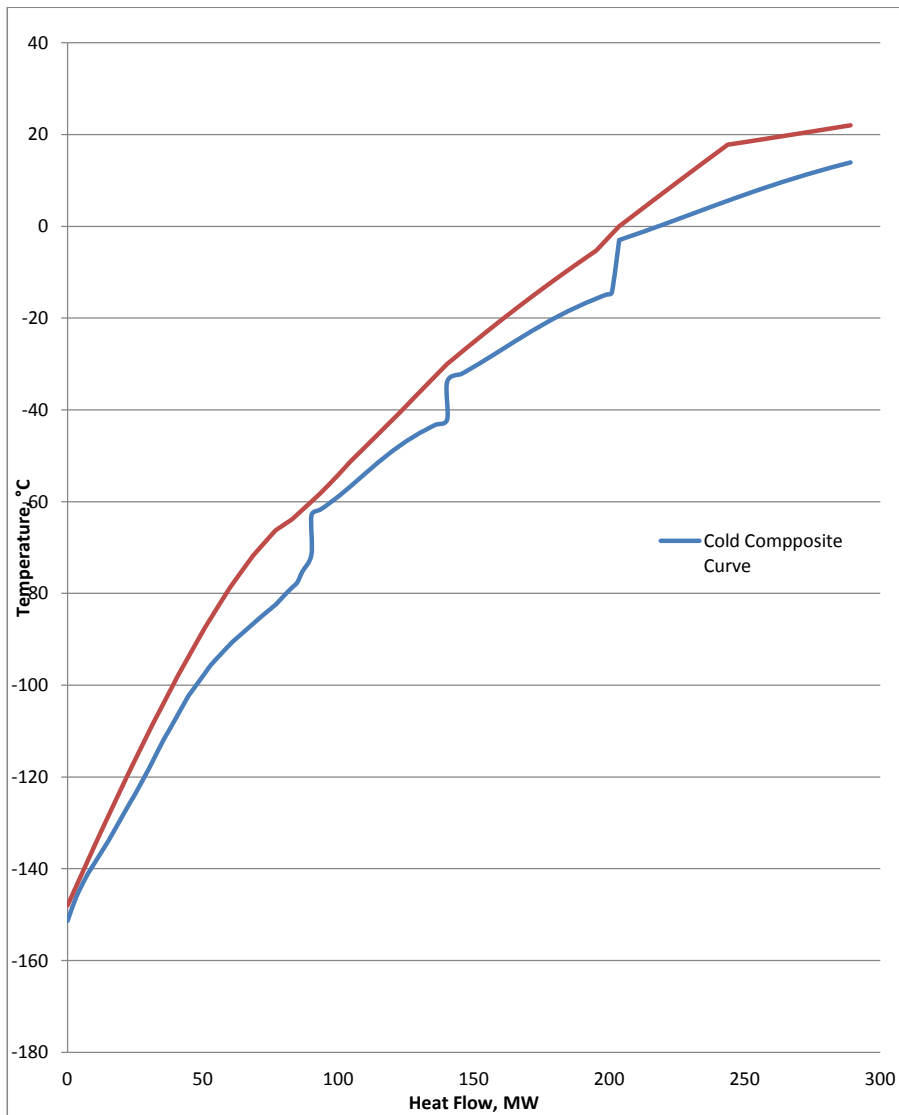
Appendix K Composite Curves Diagram for Initial Tealarc Alternative Liquefaction



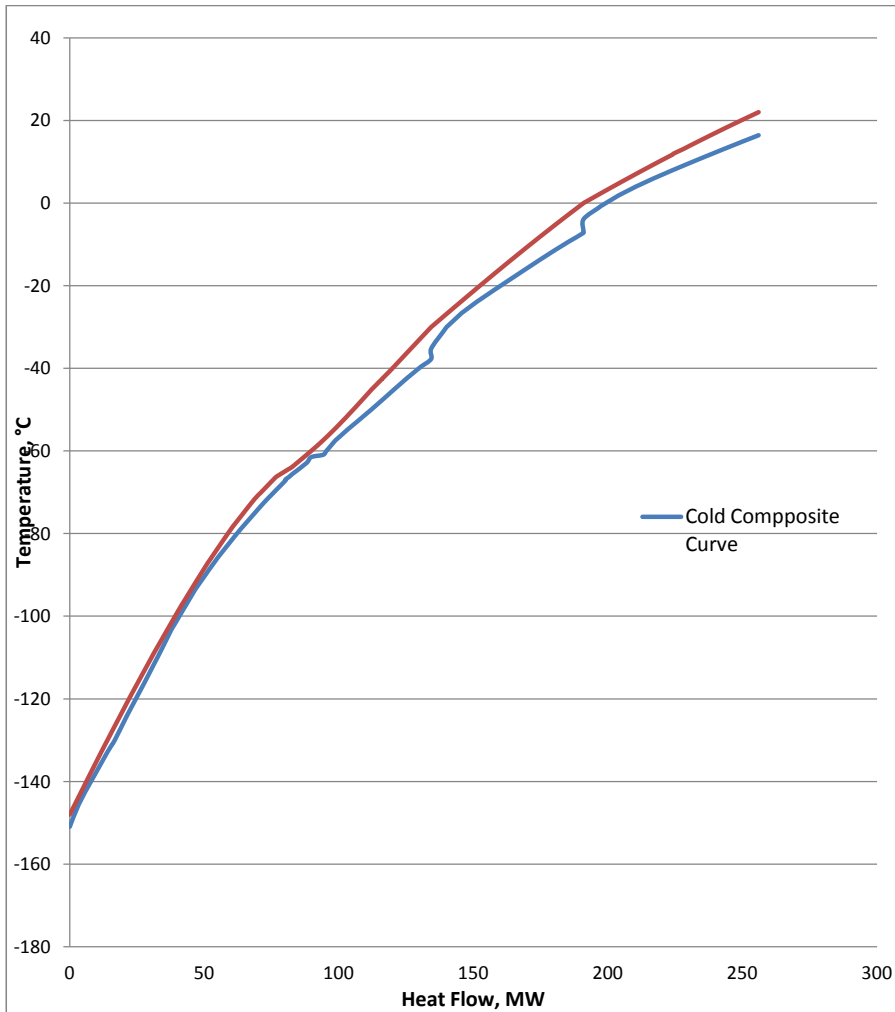
Appendix L Composite Curves Diagram for Optimized Tealarc Alternative Liquefaction



Appendix M Composite Curves Diagram for Initial Liquefin Alternative



Appendix N Composite Curves Diagram for Optimized Liquefin Alternative



Appendix O Material Stream Values from HYSYS for Initial Shell DMR Process

Stream Name	Vapor Fraction	Temperature [°C]	Pressure [bar]	Molar Flow [kgmole/h]	Mass Flow [kg/h]	Liquid Volume Flow [m ³ /h]
1	1.00	22.00	60.0	23365.5	412548	1305
201	0.97	22.00	48.6	30018.0	812000	2061
2	1.00	0.00	60.0	23365.5	412548	1305
102	0.00	0.00	18.0	23717.3	1000000	2083
202	0.62	0.00	48.6	30018.0	812000	2061
102b	0.00	0.00	18.0	10910.0	460000	958
102d	0.93	17.72	7.5	12807.3	540000	1125
102a	0.00	0.00	18.0	12807.3	540000	1125
102c	0.03	-3.48	7.5	12807.3	540000	1125
1	1.00	21.39	7.5	23717.3	1000000	2083
2	1.00	66.59	18.0	23717.3	1000000	2083
103	0.00	-33.00	18.0	10910.0	460000	958
203	0.29	-33.00	48.6	30018.0	812000	2061
3	1.00	-33.00	60.0	23365.5	412548	1305
104	0.02	-36.06	2.9	10910.0	460000	958
105	1.00	-3.01	2.9	10910.0	460000	958
106	1.00	41.96	7.5	10910.0	460000	958
1heated	1.00	21.39	7.5	23717.3	1000000	2083
4	0.00	-128.40	60.0	23365.5	412548	1305
203v	1.00	-33.00	48.6	8705.5	182801	486
203l	0.00	-33.00	48.6	21312.6	629199	1574
204l	0.00	-128.40	48.6	21312.6	629199	1574
204v	0.00	-128.40	48.6	8705.5	182801	486
205l	0.08	-133.95	3.0	21312.6	629199	1574
206	0.23	-135.92	3.0	30018.0	812000	2061
207	1.00	-39.18	3.0	30018.0	812000	2061
5	0.00	-148.00	60.0	23365.5	412548	1305
205v	0.00	-148.00	48.6	8705.5	182801	486

206v	0.16	-160.99	3.0	8705.5	182801	486
207v	0.61	-143.43	3.0	8705.5	182801	486
prod LNG	0.00	-157.59	1.4	21377.5	378697	1202
flash gas	1.00	-157.59	1.4	1988.0	33851	103
6	0.09	-157.59	1.4	23365.5	412548	1305
208	1.00	49.66	12.0	30018.0	812000	2061
209	1.00	15.16	12.0	30018.0	812000	2061
210	1.00	70.47	26.5	30018.0	812000	2061
211	1.00	14.97	26.5	30018.0	812000	2061
212	1.00	59.22	48.6	30018.0	812000	2061

Appendix P Material Stream Values from HYSYS for Initial APCI DMR Process

Stream Name	Vapor Fraction	Temperature [°C]	Pressure [bar]	Molar Flow [kmole/h]	Mass Flow [kg/h]	Liquid Volume Flow [m³/h]
1	1.00	22.00	60.0	23371.1	412646	1305
101	0.00	22.00	48.0	37504.6	1204724	3086
201	1.00	22.00	55.5	31032.2	772405	2034
102	0.00	-48.30	48.0	37504.6	1204724	3086
202	0.27	-48.30	55.5	31032.2	772405	2034
2	0.98	-48.30	60.0	23371.1	412646	1305
103	0.08	-55.11	10.0	37504.6	1204724	3086
104	1.00	19.00	10.0	37504.6	1204724	3086
105	1.00	19.00	10.0	37504.6	1204724	3086
no liquid	0.00	19.00	10.0	0.0	0	0
106	1.00	76.06	25.0	37504.6	1204724	3086
107	0.71	15.06	25.0	37504.6	1204724	3086
107v	1.00	15.06	25.0	26773.6	795299	2144
1071	0.00	15.06	25.0	10731.0	409425	942
108v	1.00	61.45	48.0	26773.6	795299	2144
1081	0.00	18.13	48.0	10731.0	409425	942
109	0.73	43.39	48.0	37504.6	1204724	3086
202v	1.00	-48.30	55.5	8322.8	184827	438
2021	0.00	-48.30	55.5	22709.4	587578	1597
3	0.00	-124.00	60.0	23371.1	412646	1305
2031	0.00	-124.00	55.5	22709.4	587578	1597
203v	0.00	-124.00	55.5	8322.8	184827	438
2041	0.11	-130.85	5.8	22709.4	587578	1597
205	0.28	-128.86	5.8	31032.2	772405	2034
206	1.00	-56.52	5.8	31032.2	772405	2034

4	0.00	-148.00	60.0	23371.1	412646	1305
204v	0.00	-148.00	55.5	8322.8	184827	438
205v	0.20	-162.23	5.8	8322.8	184827	438
206v	0.76	-126.94	5.8	8322.8	184827	438
5	0.09	-157.59	1.4	23371.1	412646	1305
flash gas	1.00	-157.59	1.4	1988.5	33859	103
prod LNG	0.00	-157.59	1.4	21382.6	378787	1202
207	1.00	17.92	17.4	31032.2	772405	2034
208	1.00	14.92	17.4	31032.2	772405	2034
209	1.00	80.32	39.9	31032.2	772405	2034
210	1.00	15.32	39.9	31032.2	772405	2034
211	1.00	41.09	55.5	31032.2	772405	2034

Appendix Q Material Stream Values from HYSYS for Initial Liquefin DMR Process

Stream Name	Vapor Fraction	Temperature [°C]	Pressure [bar]	Molar Flow [kmole/h]	Mass Flow [kg/h]	Liquid Volume Flow [m³/h]
1	1.00	22.00	60.0	23371.1	412646	1305
201	1.00	22.00	55.5	24166.4	570000	1622
101	0.27	22.00	20.0	46381.9	1720000	3979
2	1.00	0.00	60.0	23371.1	412646	1305
102	0.00	0.00	20.0	46381.9	1720000	3979
202	1.00	0.00	55.5	24166.4	570000	1622
102a	0.00	0.00	20.0	22263.3	825600	1910
102b	0.00	0.00	20.0	24118.6	894400	2069
102c	0.03	-3.00	12.3	22263.3	825600	1910
102d	0.99	13.91	12.3	22263.3	825600	1910
3	1.00	-30.00	60.0	23371.1	412646	1305
203	0.37	-30.00	55.5	24166.4	570000	1622
103	0.00	-30.00	20.0	24118.6	894400	2069
103a	0.00	-30.00	20.0	13723.5	508914	1177
103b	0.00	-30.00	20.0	10395.1	385486	892
103c	0.03	-33.84	5.2	13723.5	508914	1177
103d	1.00	-3.00	5.2	13723.5	508914	1177
4	0.86	-60.00	60.0	23371.1	412646	1305
204	0.00	-60.00	55.5	24166.4	570000	1622
104	0.00	-60.00	20.0	10395.1	385486	892
105	0.02	-63.00	1.8	10395.1	385486	892
106	1.00	-42.09	1.8	10395.1	385486	892
5	0.00	-148.00	60.0	23371.1	412646	1305
205	0.00	-148.00	55.5	24166.4	570000	1622
206	0.01	-146.11	5.7	24166.4	570000	1622
207	0.01	-146.11	5.7	15708.2	370500	1054
208	0.01	-146.11	5.7	8458.2	199500	568

209	0.06	-151.36	2.7	15708.2	370500	1054
210	1.00	-71.50	2.7	15708.2	370500	1054
211	0.84	-71.50	5.7	8458.2	199500	568
21	1.00	-25.30	5.7	15708.2	370500	1054
22	1.00	-60.19	5.7	24166.4	570000	1622
23	1.00	24.83	20.0	24166.4	570000	1622
24	1.00	15.03	20.0	24166.4	570000	1622
25	1.00	96.63	55.5	24166.4	570000	1622
6	0.09	-157.59	1.4	23371.1	412646	1305
flash gas	1.00	-157.59	1.4	1988.5	33859	103
prod LNG	0.00	-157.59	1.4	21382.6	378787	1202
1	1.00	9.41	5.2	10395.1	385486	892
2	1.00	2.38	5.2	24118.6	894400	2069
3	1.00	48.64	12.3	24118.6	894400	2069
4	1.00	30.85	12.3	46381.9	1720000	3979
5	1.00	43.85	20.0	46381.9	1720000	3979
4 cooled	1.00	15.35	12.3	46381.9	1720000	3979

Appendix R Material Stream Values from HYSYS for Initial Tealarc Process

Stream Name	Vapor Fraction	Temperature [°C]	Pressure [bar]	Molar Flow [kmole/h]	Mass Flow [kg/h]	Liquid Volume Flow [m ³ /h]
1	1.00	22.00	60.0	23371.1	412646	1305
101	0.00	22.00	22.0	25647.9	1000000	2217
201	1.00	22.00	40.0	33491.0	820000	2223
202	1.00	8.50	40.0	33491.0	820000	2223
102	0.00	8.50	22.0	25647.9	1000000	2217
102a	0.00	8.50	22.0	5129.6	200000	443
102b	0.00	8.50	22.0	20518.4	800000	1774
102c	0.05	2.82	11.8	5129.6	200000	443
102d	0.91	18.87	11.8	5129.6	200000	443
203	0.72	-24.58	40.0	33491.0	820000	2223
103	0.00	-24.58	22.0	20518.4	800000	1774
103a	0.00	-24.58	22.0	11900.6	464000	1029
103b	0.00	-24.58	22.0	8617.7	336000	745
103c	0.02	-27.73	5.2	11900.6	464000	1029
103d	1.00	4.26	5.2	11900.6	464000	1029
204	0.37	-51.86	40.0	33491.0	820000	2223
104	0.00	-51.86	22.0	8617.7	336000	745
105	0.02	-54.86	2.1	8617.7	336000	745
106	1.00	-28.67	2.1	8617.7	336000	745
204v	1.00	-51.86	40.0	12245.3	256271	667
204l	0.00	-51.86	40.0	21245.7	563729	1555
2	1.00	-40.00	60.0	23371.1	412646	1305
3	0.00	-116.70	60.0	23371.1	412646	1305
205l	0.00	-116.70	40.0	21245.7	563729	1555
205v	0.00	-116.70	40.0	12245.3	256271	667
4	0.00	-148.00	60.0	23371.1	412646	1305
206v	0.00	-148.00	40.0	12245.3	256271	667
207v	0.12	-156.64	6.0	12245.3	256271	667

208v	0.72	-127.15	6.0	12245.3	256271	667
206l	0.07	-121.34	6.0	21245.7	563729	1555
209	0.30	-122.20	6.0	33491.0	820000	2223
210	0.99	-47.86	6.0	33491.0	820000	2223
211	1.00	1.66	6.0	33491.0	820000	2223
1	1.00	15.50	5.2	8617.7	336000	745
2	1.00	9.01	5.2	20518.4	800000	1774
3	1.00	50.88	11.8	20518.4	800000	1774
4	1.00	25.88	11.8	20518.4	800000	1774
5	1.00	21.00	11.8	25647.9	1000000	2217
6	1.00	56.66	22.0	25647.9	1000000	2217
21	1.00	81.52	17.4	33491.0	820000	2223
22	1.00	15.02	17.4	33491.0	820000	2223
23	1.00	79.47	40.0	33491.0	820000	2223
5	0.09	-157.59	1.4	23371.1	412646	1305
flash gas	1.00	-157.59	1.4	1988.5	33859	103

Appendix S Material Stream Values from HYSYS for Optimized Shell Process

Stream Name	Vapor Fraction	Temperature [°C]	Pressure [bar]	Molar Flow [kmole/h]	Mass Flow [kg/h]	Liquid Volume Flow [m ³ /h]
1	1.00	22.00	60.0	23362.8	412500	1305
101	0.15	22.00	16.5	30757.4	1215972	2662
201	1.00	22.00	49.0	28800.0	759166	2006
2	1.00	0.00	60.0	23362.8	412500	1305
202	0.61	0.00	49.0	28800.0	759166	2006
102	0.00	0.00	16.5	30757.4	1215972	2662
102a	0.00	0.00	16.5	18454.4	729583	1597
102b	0.00	0.00	16.5	12303.0	486389	1065
102c	0.03	-3.02	9.7	18454.4	729583	1597
102d	0.95	15.59	9.7	18454.4	729583	1597
3	1.00	-33.00	60.0	23362.8	412500	1305
203	0.20	-33.00	49.0	28800.0	759166	2006
103	0.00	-33.00	16.5	12303.0	486389	1065
104	0.02	-36.09	3.7	12303.0	486389	1065
105	1.00	-8.52	3.7	12303.0	486389	1065
203v	1.00	-33.00	49.0	5752.3	114833	333
203l	0.00	-33.00	49.0	23047.7	644333	1674
4	0.00	-128.40	60.0	23362.8	412500	1305
204l	0.00	-128.40	49.0	23047.7	644333	1674
204v	0.00	-128.40	49.0	5752.3	114833	333
205l	0.06	-132.26	3.4	23047.7	644333	1674
206	0.18	-131.47	3.4	28800.0	759166	2006
207	1.00	-39.27	3.4	28800.0	759166	2006
5	0.00	-148.00	60.0	23362.8	412500	1305
205v	0.00	-148.00	49.0	5752.3	114833	333
206v	0.07	-153.43	3.4	5752.3	114833	333
207v	0.70	-132.42	3.4	5752.3	114833	333
6	0.09	-157.59	1.4	23362.8	412500	1305
flash gas	1.00	-157.59	1.4	1987.8	33847	103

LNG	0.00	-157.59	1.4	21375.0	378653	1202
106	1.00	38.97	9.7	12303.0	486389	1065
107	1.00	19.16	9.7	30757.4	1215972	2662
108	1.00	48.02	16.5	30757.4	1215972	2662
208	1.00	49.95	13.6	28800.0	759166	2006
209	1.00	15.00	13.6	28800.0	759166	2006
210	1.00	70.74	29.9	28800.0	759166	2006
211	1.00	15.00	29.9	28800.0	759166	2006
212	1.00	51.13	49.0	28800.00	759166	2006
1	1.00	22.00	60.0	23362.8	412500	1305
101	0.15	22.00	16.5	30757.4	1215972	2662
201	1.00	22.00	49.0	28800.0	759166	2006
2	1.00	0.00	60.0	23362.8	412500	1305
202	0.61	0.00	49.0	28800.0	759166	2006
102	0.00	0.00	16.5	30757.4	1215972	2662

Appendix T Material Stream Values from HYSYS for Optimized APCI Process

Stream Name	Vapor Fraction	Temperature [°C]	Pressure [bar]	Molar Flow [kmole/h]	Mass Flow [kg/h]	Liquid Volume Flow [m ³ /h]
WMR1	0.17	22.00	48.0	40303.8	1315636	3279
Natural Gas	1.00	22.00	60.0	23371.1	412646	1305
CMR1	1.00	22.00	55.5	31373.9	761018	2037
NG2	0.98	-48.30	60.0	23371.1	412646	1305
CMR2	0.28	-48.30	55.5	31373.9	761018	2037
WMR2	0.00	-48.30	48.0	40303.8	1315636	3279
WMR3	0.10	-56.30	12.2	40303.8	1315636	3279
WMR4	1.00	18.64	12.2	40303.8	1315636	3279
WMR4VAP	1.00	18.64	12.2	40303.8	1315636	3279
WMR4LIQ	0.00	18.64	12.2	0.0	0	0
WMR5	1.00	61.37	24.4	40303.8	1315636	3279
WMR6	0.66	15.00	24.4	40303.8	1315636	3279
WMR6VAP	1.00	15.00	24.4	26684.6	765703	2068
WMR6LIQ	0.00	15.00	24.4	13619.2	549933	1211
WMR7	1.00	63.10	48.0	26684.6	765703	2068
HPWMRLIQ	0.00	17.82	48.0	13619.2	549933	1211
WMR8	0.63	42.91	48.0	40303.8	1315636	3279
CMR2VAP	1.00	-48.30	55.5	8857.1	190186	473
CMR2LIQ	0.00	-48.30	55.5	22516.8	570833	1564
NG3	0.00	-124.00	60.0	23371.1	412646	1305
CMR3VAP	0.00	-124.00	55.5	8857.1	190186	473
CMR3LIQ	0.00	-124.00	55.5	22516.8	570833	1564
CMR4LIQ	0.08	-128.59	7.2	22516.8	570833	1564
CMR4	0.25	-126.40	7.2	31373.9	761018	2037
CMR5	1.00	-50.66	7.2	31373.9	761018	2037
CMR4VAP	0.00	-148.00	55.5	8857.1	190186	473
NG4	0.00	-148.00	60.0	23371.1	412646	1305
CMR5VAP	0.13	-156.74	7.2	8857.1	190186	473
CMR6VAP	0.70	-126.92	7.2	8857.1	190186	473
NG5	0.09	-157.59	1.4	23371.1	412646	1305

End Flash	1.00	-157.59	1.4	1988.5	33859	103
LNG	0.00	-157.59	1.4	21382.6	378787	1202
CMR6	1.00	47.77	28.9	31373.9	761018	2037
CMR7	1.00	15.00	28.9	31373.9	761018	2037
CMR8	1.00	38.76	39.0	31373.9	761018	2037
CMR9	1.00	15.00	39.0	31373.9	761018	2037
CMR10	1.00	43.09	55.5	31373.9	761018	2037
WMR1	0.17	22.00	48.0	40303.8	1315636	3279
Natural Gas	1.00	22.00	60.0	23371.1	412646	1305
CMR1	1.00	22.00	55.5	31373.9	761018	2037
NG2	0.98	-48.30	60.0	23371.1	412646	1305
CMR2	0.28	-48.30	55.5	31373.9	761018	2037
WMR2	0.00	-48.30	48.0	40303.8	1315636	3279
WMR3	0.10	-56.30	12.2	40303.8	1315636	3279

Appendix U Material Stream Values from HYSYS for Optimized Liquefin Process

Stream Name	Vapor Fraction	Temperature [°C]	Pressure [bar]	Molar Flow [kmole/h]	Mass Flow [kg/h]	Liquid Volume Flow [m ³ /h]
1	1.00	22.00	60.0	23371.1	412646	1305
101	0.00	22.00	41.1	47068.8	1599639	3956
201	0.88	22.00	53.7	23708.5	643799	1667
2	1.00	0.00	60.0	23371.1	412646	1305
202	0.50	0.00	53.7	23708.5	643799	1667
102	0.00	0.00	41.1	47068.8	1599639	3956
102a	0.00	0.00	41.1	22593.0	767827	1899
102b	0.00	0.00	41.1	24475.8	831812	2057
102c	0.04	-3.90	19.3	22593.0	767827	1899
102d	0.85	16.43	19.3	22593.0	767827	1899
3	1.00	-30.00	60.0	23371.1	412646	1305
203	0.15	-30.00	53.7	23708.5	643799	1667
103	0.00	-30.00	41.1	24475.8	831812	2057
103a	0.00	-30.00	41.1	13926.7	473301	1170
103b	0.00	-30.00	41.1	10549.1	358511	887
103c	0.05	-35.23	8.9	13926.7	473301	1170
103d	1.00	-6.82	8.9	13926.7	473301	1170
4	0.86	-60.00	60.0	23371.1	412646	1305
204	0.00	-60.00	53.7	23708.5	643799	1667
104	0.00	-60.00	41.1	10549.1	358511	887
105	0.06	-66.88	3.2	10549.1	358511	887
106	0.95	-37.70	3.2	10549.1	358511	887
5	0.00	-148.00	60.0	23371.1	412646	1305
205	0.00	-148.00	53.7	23708.5	643799	1667
206	0.00	-145.60	5.5	23708.5	643799	1667
206lp	0.00	-145.60	5.5	15410.5	418469	1083
206hp	0.00	-145.60	5.5	8298.0	225330	583
207lp	0.06	-150.97	2.2	15410.5	418469	1083
208lp	0.91	-61.50	2.2	15410.5	418469	1083
207hp	0.66	-61.50	5.5	8298.0	225330	583

107	1.00	2.94	8.9	10549.1	358511	887
108	1.00	-2.61	8.9	24475.8	831812	2057
109	1.00	43.10	19.3	24475.8	831812	2057
110	0.99	19.42	19.3	47068.8	1599639	3956
111	0.78	15.00	19.3	47068.8	1599639	3956
112	0.85	47.65	41.1	47068.8	1599639	3956
209	0.97	-37.39	5.5	15410.5	418469	1083
210	0.86	-44.46	5.5	23708.5	643799	1667
211	1.00	8.84	27.3	23708.5	643799	1667
212	1.00	15.00	27.3	23708.5	643799	1667
213	1.00	64.40	53.7	23708.5	643799	1667
6	0.09	-157.59	1.4	23371.1	412646	1305
flash gas	1.00	-157.59	1.4	1988.5	33859	103
LNG	0.00	-157.59	1.4	21382.6	378787	1202

Appendix V Material Stream Values from HYSYS for Optimized Tealarc Process

Stream Name	Vapor Fraction	Temperature [°C]	Pressure [bar]	Molar Flow [kmole/h]	Mass Flow [kg/h]	Liquid Volume Flow [m ³ /h]
1	1.00	22.00	60.0	23371.1	412646	1305
101	0.00	22.00	20.2	26886.2	1050917	2336
201	1.00	22.00	38.8	34531.5	840314	2305
202	1.00	8.50	38.8	34531.5	840314	2305
102	0.00	8.50	20.2	26886.2	1050917	2336
102a	0.00	8.50	20.2	4812.6	188114	418
102b	0.00	8.50	20.2	22073.6	862803	1918
102c	0.10	-2.29	10.4	4812.6	188114	418
102d	0.99	19.47	10.4	4812.6	188114	418
103	0.00	-24.58	20.2	22073.6	862803	1918
203	0.71	-24.58	38.8	34531.5	840314	2305
103a	0.00	-24.58	20.2	12957.2	506465	1126
103b	0.00	-24.58	20.2	9116.4	356338	792
103c	0.02	-26.75	5.6	12957.2	506465	1126
103d	1.00	-0.88	5.6	12957.2	506465	1126
204	0.35	-51.86	38.8	34531.5	840314	2305
104	0.00	-51.86	20.2	9116.4	356338	792
105	0.02	-54.18	2.2	9116.4	356338	792
106	0.98	-26.73	2.2	9116.4	356338	792
107	1.00	12.05	5.6	9116.4	356338	792
108	1.00	3.88	5.6	22073.6	862803	1918
109	1.00	35.77	10.4	22073.6	862803	1918
110	1.00	32.64	10.4	26886.2	1050917	2336
111	0.82	15.00	10.4	26886.2	1050917	2336
112	0.83	41.02	20.2	26886.2	1050917	2336
204v	1.00	-51.86	38.8	12257.5	250370	676
204l	0.00	-51.86	38.8	22274.0	589944	1629
2	1.00	-40.00	60.0	23371.1	412646	1305
3	0.00	-116.70	60.0	23371.1	412646	1305
205l	0.00	-116.70	38.8	22274.0	589944	1629

205v	0.00	-116.70	38.8	12257.5	250370	676
4	0.00	-148.00	60.0	23371.1	412646	1305
206v	0.00	-148.00	38.8	12257.5	250370	676
207v	0.07	-152.41	7.1	12257.5	250370	676
208v	0.68	-124.75	7.1	12257.5	250370	676
206l	0.04	-118.99	7.1	22274.0	589944	1629
209	0.26	-119.25	7.1	34531.5	840314	2305
210	0.97	-47.40	7.1	34531.5	840314	2305
211	1.00	-6.50	7.1	34531.5	840314	2305
212	1.00	74.82	21.4	34531.5	840314	2305
213	1.00	15.00	21.4	34531.5	840314	2305
214	1.00	60.90	38.8	34531.5	840314	2305
5	0.09	-157.59	1.4	23371.1	412646	1305
flash gas	1.00	-157.59	1.4			

988.5	33859	103
-------	-------	-----